
Roma Tre University

Doctoral School in Computer Science and Automation
Ciclo XXVIII

# The Cell Transmission Model for Urban Traffic: a Robust Optimization Algorithm for Signal Setting Problem

Author:
**Marco Tiriolo**

Advisor: **Prof.ssa Ludovica Adacher**

Spring 2017

ROMA TRE
UNIVERSITÀ DEGLI STUDI

SCUOLA DOTTORALE IN INFORMATICA ED AUTOMAZIONE

XXVIII
CICLO DEL CORSO DI DOTTORATO

# The Cell Transmission Model for Urban Traffic: a Robust Optimization Algorithm for Signal Setting Problem


Marco Tiriolo
Nome e Cognome del dottorando

firma

Ludovica Adacher
Docente Guida/Tutor: Prof.

firma

Stefano Panzieri
Coordinatore: Prof.

firma

# Summary

The main goal of this research is to define a robust method to solve combined signal setting problem.
Signalized junctions represent critical points of an urban transportation network, and the efficiency of their traffic signal setting influences overall network performance. Since road congestion usually takes place at or close to junction areas, an improvement in signal settings contributes to improve travel times, driver comfort, fuel consumption efficiency, pollution and safety. In a traffic network, the signal control strategy affects the travel time on the roads and influences the drivers' route choice behavior.
Usual traffic signal optimization methods seek either to maximize the green bandwidth or to minimize a general objective function that typically includes delays, number of stops, fuel consumptions and some external costs like pollutant emissions. A major objective of Traffic Signal Synchronization at intersection is to clear maximum traffic throughput in a given time with least number of accidents, at maximum safe speed and with minimum delay. It has been widely accepted that improving traffic flow has been one of the strategies to reduce vehicle emissions and fuel consumption. In urban areas, frequent stop-and-go driving and excessive speed variations contribute to higher fuel consumption and emissions. During the implementation of the research project presented in this PhD Thesis, three main areas of research have been explored: urban traffic modeling, traffic control, network clustering.

This thesis presents a new framework for traffic modeling, based on Cell Transmission Model. The Cell Transmission Model for Urban Traffic (CTM-UT) proposes new methods to model complex traffic dynamics on arterial and node. Its two most important features consist in the representation of (i) the traffic flow interactions between neighboring movements when entering in the channelized lanes upstream intersection and (ii) the conflict among crossing flows at intersection with the capacity determination of minor flows.
The experiments (presented in [Adacher et al., (2014)] , [Adacher and Tiriolo (2015b)] and [Adacher and Tiriolo (2015b)]) demonstrate that the CTM-UT is suitable to obtain good accuracy (between the 2% and 4%) compared to microscopic simulation tools (i.e., VISSIM and SUMO). At the same time, the CTM-UT framework is suitable to take into account the urban complexity keeping the benefits of macroscopic model (i.e., low computational time and not too many information to manage).
To improve the calibration process of macroscopic models, which require a great effort in terms of time and resources, a new method to calibrate the congestion wave speed via optimization is proposed.

In order to minimize total traffic delay with signal synchronization,
[Adacher and Tiriolo (2016c)] describe how the Surrogate Method (SM), based on robust gradient approach, has been improved. The new version of the optimization model is suitable to obtain solution with more efficiency (at least the 4%) and efficacy (at least the 10%) compared to the classic SM.

Lastly, new "hybrid" decompositions of network nodes are proposed and the classification of nodes is integrated with a clustering algorithm based on topological characteristics of the network. Given the network partitions (subnetworks), the SM is applied to solve the traffic signal synchronization problem. Compared to considering the total network, the optimization integrated with the new "hybrid"

decomposition approaches can reduce the computational time with a slight loss of accuracy. For example, on a small network, an improved efficiency of 78% and a efficacy loss of 0.6% have been obtained (see [Adacher and Tiriolo (2016a)] and [Adacher and Tiriolo (2016b)]). While, on a large network, an improved efficiency of 53% and a efficacy loss of 0.09% have been obtained (see [Adacher and Tiriolo (2016c)]).

The results presented in this thesis demonstrate that the new version of optimization model, applied with proposed decomposition algorithm, are suitable to minimize, through the traffic signal synchronization, the total network delay in real time and for large-scale networks. The traffic model proposed is applied to estimate, with accuracy and efficiency, the total delay taking into account of complex urban dynamics.

The knowledge of travel time variations is fundamental in the evaluation of Dynamic Traffic Assignment (DTA) strategies and in the travelers' choices. Since that the CTM-UT is suitable to predict the travel time for traffic demands detailed at urban level (link, lane, turning movement), an interesting future research will be focused to the application of the DTA combined to the new proposed optimization algorithm. The integration of the assignment model into the defined control strategy might lead to increase the computational time but this problem can be reduced with the presented decomposition approaches.

# Contents

# List of Tables

# List of Figures

# Notation

# Cell Transmission Model notation

| Notation | Definition |
|---|---|
| $in$ | inflow in the node from upstream link |
| $out$ | outflow from the node to downstream link |
| $IN$ | set of inflows in the node |
| $O$ | set of outflows from the node |
| $\Phi$ | flow function |
| $\Sigma$ | supply flow function of node |
| $\Delta$ | demand flow function of node |
| $N$ | number of cells |
| $I$ | number of cells belong to merging zone |
| $\Delta t$ | sampling period (time step) |
| $\Delta x_i$ | cell length |
| $v_i$ | free flow speed (mph) |
| $w_i$ | congestion wave speed (mph) |
| $\bar{\rho}_i$ | jam density (vpm) |
| $\rho_i^c$ | critical density (vpm) |
| $k$ | period number |
| $f_i(t)$ | flow into cell $i$ at the time $t$ (vph) |
| $\rho_i^a(k)$ | the density for link $a$ and cell $i$ (vpm) in period $k$ |
| $\rho_i^{ab}(k)$ | considering the period $k$ is the density (vpm) from link $a$ to link $b$ for cell $i$ |
| $G = (U, A)$ | road network |
| $U$ | set of nodes (intersection) |
| $A$ | set of links |
| $B_m$ | set of links leaving node $m$ |

Table 1: Cell Transmission Model notation (1 of 2)

| Notation | Definition |
|---|---|
| $V_i^a(k)$ | actual speed in cell $i$ of link $a$ in period $k$ (mph) |
| $TT(k)$ | travel time in period $k$ (h) |
| $MTT$ | mean travel time (h) |
| $n_i^a(k)$ | vehicles contained in cell $i$ of link $a$ and during the period $k$ (vp$\Delta t$) |
| $n_i^{ab}(k)$ | vehicles contained in cell $i$ of link $a$ addressed to link $b$ of during the period $k$ (vp$\Delta t$) |
| $y_i^a(k)$ | incoming flow in cell $i$ of link $a$ in period $k$ (vp$\Delta t$) |
| $y_i^{ab}(k)$ | incoming flow in cell $i$ of link $a$ and addressed to link $b$ in period $k$ (vp$\Delta t$) |
| $Y_i^a(k)$ | maximum number of vehicles that can flow in cell $i$ of link $a$ in period $k$ (vp$\Delta t$) |
| $F_i^a(k)$ | total capacity of cell $i$ of link $a$ in period $k$ (vp$\Delta t$) |
| $\phi^{ab}$ | rate of vehicles traveling from link $a$ to link $b$ |
| $\alpha^{ab}$ | rate of stop line width for vehicles from link $a$ to link $b$ |

Table 2: Cell Transmission Model notation (2 of 2)

# Chapter 1

# Introduction

## 1.1 An overview on traffic problem

Transport represents a crucial aspect of the our lives at worldwide level. One of the main aims of the EU is the reducing global greenhouse emissions by the 80%. To keep climate change within safe limits (a temperature increase below the 2°C) is necessary a deep reduction of the transport sector emissions by 60% by 2050 ([EU Explained: Transport (2016)]).

In [EU Explained: Transport (2016)] it has been estimated that the road is the largest mode of transport used, only the passenger cars cause around two thirds of the 71% of overall transport CO2 emissions. Other transports pollute significantly less: maritime and aviation 14% and 13% respectively; inland navigation 2%; rail less than 1%.

In the last years the increasing volume of traffic has led to a worsening in congestion phenomena, with a variety of subsequent negative effects on the environment, safety and quality of life. The urban population in Europe still will increase, the forecasts indicate that in 2050 around 82% of the European population will be concentrated in urban areas. At the same time, also the demand for transport is expected to grow with a significant estimated increase by 80% by 2050 (second

the forecasts presented in [EU Explained: Transport (2016)] ).
To improve the urban transport is needed tackle many challenges, foremost among them traffic congestion as urbanization and a high dependence on cars for passengers and on trucks for freight.

Transport also represents a crucial sector of the economy. The traffic congestion, one of the worst transport problems, costs Europe about 1% of its GDP every year an also causes heavy amounts of carbon and other unwelcome emissions. The traffic congestion translates into a series of issues spanning from pollution, noise emissions, road safety problems and high levels of CO2 (urban areas represent around 23% of all CO2 emissions from transport and are also responsible for other emissions from road transport [Urban mobility (2014)]). In Europe, the congestion incurs an estimated annual cost of 80billion. According the analysis of the [Urban Mobility Scorecard (2015)] on the 471 U.S. urban areas, in the 2014 the cost in terms of delay and fuel has been of $160 billion.

The cost in terms of time that the population has been paying is enormous and there is a concrete risk that the increasing growth in transport demand may cause this cost not to be sustainable anymore. One of the key scopes of the EU's policy is to cut pollution caused by transport, which is backed by numerous projects and initiatives to cut urban congestion, encourage more use of cleaner forms of travel (e.g. rail) and promote clean fuels. Until now, the spread of transports that use fuel alternatives have been held back by scant infrastructure for recharging, by the high cost of vehicles and low level of consumer acceptance.
The reduction of the urban congestion play a key role in mitigating the effects of the global climate change. To achieve this scope, EU-funded research on urban transport is directed to improving traffic planning and demand management with the use of intelligent transport systems, and to facilitating high-quality public transport and non-motorized transport. Concrete solutions to go toward a sus-

tainable urban mobility can be provided by the Intelligent Transport Systems (ITS). The ITS are now being employed to optimize use of road infrastructure and to manage urban traffic flows by balancing road use by private cars, public transport and freight vehicles, optimizing energy consumption, and reducing congestion and transport emissions.

## 1.2 Traffic management

There are several ways to reduce the congestion: change the road infrastructure; a good management of traffic demand; traffic control (e.g. ramp metering, route guidance, variable speed limits, traffic signal synchronization (TSS), etc.). The TSS is a traffic engineering technique of matching the green light times for a series of intersections to enable the maximum number of vehicles to pass through, thereby reducing stops and delays experienced by motorists. Detailed overview of traffic control strategies is presented in [Papageorgiou et al., (2003)]. In this study, Papageorgiou argued that urban traffic network control is an urgent and challenging task, which if solved, could improve the economic and social effects related to traffic.

The activity of the urban traffic network remains a challenge within the ITS due to the intrinsic complexity of traffic systems. An updated, reliable and real-time urban traffic flow prediction is the groundwork of traffic management and control in the urban context. Research studies and literature reviews have demonstrated that the application of ITS has the potential to lead to a decrease in congestion; but as ITS technology solutions are also based on their ability to provide an accurate estimate of travel time prediction, it is necessary that this prediction is accurate so as to obtain the expected benefits on transport costs.

In order to face this serious problem concerning urban mobility, it is necessary to

adopt a "system" approach, where information, management and control work in synergy, optimizing the use of infrastructures and vehicles in a multimodal perspective. The travelers' time depends both on the maximum free flow time, in relation to the infrastructures, and on the delay due to congestion in the network. The problem of transportation is often posed in terms of delay so as to optimize the functioning of the network and minimize both travel time and energetic consumption, still ensuring and improving personal safety. The delay produced by slowdown and congestion is one of the costs associated to the use of transport systems. The term traffic refers to the movement of vehicles on a transport infrastructure. It differs for types of vehicles (e.g. cars, ships, etc.) and transport modes (e.g. highway, sea, etc.). A further differentiation concerns its type (public or private), and he environment (e.g. urban or intercity). In transport, the term intermodal refers to the use of different modes of conveyance on the same trip. Examples of inter-modal transfer facilities are: ports, airports, terminals, stations. This thesis focuses on the cars driving through urban traffic environments and offers a short overview of highway traffic flows.

Although the information about travel-time estimation has been used in various fields and applications, the complexity of the urban network and the randomness of the traffic demand has made reliable prediction of travel time on urban networks, a research area that still requires significant development. Research studies have confirmed that the traffic simulation techniques are among the few ones able to predict urban traffic travel time at the network level.
To obtain an urban traffic model with a good approximation of reality, it is necessary to define a formulation that takes into account the urban complexity, as far as it concerns both the network and the drivers' behaviors. These elements can be represented with high accuracy, simulating single vehicle-driver units, by a microscopic model. However different disadvantages, as the high computational time and the detailed information required, limits the applicability of micro-

scopic model to medium networks and no-real-time. Several studies about traffic simulation (as e.g. [Papageorgiou et al., (2003)], [Alecsandru and Ishak (2007)], [Flötteröd and Nagel (2005)]) have shown that, among various macroscopic simulation models, the Cell Transmission Model (CTM) by Daganzo has the potential to mimic the accuracy of microscopic simulators in urban traffic environments maintaining the benefits of the macroscopic models.

## 1.3 Research objectives and scope

The main goal of this research is to obtain a general framework for an urban traffic model suitable for real applications and large-scale networks.
The robust optimization model used works well under a different set of assumptions and with robust performances. A solution to an optimization model is defined as robust if it remains "close" to optimal for all scenarios of the input data, and a model is robust if it remains "almost" feasible for all data scenarios. The new framework is used to tackle the critical traffic issue on how to minimize the network delay through optimization of traffic signal synchronization. As traffic lights timing is a non-convex problem, to increase the efficiency and applicability of optimization methods, a spatial decomposition of network nodes is proposed.

The following objectives have been pursued in this study:

- The first objective is to design a model to simulate complex urban traffic dynamics with an accurate prediction of travel time, along with efficiency in terms of computational time and resources.
- Defining a general node approach that takes different aspects of conflicts at intersections into account. Such modeling must be suitable to represent both complex urban intersections and unsignalized intersections.

- Defining a solution to calibrate key elements of the macroscopic fundamental diagram (MFD). In order to solve the difficulty in tuning and setting the simulation parameters, a target of this thesis is to improve the calibration process of congestion wave speed in terms of accuracy and efficiency.
- Improving the efficiency and robustness of the surrogate method (SM) to extend its application to effectively optimize the urban traffic signal synchronization.
- Designing a decomposition method of the traffic network suitable for cooperative, centralized and decentralized control applications.
- The last general object is to integrate the optimization and decomposition approaches for a decentralized signal control system based on macroscopic urban traffic framework.

## 1.4 Thesis outline

This paragraph briefly describes the chapters of this thesis. In particular, articles that have already been published or submitted for publication will be mentioned. These describe how the research objects of this thesis have been tackled.

During the achievement of objectives listed above, three main areas of scientific discipline have been explored.

- **Urban Traffic Modeling:** the contents of Chapters 2-4 refer to basic concepts of traffic modeling and traffic simulators. Furthermore an in-depth description of the CTM state of art and its formulation is included. Chapter 4 shows the details of the formulations made in order to develop a new framework, the Cell Transmission Model for Urban Traffic (CTM-UT). Case

studies and preliminary results of this chapter are presented in the following paper.

Tiriolo M., Adacher L. and Cipriani E., An urban traffic flow model to capture complex flow interactions among lane groups for signalized intersections , *Procedia - Social and Behavioral Sciences Volume 111, 5 Pages 839-848* , 2014

Adacher L. and Tiriolo M., A New Node Model based on CTM-UT with Capacity Determination , *Transportation Research Procedia - Social and Behavioral Sciences Volume 10, Pages 21-30* , 2015

Chapter 4 also shows the method to calibrate the congestion wave speed for the macroscopic fundamental diagram presented in the following articles:

Adacher L. and Tiriolo M., 'A New Methodology to Calibrate the Congestion Wave for the Cell Transmission Model for Urban Traffic.' *IEEE 18th International Conference on Intelligent Transportation Systems, Las Palmas* , 2015, pp.606-611

- **Traffic Control:** Chapter 5 presents a general overview on traffic signal control and the background of the (SM). The chapter also shows the extensions of the SM for urban large-scale networks. The first results of this optimization method are presented in the following articles:

  Adacher L. and Tiriolo M., 'Stochastic Optimization for Macroscopic Urban Traffic Model with Microscopic Elements' *Computer Modelling and Simulation (UKSim), 2016 UKSim-AMSS 18th International Conference on, IEEE*,

2016

- **Network Clustering:** Chapter 6 proposes a decomposition approach, considering different levels of cooperation between subnetworks. Moreover, the Chapter demonstrates that the network decomposition allow to make Synchronizing Traffic Signals suitable for real-time decision and for large-scale networks.
  First, background formulation of clustering methods used is presented. Second, the cooperation methods are exhibited. Thirdly, the proposed methods identify the subnetworks through an algorithm that is based on classification or topological characteristics of the network. In Chapter 6, given the subnetworks, the surrogate method is applied to solve the Traffic Signal Synchronization problem. Furthermore, a comparison of several proposed decomposition methods has been made. The early results are presented in the following papers.

  Adacher L. and Tiriolo M., 'Distributed urban traffic signal optimization based on macroscopic model ' , *Innovative Computing Technology (INTECH) 2016 Sixth International Conference on, pp. 605-610, Dublin (Ireland), IEEE*, 2016

  Adacher L. and Tiriolo M., 'A Distributed Approach for Traffic Signal Synchronization Problem ' , *Mathematics and Computers in Sciences and in Industry (MCSI), 2016 Third International Conference on, Chania(Greece), IEEE*, 2016

  Adacher L. and Tiriolo M., 'Decentralized Vs Centralized Traffic Signal

Optimization' , *IEEE ITS Transactions*, 2016, submitted

This part about network clustering is still research in progress.

During the achievement of the research objects, listed in the previous paragraph, have been developed three main models and methods: one for each areas of research explored. These independents software can be integrated between them to define a robust optimization algorithm for signal setting problem.
The following Fig.1.1 presents a schematic overview of the architecture system which explains the data flow between the components software. The flowchart also shows the articles grouped for research areas.

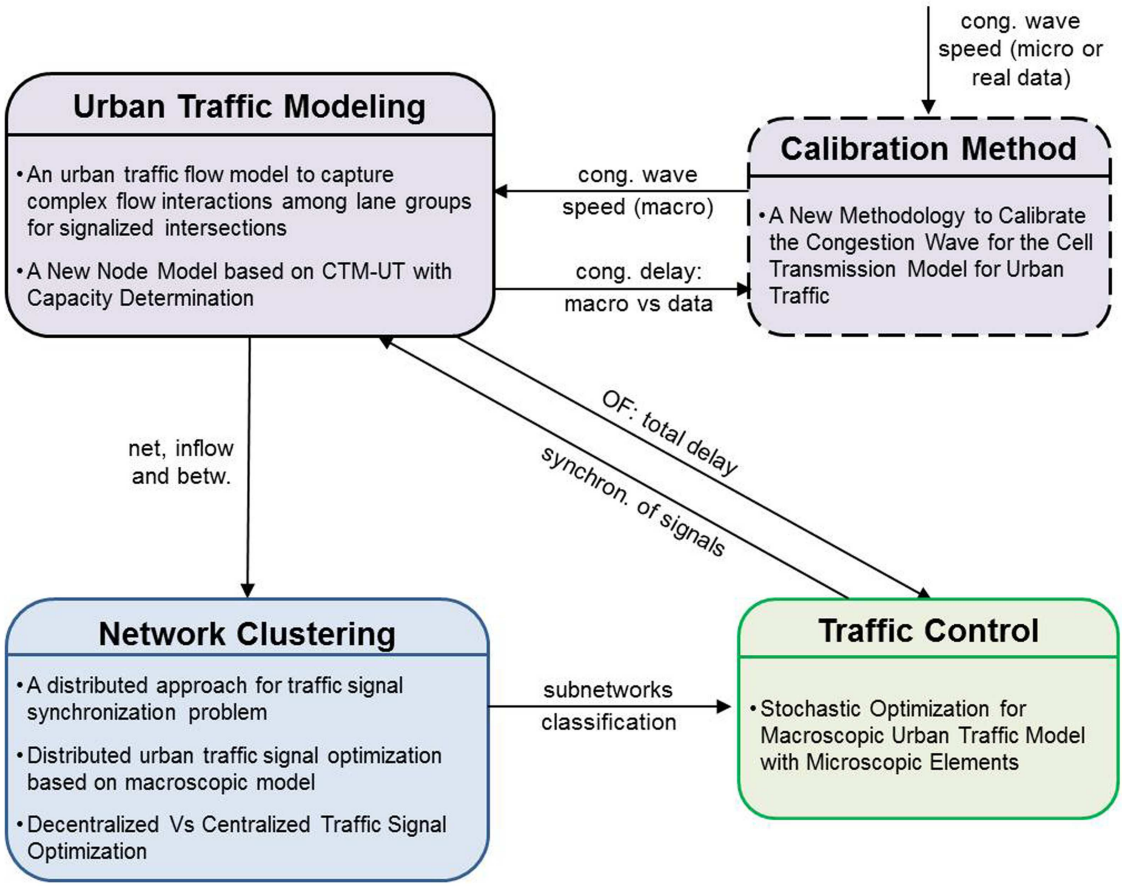


Figure 1.1: Schematic overview of the architecture system

# Chapter 2

# Traffic Flow Modeling

## 2.1 Introduction

The core of the research project presented in this PhD Thesis is represented by the new modeling framework for urban traffic systems. A traffic simulator has been developed to test the new framework. In this chapter the basic concepts of the traffic simulators and of the urban traffic will be described. In this thesis, the urban traffic aspects have been conventionally subdivided into arterial and intersection traffic flow. Lastly, a comparison between the main types of the traffic simulation models is presented.

## 2.2 System Architecture of Traffic Simulator

The traffic simulation software is basically a computerized version of a traffic model which is run over time to study the behavior of the system and the interactions between the subsystems. Therefore, the simulation software plays a fundamental role in the analysis and the improvement of transportation. Each traffic simulator uses a mathematical model to manage the data provided by the two components of road infrastructure. The first one is represented by trans-

portation supply, defined as the system of all elements, fixed or not, that allow or facilitate the transportation of people and things. The second is represented by transportation demand, which can be defined as the number of transfers effected on a given means of transport during a specified period of time. Generally, the simulator contains the following three main sets of elements, plus an additional one used to generate and manage the results of each simulation:

- ***Infrastructure*** is composed by: stations and parking that represent starting (origin) and ending (destination) points of trips; roads; tracks and many other elements. All these fixed elements are connected and define the traffic network. Roads are generally classified on the base of travel speed limits. The freeways are characterized by grade-separated and limited access, they carry heavy flows, have high speeds and are multilane divided. They do not present traffic lights on the mainline and are generally financed with tolls, so they may have tollbooths, either across the entrance ramp or across the mainline. Another kind of roads is the arterial. Unlike freeways, the arterial may not be grade-separated they serve both a movement and an access function. Their access is still generally limited, but it is not limited to the same extent as freeways. Below arterial are collector roads. These serve more of an access function, allowing vehicles to access the network from origins and destinations. In the end there are the local roads. These are designed to be low speed and carry relatively little traffic. Unlike collector, the local roads have only an access function, and are not intended for the movement of vehicles with neither a local origin nor destination.

- ***Traffic*** represents the technical features of a vehicle and specifications of traffic flows. Generally, the traffic supply is defined by origin-destination matrices.

- ***Traffic control***: all elements required for the management of the traffic, such as lighting, level crossing, etc.

- ***The results of simulations*** (i.e. output) can be provided online or at the end of all algorithm iterations. Generally, the indices of performance of the traffic network are generated during the simulation. these can be visualized during the evolving of the simulation or at the end of it.

The level of detail required to simulate the modeled roadway infrastructure depends on the purpose of the simulation. For example, elements as centroids, representing a traffic analysis zone or more roads which are very close to each other, can be simplified in one single road. The key elements in the representation of traffic networks are the following.

- Zone centroids: special nodes which are thought as source and sink of all transportation demand on the network.

- Node (vertices): intersection of links.

- Links (arcs): road segments indexed by from and to nodes (including centroid connectors), attributes can include lanes with the indications of turn direction (movement).

## 2.3 Basic concepts of urban traffic flow

Given the characteristics of freeway, the control of freeway traffic consists in ramp metering, route guidance, variable speed limits, etc. Instead, model and control of urban traffic is more complex because there are many elements, frequent congestion and more uncertainty to model it than freeway traffic.
In the urban traffic network the travel time of arterial is primarily determined by the time a vehicle takes to traverse the link, with a speed, which is also influenced by the presence of other vehicles on the street (density). While, the

waiting times at intersections are determined by the interaction between different streams converging to the node and the way traffic is regulated.
In the study by [Kang (2000)] there is a categorization of traffic flows. The author defines the traffic flow as uninterrupted and interrupted. The first one defines the flow category where the only interaction is among vehicles belonging to the same flow. In this category the are also the flows in facilities and freeways where there are no intersections or other external factors. Interrupted flow defines a category of traffic facilities having traffic signals, stop signs and other types of control devices which influence the progression of vehicles along the section. Examples of such facilities include intersections and arterial. The flow can be obstructed by interaction among vehicles belonging to the same flow, interactions among flows or by traffic control. The travel time for interrupted flow is primarily influenced by the waiting time at the intersections. Depending on the type of traffic regulation, the interrupted flow at intersection regards two different types, non-signalized and signalized. The through time of non-signalized intersection depends on the probability for a driver to have enough space between vehicles on the conflicting streams to pass the intersection safely. Instead, the through time for the second type is determined by the traffic light cycle time. Because signalized intersection has a main role on the urban traffic flow, such element is best described in the next section.

### 2.3.1 Arterial Modeling

In order to define a traffic model, it is required to have a comprehensive knowledge of traffic flow theories on freeways and urban streets. As it has been already pointed out, to obtain a urban traffic model with a good approximation of reality, it is necessary to define a formulation that takes into account the urban complexity, as far as it concerns both the network and the drivers' behaviors. In the urban environment traffic is interrupted by intersections along urban roads. Vehicles need to decelerate when approaching stop lines in red phases and ac-

celerate when departing in green phases. The speed equations used for freeways are not sufficient to describe the dynamic speed changes on urban roads. For this reasons, traffic models designed for freeway are not easily translated to urban environments. This paragraph describes some modeling features of traffic on arterial.

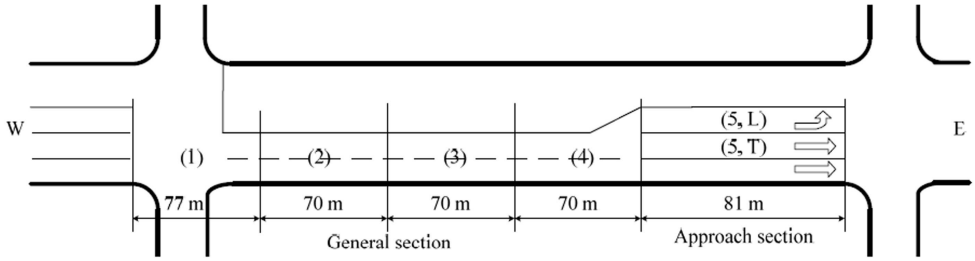


Figure 2.1: Example of arterial (see [Hu et al., (2010)]).

There are two ways to analyze queuing, vertical and horizontal. The first is only interested in processing the expected vehicles number at one point in time and does not consider the physical space occupied by them. This analysis does not allow any investigation of spillback effects of this queue on other links or nodes. The horizontal queuing analysis can be made by microscopic and macroscopic models. For microscopic models, the representation of the spillback phenomenon (horizontal queuing) requires high computational complexity, making these models not applicable for some transportation problems (e.g. traffic assignment, signal optimization, etc.).

The Cell Transmission Model (CTM) [Daganzo (1994)] is an example of macroscopic modeling approach applied to the horizontal queuing process. It represents the dynamics of queuing by subdividing a link into cells. The propagation of queues in time and space can also be computed using shockwave theory

(by products of traffic congestion and queuing). In particular, the propagation of traffic flow and especially the congestion effects can be represented using fluid-dynamic relationships. For example, the CTM adopts the LWR model ([Lighthill and Whitham (1955)] and [Richards (1956)]) to model the shockwave propagation in time and space in highways.

The shockwave are transition zones between two traffic states. On the urban street, most drivers can identify them as a transition from a moving to a congested state and vice versa. The shockwave can be caused by a change in capacity on the roadways (e.g. from three lane to two), a traffic signal on an arterial or an incident.

Simulating the traffic for multilane road sections is more complicated than for roads with only one lane, because it is necessary to take into account any risky behaviors displayed by drivers (e.g. lane-changing and platooning effects). The lane-changing model requires the estimation of the accepted deceleration. A driver is willing to accept that he forces a lag vehicle on the desired lane to decelerate.

Signalized intersections can strongly influence the propagation of queues and delays on the multilane road (and upstream of lane group). For example, it is possible to have one lane blocked while the others are flowing freely. Such queues depend on the relative density among lanes.

### 2.3.2 Intersection Modeling

Signalized intersections are the most common among various types of traffic control. The traffic signals allow certain streams of the intersection to move while forcing the others to wait, through a set of alternative light phases. Often, the yellow time is included in the green time to simplify the defining of traffic data and models. The main purposes of traffic signals are to improve overall safety, decrease average travel time through an intersection, and equalize the quality of services for all or most traffic streams. On the other hand, they may increase

both delays and the probability of congestions and rear-end collisions.

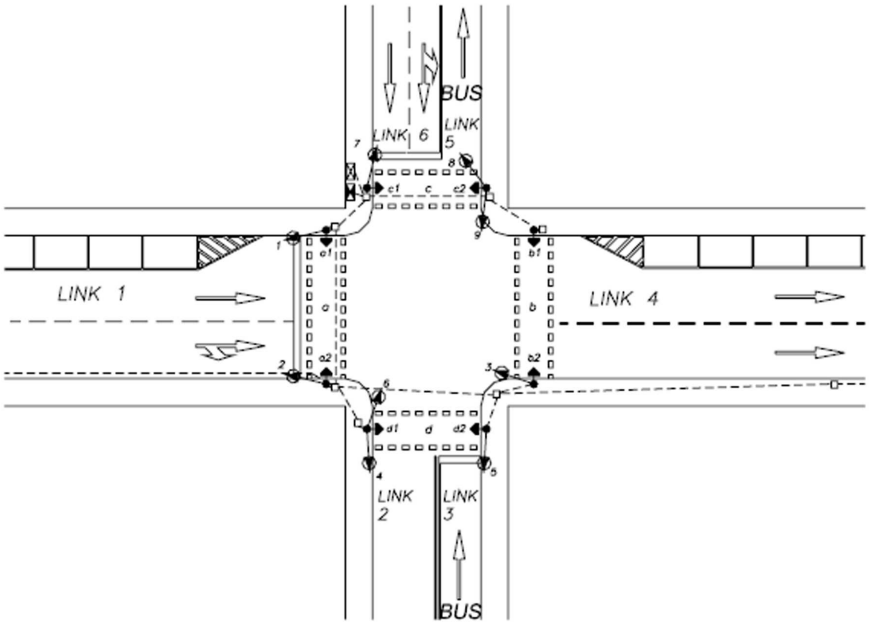


Figure 2.2: Example of urban intersection (see [Dotoli and Fanti (2006)]).

The Highway Capacity Manual [HCM (2010)] includes some useful guidelines to estimate delay, queue length, and number of stops for fixed-time signal settings (pre-timed control). The most important traffic performance, which determines the functionality of signalized intersections, is the signal delay. This measure is defined by the waiting (or delay) time and is calculated as the difference between the time spent to be served at the signal and the time the driver would have spent if the road section had been uninterrupted. In research, particular interest is given to queue modeling. This type of modeling can influence the fundamental aspects of traffic management such as optimization of signal control, measurement of network performance and other particular driving behaviors (e.g. uncertainty, driver choice).

Another characteristic of signalized intersections is that they might have to man-

age a multilane link. The time signal can manage lane group movements defining the one lane group that will dictate the necessary green time during a particular phase (critical lane group). The next section will present a description of the characteristics of multilane links.

## 2.4 Micro vs Macro for Traffic Simulation Models

The evolution of IT (Intelligent Transportation) and the increased power of computer calculations have brought a greater use of traffic simulation models. These are very powerful instruments that allow the analysis of those transportation problems which would not be solved by other means.
Microscopic traffic flow models are a class of analytical models for vehicular traffic dynamics. In contrast to macroscopic models, microscopic traffic flow models simulate single vehicle-driver units, so the dynamic variables of the models represent microscopic properties like the position and velocity of single vehicles. A microscopic traffic flow model calculates the position, speed and acceleration of every vehicle in the network at any moment. It can provide great deal of information to traffic management and simulation. For these reasons, the microscopic models are applied to small and medium no-real-time networks. Microscopic models are based on the simulation of single vehicle-driver units as their drivers respond to surrounding conditions by adjusting speeds and changing lanes.

- Benefits of microscopic models:
  - high accuracy of analysis;
  - high capacity to represent complex conditions of traffic.
- Disadvantages of microscopic models:
  - require high computational time and detailed information;

- difficulty to represent the drivers' behaviors.

Most applications of microscopic models are applied on networks that are not used to carrying too many vehicles, single intersection and urban traffic. It is clear that, for every time period, the microscopic models need information on all vehicles in the network. Also, it is very difficult to represent the real aspect of the complex traffic network by using an analytical model. However, different microscopic traffic simulation software are used to simulate the real urban traffic (i.e. SYNCHRO, MITSIM, VISSIM, SUMO). Microscopic traffic simulation models depend on the accuracy of the coding of network features. Network coding uses a node and link based network system, where each link is codified as a connector between two nodes. Network creation is accomplished within a graphical user interface that allows the user to build the network on top of a template road geometry file. Details on each link specify the characteristics of roadway such as the number of lanes, lane width, types of roadway, design and speeds. A microscopic traffic simulation model generally includes physical components, such as the roadway network, traffic control systems, driver-vehicle units, etc., and its associated behavioral models, such as driving behavior models and route choice models. These components and models have complex data requirements and numerous model parameters.

Even though simulation models offer the possibility to select entry parameters based on the available transport literature, it is necessary to calibrate these models according to a specific type of transport network and application. Such a calibration procedure involves the regulation of the parameters until there is a correct relation between the data collected by direct observation and those reproduced by the model. This calibration process requires a great effort in terms of time and resources. It becomes more difficult in relation to the number of calibration parameters and the impossibility to gather real data. In order to solve calibration problems, not only a trial-and-error method can be used, but also better structured approaches which consider calibration models as an optimization

problem, where a combination of values that best satisfies an objective function is searched. In the light of what it has been said, in particular, microscopic simulation requires greater efforts in calibration than the macroscopic one. This is due both to the fact that it is necessary to determine the data pertaining to each individual vehicle and route (Origin-Destination matrix) and to the fact that there is a greater number of stochastic factors linked to the estimate of the data. This is the reason why it is wise to run a series of simulations and use statistical estimators to compute, in compliance with the commonly accepted statistical principles, the number of simulations required to meet a stated objective.

Macroscopic models simulations are based on a section-by-section transmission rather than by tracking individual vehicles. Macroscopic models focus on basic hypothesis such as the conservation of flow and the state equation. The first one affirms that the vehicles' flow is conserved and as such it must comply with the mass conservation law, as it happens with fluids. On the contrary, the continuity equation shows the biunivocal correspondence among the three characteristic measures of the flow. Macroscopic models are based on hydrodynamic analogy representing traffic in terms of flow, density and speed. Benefits of macroscopic models include their capacity to model a large-scale network with heterogeneous elements (e.g. streets of different length, different level of traffic demand) and their ability to simulate freeway traffic connected to urban zone. The model requires low computational time and not too many information while the results of the simulations are easy to be managed on an IT level. On the other hand, the disadvantages of macroscopic models include their difficulty in tuning and setting the physical and simulation parameters and their lower accuracy compared to microscopic models. The application of macroscopic models allows validation of control strategies and they are suitable both for a large network scale and real-time solutions. Macroscopic models for traffic flows in urban arterial are frequently proposed in literature. [van den Berg et al., (2003)] presents a macroscopic model based on the model developed by [Kashani and Saridis (1983)] for

mixed urban and freeway traffic networks. A dynamic macroscopic model proposed by [Chevallier and Leclercq (2007)], for unsignalized intersections, accounts for time-limited disruptions in the minor stream flow, even in free-flow conditions when the mean flow demand is satisfied. [Abu-Lebdeh et al., (2007)] designed models that can represent the traffic output of intersections under congested flow conditions and, in particular, considered the interactions among traffic streams at successive signals. [Tonguz et al., (2009)] proposed a new cellular automata approach to formulate an urban traffic mobility model. He has shown that different control mechanisms used at intersections such as cycle duration, green split, and coordination of traffic lights, have a considerable effect on inter vehicle spacing distribution and traffic dynamics. In literature the CTM is identified as a macroscopic simulation method with specific features which are quite close to microscopic capabilities ([Flötteröd and Nagel (2005)]).

## 2.5 Conclusions

One of the primary goal of transport research is to develop a general framework for urban traffic network modeling that could be suitable for real applications. Several studies about traffic simulation have shown that, among various macroscopic simulation models, the CTM by Daganzo has the potential to achieve this objective. The CTM is one of the most standard traffic models, it has the potential to be applied for real-time application on a large network scale, because the model doesn't have a complex formulation and it is robust.

# Chapter 3

# State-of-art and development of the Cell Transmission Model (CTM)

## 3.1 Introduction

This chapter aims at presenting the background formulation and the state of the art of the CTM. In the last years researchers have attempted to increase the level of detail by extending CTM and introducing new formulations to improve the practical application of the model. Relevant research contributions on intersection and arterial modeling are conventionally reported in dedicated sections. Lastly, the advantages and the limitations of the CTM and its applicability to transport management are summarized.

## 3.2 The CTM model

The CTM proposed by Daganzo ([Daganzo (1994), Daganzo (1995)]), based on the hydromechanical theory, is a discrete approximation of the LWR model

([Lighthill and Whitham (1955)] and [Richards (1956)]). The CTM was proposed to represent the highway traffic. Through important features such as queue formation, queue dissipation and kinematic waves, the CTM can give a faithful representation of the real dynamics of traffic. This model can adopt a trapezoidal or triangular flow-density relation and each road section (link) is modeled as a sequence of heterogeneous cells. The example of figure 3.1 shows as the CTM represents an highway section with four cells. In the example, the flow propagation for the cell 2 is calculated with the number of vehicles in the cell 2 plus the inflow ($y_2$) and onramp flow ($r_2$) less the total outflow ($y_3$). While for the cell 3, the flow propagation is calculated with the number of vehicles in the cell 3 plus the inflow ($y_3$) less the total outflow ($y_4$) and offramp flow ($s_3$).

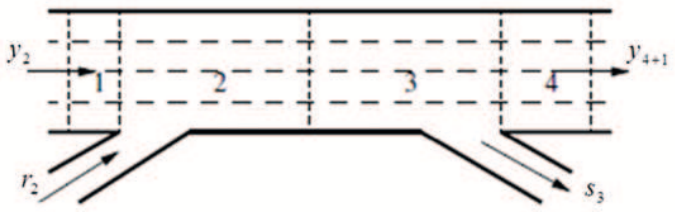


Figure 3.1: CTM Link subdivided.

Generally, a macroscopic simulation model for freeway traffic networks keeps track of the number of vehicles in distinct sections of the network as time passes. The vehicle occupancy in each section is increased (or decreased) by the number of vehicles allowed to enter (or leave) the section. To estimate the maximum outflow by a section, it is also employed the kinematic wave model that provides a measurement of the occupancy of the downstream section. Daganzo develops a freeway network representation based on CTM [Daganzo (1995)]. He defines three types of junction (connection between road sections): merging if two links enter and one leaves figure 3.2(a), diverging if only one link enters in the section but two leave it figure 3.2(b), and ordinary if one enters and one leaves. In

Fig.3.2, to identify all the components of the junction (merge or diverge), a link is denoted with "links" and it connects the cell "B" with the "E". With "clinks" is denoted the complementary link relative to "links", "clinks" is connected with "C" that is the third (complementary) cell belonging to the modeling block.

Daganzo explains that each arc can be treated as in section, defining for it boundary conditions specified by means of input and output cells. Such conditions are based on the number of vehicles existing in a cell at a specific time, the maximum number of vehicles that can be present in a cell and maximum number of vehicles that can flow into a cell. More details on the formulation will be provided later in this chapter.

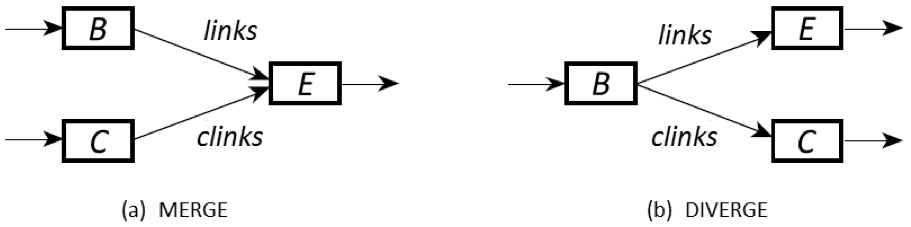


Figure 3.2: Representation of merge and diverge (see [Daganzo (1995)]).

### 3.2.1 CTM formulation

In tables 1 and 2 parameters and variables of the CTM and of the own extensions are reported.

The dynamic behavior of traffic, considering also the queues characteristics ( i.e.: formation, propagation, and dissipation) can be represented by the hydrodynamic theory of traffic flow. The hydrodynamic theory of traffic flow is based on the classic continuity flow conservation. This equation (3.1), considering time

$(t)$ and space $(x)$, gives a relationship between the density $(\rho)$ and flow function $(\Phi)$:

$$\rho_t + (\Phi(\rho))_x = 0 \tag{3.1}$$

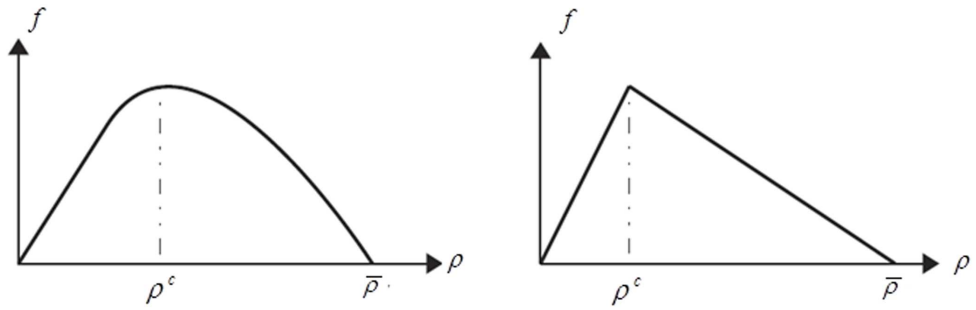


Figure 3.3: Fundamental diagrams for LWR (left) and the cell transmission model (right) [Kurzhanskiy (2007)].

The flow function, also known like the fundamental diagram, $\Phi(\rho) = \rho \cdot v(\rho)$ is assumed to be concave. $v = v(\rho)$ is the speed and it is a function of density. $\Phi$ is defined for $\rho \in [0, \bar{\rho}]$. At jam density $\bar{\rho}$ the vehicles are not moving and the flow is considered equal to zero. The maximum flow corresponds to the critical density $\rho^c$. The speed in which the vehicle can travel in optimal conditions is called free flow speed and the $v \geq \Phi(\rho^c) \ / \ \rho^c$. The free flow speed for a specific cell $i$ is represented as $v_i$. The road becomes congested when the density exceeds the critical value.

The conservation law in (3.1) defines a fundamental diagram. Compared to the approximation of the conservation law, for a given density, many speed values are actually measured. The flow-speed-density relations are location-specific, i.e. different locations and roads may be based on different fundamental diagrams and, furthermore, they are equilibrium models, i.e. they describe a steady-state behavior in the long run, and hence not specific to a particular time. If initial and boundary conditions are known, these assumptions can be solved at equilibrium

condition, when the speed is a function of density and if flow, speed, density are referred to the same location and time.

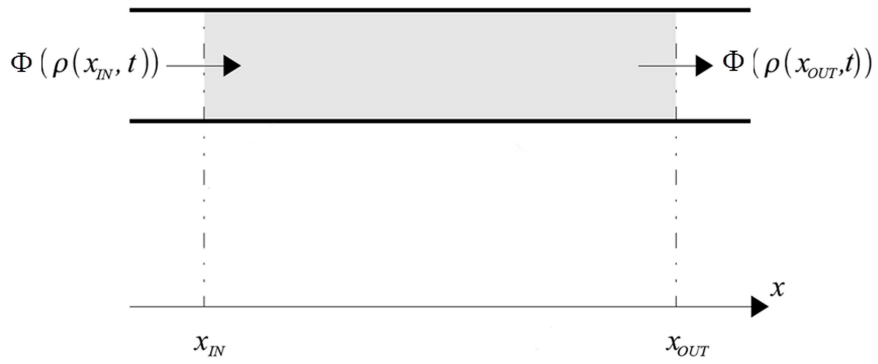


Figure 3.4: Representation of flow in road section.

For convention we use $f(t)$ when the flow is expressed in continuous time and $y(k)$ when the flow is expressed in discrete time, where the period $k$ is equal to sampling period $\Delta t$. To simplify the formulation sometimes time can be not explicate. $f(x,t) = \rho(x,t) \cdot v(x,t)$ is the flow at time $t$ for the position $x$ on a road. To represent the flow is possible rewrite in an integral form the (3.1)(see also Fig.3.4)

$$\frac{d}{dt}\int_{x_{OUT}}^{x_{IN}} \rho(x,t)dx = \Phi(\rho(x_{IN},t)) - \Phi(\rho(x_{OUT},t)) \tag{3.2}$$

The conservation laws can have discontinuous solutions and a numerical integration of standard methods like finite difference can generate instability and wrong shock velocities. Among numerical schemes for the conservation laws, the Godunov's scheme is often employed because it can solve partial differential equation. With this method the conservation variables are considered like constant piecewise. Godunov's scheme belongs to the first order, it is used for integration of relativistic fluid dynamic equations, it is free from oscillating behaviors and has a physical interpretation. The spatial domain is divided into cells, the cell $i$ comes before the cell $i+1$, the cell length is represented as $\Delta x_i$, the time is

discretized and $\tilde{\rho}$ can approximate the solution of (3.2):

$$\tilde{\rho}(x, k\Delta t) = \rho_i(k) \quad \forall i,\ \forall x \in [x_{i-1}, x_i] \tag{3.3}$$

the $\tilde{\rho}(x,\ (k+1)\Delta t)$ is calculated in two steps:

1. on the bases of initial conditions calculate the solution $\tilde{\rho}(x, (k+1)\Delta t)$ of (1)

$$\rho(x, k\Delta t) = \widetilde{\rho}(x, k\Delta t) = \rho_i(k), \quad \forall i,\ \forall x \in [x_{i-1}, x_i] \tag{3.4}$$

2. on the bases of the averages of $\tilde{\rho}(x, (k+1)\Delta t)$ of all cells $[x_{i-1}, x_i]$:

$$\rho_i(k+1) = \frac{1}{\Delta x_i} \int_{x_{i-1}}^{x_i} \tilde{\rho}(x, (k+1)\Delta t)\ \ dx \tag{3.5}$$

It is possible combine such steps like in the following equation

$$\rho_i(k+1) = \rho_i(k) + \frac{\Delta t}{\Delta x_i}(y_{i-1}(k) - y_i(k)) \tag{3.6}$$

where

$$y_i(k) = \frac{1}{\Delta t} \int_{k\Delta t}^{(k+1)\Delta t} \Phi(\rho(x_i, s))\ \ ds \tag{3.7}$$

stand for the average of crossing flow $x_i$, during the time interval $[k\Delta t, (k+1)\Delta t]$, from cell $i$ to cell $i+1$.

$\Phi$ is a concave function, and for this reason, it is possible reformulate the (3.7) as

$$y_i(k+1) = \begin{cases} \min\limits_{\rho_i(k) \le \rho \le \rho_{i+1}(k)} \Phi(\rho)\ , & if\ \ \rho_i(k) \le \rho_{i+1}(k) \\ \min\limits_{\rho_{i+1}(k) \le \rho \le \rho_i(k)} \Phi(\rho)\ , & if\ \ \rho_i(k) \ge \rho_{i+1}(k) \end{cases} \tag{3.8}$$

In case of discontinuity, this conservative Godunov's scheme can converge to solution without oscillations and with first order accuracy [Godunov (1959)]. The change flow direction, by approximating piecewise the state (density), for each time step in each cell of the spatial grid it is taken in consideration. For small

time intervals with Heaviside initial conditions when the the solution of initial problem is known it is possible to calculate the state evolution (the Heaviside step function is a discontinuous function whose value is zero for negative argument and one for positive argument).

$$\rho(x) = \begin{cases} \rho^- \ , & x < 0 \\ \rho^+ \ , & x > 0 \end{cases} \tag{3.9}$$

The scheme of Godunov is a good method to simulate the macroscopic traffic models, it solves a succession of local Riemann problems. For the triangular fundamental diagram the CTM is a particular case of the Godunov's scheme. This scheme can be simplified for the triangular diagram with free flow speed $v_i > 0$ and congestion wave $-w_i < 0$ speed as:

$$\rho_i(t+1) = \rho_i(t) + \frac{\Delta t}{\Delta x_i}(f_{i-1}(t) - f_i(t)) \tag{3.10}$$

where $\Delta t$ is the period, $\Delta x_i$ is the ith cell length, $f_i$ the flow from cell $i$ to $i+1$, $F_i$ is the total capacity (max number of vehicle) of cell $i$, and the flow is obtained by

$$f_i(t+1) = min\left\{v_i \cdot \rho_i(t),\ w_i\ (\bar{\rho} - \rho_i(t)),\ F_i\ \right\} \tag{3.11}$$

If $f_{i-1} = min\left\{v_{i-1} \cdot \rho_{i-1},\ F_{i-1}\ \right\}$ cell $i$ operates in free flow mode, or if $f_{i-1} = w_{i-1}(\bar{\rho} - \rho_i)$ it works in congested mode ( see [Daganzo (1994), Kurzhanskiy (2007)] for more details)

### 3.2.2 Formulation overview of the CTM extensions

The original CTM formulation is simple and robust, but it poses several restrictions on cell linkage. To overcome such limitations, different CTM extensions have been proposed to simulation the traffic flow for urban environment. Compared to urban environments, this section gives a concise overview of the variables

of the original CTM in relation to those of the new extensions introduced in the last years. More than representing the values of the cells, the variables have to represent the value for the lanes belongs to cells and the cells belongs to links. The flow conservation model is applied to update the number of vehicles contained in each cell, instead of use the values of density and flow it's possible formulated such update as

$$n_i^a(k+1) = n_i^a(k) + y_i^a(k) - y_{i+1}^a(k) \quad 1 \leq i \leq N \tag{3.12}$$

and

$$n_i^{ab}(k+1) = n_i^{ab}(k) + y_i^{ab}(k) - y_{i+1}^{ab}(k) \quad 1 \leq i \leq N \tag{3.13}$$

, where the number of vehicles is meant as a flow (vehicles per time), while the second one represent the number of vehicles contained in cell $i$ of link $a$ and direct to link $b$ in period $k$.

[Daganzo (1994), Daganzo (1995)] presents the CTM which simplified the solution scheme of the LWR model by adopting the following relationship between traffic flow ($f$) and density ($\rho$) :

$$f = min\{\, v\ \rho\ ,\ w\ (\bar{\rho} - \rho)\ ,\ F\,\} \quad 0 \leq \rho \leq \bar{\rho} \tag{3.14}$$

, where $F$ represents the total capacity of cell (storage capacity). With the previous equation the number of vehicles that flow from cell $i+1$ into cell $i$ in time interval $t$ ($\Delta t$) can be estimated as

$$y_i^a(t) = f_i^a(t)\ \Delta t = min \begin{cases} v\ \rho_{i-1}^a(t)\ \Delta t\ , \\ w\ (\bar{\rho} - \rho_i^a(t))\ \Delta t\ , \\ F_i^a(t)\ \Delta t \end{cases} \tag{3.15}$$

, via the relationship $n_i^a(t) = v\ \rho_i^a(t)\ \Delta t$, between the density and the number of vehicles contained in cell $i$, it's possible rewrite the inflow in the cell $i$ of link $a$ as:

$$y_i^a(t) = min \left\{ n_{i-1}^a(t),\ Y_i^a(t),\ \frac{w\ (F_i^a(t) - n_i^a(t))}{v} \right\} \tag{3.16}$$

Therefore, the inflow in a cell is given by:

- $n_{i-1}^a(t)$ : number of vehicles contained in cell $i$ in the upstream cell $i-1$ of link $a$ in time $t$;
- $Y_i^a(t)$ : maximum capacity of cell $i$ of link $a$ in time $t$; the value of the maximum capacity can change over the time in function of the traffic incident/blocking or signalized phases of red;
- $\frac{w\ (F_i^a(t) - n_i^a(t))}{v}$ : the necessary restriction to ensure that the inflow doesn't exceeds the available capacity, it represents the total space available in the downstream cell $i$.

Finally, with such notation, the flow conservation equation of the LWR model can be expressed as

$$n_i^a(t+1) = n_i^a(t) + y_i^a(t) - y_{i+1}^a(t) \tag{3.17}$$

, where the number of vehicles presents in each cell $i$ in time $t+1$ is equal to the sum of the number of vehicles presents in the cell $i$ in the prior time $t$ ($n_i^a(t)$); to this sum is subtracted the number of vehicles moving from the cell $i$ to the cell $i+1$.

As reported in the following chapters, the formulation of the CTM-UT is based on the flow conservation of the equations (3.12) and (3.13). Moreover, the CTM-UT formulation extends the representation of the inflow above-described (3.16).

## 3.3 Development of the CTM

The Tab. 3.1 reports the papers described in Chapter 3 and 4 that have extended the CTM starting from the original model of Daganzo. This overview puts in evidence the modelling area on which the papers are focused. The modelling areas are defined in terms of types of traffic flow and contest. As reported in this thesis, the traffic aspects have been conventionally subdivided into arterial and intersection traffic flow. The CTM extensions are classified through the following modelling areas.

- **Hig. Art.**: Highway traffic for the arterial.
- **Urb. Art.**: Urban traffic for the arterial.
- **Int.**: Crossing flows at the intersection.
- **Net.**: Network. Such classification identifies the papers that propose a general modeling of macroscopic traffic flow elements suitable for the entire network (e.g.: kinematic wave, fundamental diagram, merge and diverge models, etc.).
- **R. M.**: Ramp Metering. Flows that across onramp or offramp.

The CTM has been extended by Daganzo ([Daganzo (1995), Daganzo et al., (1997), Daganzo (1997)]) to consider the general flow-density relations, priority vehicles and special lanes for freeway environment. The validation of basic CTM, when it is applied to traffic freeway, is described both in [Lin and Ahanotu (1995)] and in [Smilowitz and Daganzo (1999)]. In [Lin and Daganzo (1994)] and in [Cayford et al., (2011)] there is an analysis of NETCELL, a freeway simulation tool based on CTM.
The paper [Jin and Zhang (2004)] introduced a generalization of simple merge and diverge models proposed originally by Daganzo. In this paper, the outflow of an incoming link is equal to the demand proportional part of the total

Table 3.1: Overview of the CTM extensions

| Extension | Hig. Art. | Urb. Art. | Int. | Net. | R. M. |
|---|---|---|---|---|---|
| [Daganzo (1994)] | X | | | | |
| [Daganzo (1995)] | | | | X | |
| [Buisson (1996)] | | | X | | |
| [Ziliaskopoulos and Lee (1997)] | | | X | | |
| [Daganzo (1997)] | X | | | | |
| [Daganzo et al., (1997)] | X | | | | |
| [Daganzo (1999)] | | | | X | |
| [Lo (1999), Lo (2001), Lo (2004)] | X | X | | | |
| [Lebacque and Khoshyaran (2002)] | | | X | | |
| [Jin and Zhang (2004)] | | | X | X | |
| [Ni and Leonard (2005)] | | | X | | |
| [Ishak et al., (2006)] | | | X | | |
| [Laval and Daganzo (2006)] | X | | | | |
| [Muñoz et al., (2006)] | X | | | | X |
| [Gomes and Horowitz (2006)] | X | | | | X |
| [Szeto (2008)] | | | | X | |
| [Wang (2010)] | | | X | | |
| [Pohlmann and Friedrich (2010)] | | | X | | |
| [Li (2011)] | | X | | | |
| [Long et al. (2011)] | | X | | X | |
| [Flötteröd and Rohde (2011)] | | | X | | |
| [Tampere et al., (2011)] | | | X | | |
| [Adacher et al., (2014)] | X | X | | | |
| [Adacher and Tiriolo (2015a)] | | | X | | |
| [Adacher and Tiriolo (2015b)] | | | | X | |

flow. While, [Ni and Leonard (2005)] proposed a capacity proportional distribution into the original merge model of Daganzo.

With the method of transmission in each instant of time is calculated the average flows crossing from upstream cells to downstream cells. The average flow is based on comparison between maximum number of vehicles that can "sent" into a cell by maximum number of vehicles that can "received" into a cell. To improve the accuracy of the original CTM, Daganzo proposes the Lagged Cell

Transmission Model (L-CTM). This model is easier to apply and more accurate compared to the methods for flow density relation both of Godunov that of Newell. In [Daganzo (1999)] the author has demonstrated that the CTM's accuracy improves when the downstream density that is used to calculate the receiving flow is read in clock intervals earlier than the current time and if such lag is chosen appropriately. Moreover, L-CTM has the following properties: if a nonconcave flow-density relation is adopted, the model can also be applied for prediction of rather dense traffic in queues coasting toward the end of the queue (coasting effect); it can converge to the LWR model when the lattice spacing tends to zero; when the flow-density relation is triangular or trapezoidal and the optimal lag is used, the L-CTM has an accuracy of second-order; it is also more accurate than the CTM in terms of flow prediction. However, the L-CTM is affected by a strong disadvantage due to the fact that it can generate negative densities and densities higher than the maximum density. This aspect is to be considered a limitation of the model, because it can represent unrealistic traffic behaviors. Such problem is solved in [Szeto (2008)] both by enriching the model of two terms which produce values of density between zero and the jam density, and by keeping at the same time the most desirable features of the L-CTM. The model by Szeto is called Enhanced L-CTM (EL-CTM).

In [Muñoz et al., (2006)] the Switching-Mode Model (SMM) is proposed. The SMM is a hybrid system that on the bases of mainline boundary data values and the congestion cells status changes the sets of linear difference equations. In CTM the density is not linear while in SMM each definition of density is linear. To obtain linear densities the SMM reformulates each flow among cells making explicit the density of cells, but this can be obtained defining first, for each step, a set of logic rules to determine the congestion state of each cell considering the mainline boundary data. The application of the SMM permits to obtain additional information about highway traffic behavior, and to simplify the control analysis,

control design and data-estimation design methods. For example, the SMM can be applied to estimate the density in highway traffic context permitting to define the controllability and observability properties of the highway. Such properties are necessary to design of data estimators and ramp-metering control systems.

Gnomes and Horowitz have proposed an extension called asymmetric cell transmission model (ACTM, [Gomes and Horowitz (2006)]). The important difference between the models is in the treatment of traffic merges. In the ACTM two allocation parameters are used instead of one and the merges are limited to asymmetric connections where a minor branch feeds into a major branch (e.g. onramp-to-mainline junctions). In the figure 3.5, the demand for the onramp flow of the cell $i$ denoted by $d_i$ is reported. In the ACTM, $d_i$ considers the vehicles queuing in the onramp of the section that, together to the restrictions of maximum mainline space and ramp metering rate, limit the estimation of the onramp flow. The authors define sufficient conditions that permit to solve the optimal ramp metering problem by linear program. This has allowed to develop an efficient method for computing optimal ramp metering plans for congested freeways that allows to reduce delay.

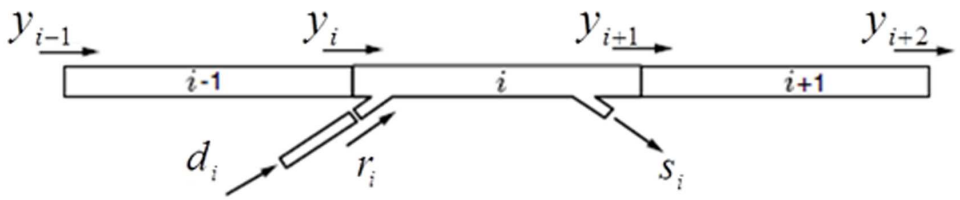


Figure 3.5: Section with on-ramp and off-ramp (see [Gomes and Horowitz (2006)]).

Some researchers have proposed traffic simulation models based on CTM. Freeway lane-changing has received increased scientific attention during the last

decade, but different issues are still raised about its impacts on traffic flow. When a vehicle changes lane it acts as a moving bottleneck on its destination lane and the resulting disruption can trigger other lane changes. To model this traffic flow behavior, the paper [Laval and Daganzo (2006)] proposed a hybrid implementation of the kinematic wave theory to account for lane-changing in traffic streams, thus improving CTM accuracy.

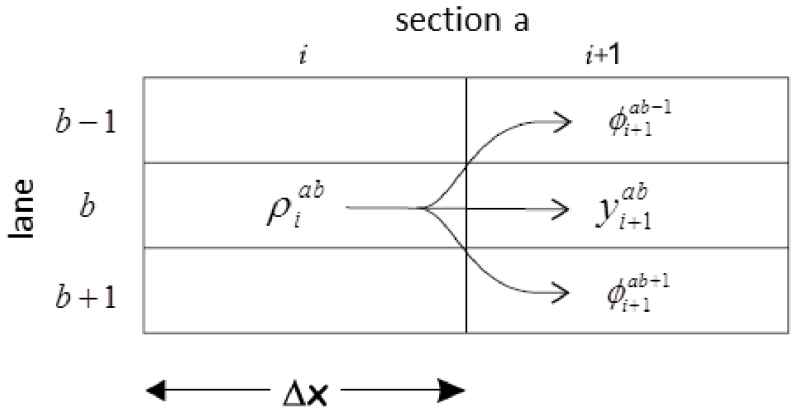


Figure 3.6: Freeway representation with multi-lane ( see [Laval and Daganzo (2006)]).

It employs a four-parameter multilane hybrid model. This model takes into account: the demand for lane-changing (from $b$ lane directed to lanes $b-1$ or $b+1$ in the Fig.3.6); desired through flows and available capacity for lanes. These traffic characteristics are obtained by the through flows (e.g., $y_{i+1}^{ab}$) and the one-directional lane-changing rates $\phi$ (i.e., the representation of the competition between drivers desires for changing lanes and the available space capacity in the target lane). The tests done on the model by Daganzo and Laval [Laval and Daganzo (2006)] show that it is able to capture the bounded accelerations of lane-changing vehicles. This model take into account of a demand for lane-changing (form $b$ to $b-1$ or $b+1$ lanes in the figure); a desired through flows for $b$ and available capacity on lane $b$. This parameters are used to define

the following variables represented in the Fig.3.6: through flows $y_{i+1}^{ab}$ and the one-directional lane-changing rates $\phi$ (representing the competition between drivers desires for changing lanes, and the available space capacity in the target lane). The tests done on the model by Daganzo and Laval [Laval and Daganzo (2006)] show it is able to capture the bounded accelerations of lane-changing vehicles.

The work presented in [Ziliaskopoulos and Lee (1997)] extended the CTM so that long homogeneous cells can be divided into small imaginary cells to maintain a constant simulation time step without increasing the number of cells. However, the presented model is affected by two problems: it may represent unrealistic propagation of traffic flow and under-utilization of road capacity; it is also limited by the fact that the length of imaginary cells has to be equal to that of the shortest cell in the network. These aspects are solved by the improvements introduced in [Ishak et al., (2006)]. The authors proposed different extensions to the original CTM formulation to account for variable cell length, non-integer movements between cells and more realistic representation of merging and diverging junctions. In this way, the authors extend the applicability of CTM for operational analysis of large-scale traffic networks.

In the last years the research has proposed other developments to realize a CTM useful in modeling and analyzing the urban traffic. The following paragraphs focus on the literature about the modeling of the propagation flow at the lane level for the multi-lane arterial and the urban traffic that crossing an intersection.

### 3.3.1 Relevant extensions of the CTM for Arterial

Differently from road sections with a single lane, the modeling of traffic that travels on multi-lane road is affected by various issues given by the lane-changing possibilities (it includes gap acceptance of vehicles and platooning effects) and in the drivers choice when one lane is preferred to another one. It is very important

to model the multi-lane arterial correctly because various aspects can strongly influence the dynamic and stochastic propagation of queues and delays in multilane signalized intersections, and upstream among lanes. To handle these problems, various studies (such as [Hoogendoorn (1996), Helbing (1996), Ngoduy (2006)] ) were concentrated on improving the accuracy of the analytic description using macroscopic formulations. Only some research works, especially on urban roads, have focused on the performance of signalized intersections with multiple lanes per stream, considering that the flow is equally distributed when approaching the intersection. On the contrary, the study of Akcelik affirms that a distinction should be made between strategic and tactical decisions [Rouphail (1989)]. It should be possible to pre-select routes for drivers on a route choice level, and at the same time give indications at intersections because this is where drivers are more sensitive to direct measures.

Liu proposes a macroscopic model of traffic to evaluate the traffic performance explicitly considering queue accumulation and dissipation at the lane-group level [Liu (2008), Liu et al., (2011)]. Through these important features, the model can capture complex phenomena that occur at signalized intersections, as queue formation, queue dissipation and blocking effects between different movements. Therefore, it can realistically represent the urban traffic dynamics upstream the intersection signalized. The test done on real cases, demonstrates the effectiveness and the accuracy of the model proposed. On the basis of such studies, it is possible to assert that the extensions of the CTM model have the potential to provide a good urban travel time prediction.

Thanks to the characteristics of macroscopic models, they are often applied to validated arterial signal optimization methods. The study by Lo ([Lo (1999), Lo (2001)]) was one of the first models to make use of CTM to capture the traffic dynamics for signal optimization models obtaining promising results. In the following years, Lo et al. in [Lo (2004)] extended this model to capture turning movements and to optimize the green splits without a constant cycle length, re-

spectively. As it has been already mentioned, the work of [Laval and Daganzo (2006)] models each lane as a separate stream interrupted by lane-changing particles that completely block traffic and the incremental-transfer principle for multilane problems ([Daganzo et al., (1997)]), coupled with a one-parameter model for lane-changing demand, is used to predict the flow transfers between neighboring lanes.

### 3.3.2 Relevant extensions of the CTM for Intersection

The macroscopic traffic simulation models are based on continuous macroscopic functions to describe traffic flow. These are only valid at a sufficiently large space in relation with the sampling period (time scale), such space exceeds the size of the most intersections.
In order to provide a correct model of traffic when crossing an intersection, it is necessary to prevent the mistakes of representing various movements that occupy the same physical space. In literature there are several methods to solve this issue. These models consider overlapping cells (the Semi-macroscopic simulation of urban traffic (SSMT) solution, [Lebacque (1984), Elloumi et al., (1994)] ), conditional cell (the CCTM [Wang (2010)]) or exchange zones ([Buisson (1996)]). Substantially, an exchange zone is similar to a cell but with a different modelling of the flow that crosses it.

In the figure 3.7 is represented a conditional cell 3 between the cell 1 and the cell 2. If cell 2 is empty or has available space the flow will go to cell 2 (crossing flow $y^{12}$). If cell 2 is full, the flow (represented as $y^{13}$) will go to the conditional cell causing a spillback queue at the intersection Afterwards to the dissipation of the queue, the vehicles that wait in the conditional cell go in the cell 2 ($y^{32}$).

In [Pohlmann and Friedrich (2010)], Pohlmann and Friedrich defined a new Adaptive Traffic Control Systems (ATCS) based on CTM. It can manage urban sub-networks with several interconnected signalized intersections. The algorithm proceeds, every 15 minutes, with the adaptation and optimization of signal plans

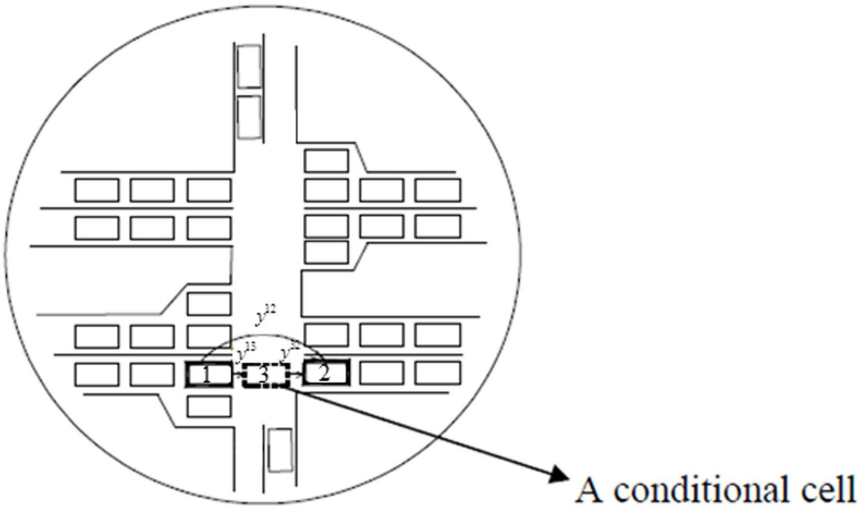


Figure 3.7: Representation of conditional cell (see [Wang (2010)]).

and coordination patterns to the currently estimated traffic demand in the network.

Despite the results obtained in literature, some critical issues remain to be solved. Most of them concern queue formation, queue dissipation and related effects of spillback upstream from link controlled by signalized intersection. These problems impact on the vehicular travel time estimated by the travel time prediction method. Usually, the urban travel time is split into the travel time spent for passing links and that for crossing the intersections. When a vehicle travels in the road network, its speed varies according to the interaction with other vehicles. This type of vehicular conflict provokes delay that significantly impacts on the total delay on urban networks. Furthermore, in the perception of travel costs, for most drivers, the waiting time at signals has a larger impact than running times.

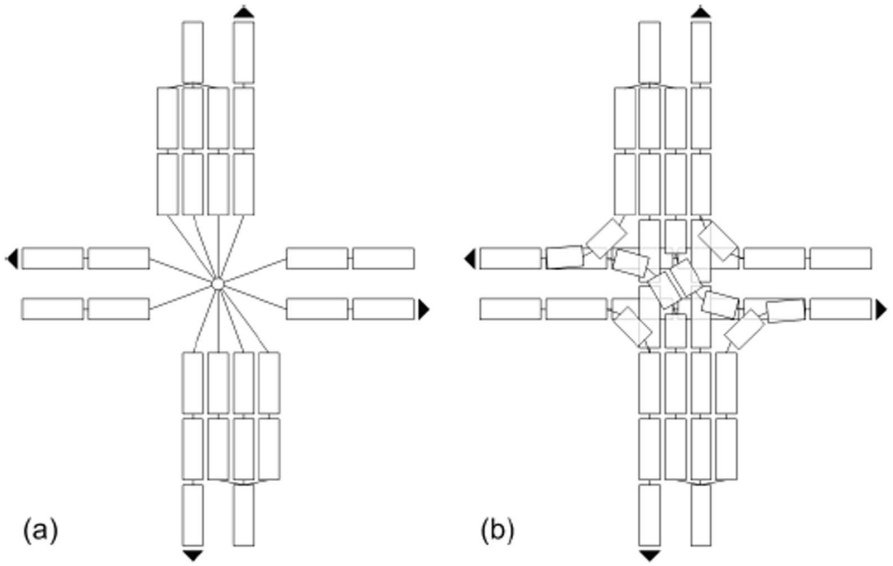


Figure 3.8: Modeling of intersections in the CTM:(a) a general n:n-connector is used whereas (b) all turnings are modeled explicitly (see [Pohlmann and Friedrich (2010)]).

## 3.4 Conclusions

The CTM is one of the most standard models for queuing phenomena observed at bottlenecks and for highway traffic modeling in general, encompasses most of the non linear phenomena observed on highways and the model is able to represent the following features:

- flow conservation;
- non-negativity;
- flow propagation;
- queues effect, as for example the spillback effect;
- the FIFO principle.

Initial studies about the validation of the CTM confirm that it is particularly suitable for planning and for operational analysis of traffic networks. However the

original version of CTM has a limited scope of applicability to realistic networks, because it does not appropriately support network facilities such as for example stopped controlled intersections, and does not consider stochastic variations of traffic. It is not suitable to make analytical operationalization that require high detail level. The original CTM is a non linear model and it presents the following limitations

- the speed of vehicles is a single-valued function of the density,
- the need of a priori definition of switching modes and the difficulty to define travel routes of drivers on the network,
- the representation of relatively short freeway sections due to the capturing of single-wave traffic behavior only,
- the not representation of the traffic behaviors at intersection,
- the cell size have to be constant,
- the not representation of lane-changing in traffic streams.

The different studies described in this chapter have extended the CTM to solve its original limitations. The literature about the CTM has demonstrated that the model is suitable to represent specific transportation facilities (e.g. signalized intersections, ramp metering systems, etc.) and it is suitable to transport applications such as

- travel time prediction,
- time signal optimization and ramp metering management,
- jam propagation and dissipation simulation,
- dynamic network design problem,
- dynamic traffic assignment problem,

- planning of disaster evacuation.

Despite the results obtained in literature, there are some critical issues to be solved to apply the CTM for urban traffic problem and on large-scale network. For example, in the work presented by [Ziliaskopoulos (2000)], the author uses the CTM to formulate the single destination system optimum dynamic traffic assignment problem as a linear program. Through numerical examples on simple networks, Ziliaskopoulos has demonstrated that the approach is both simple and applicable, except for large networks.

# Chapter 4

# Development of a CTM for Urban Traffic

## 4.1 Introduction

This chapter presents the steps of the research project made in order to develop a new framework of traffic modeling, based on CTM, named (CTM-UT). For the most important aspects of the CTM-UT, the major research contributions are highlighted. As previously described, the CTM-UT aims to mimic the accuracy of microscopic simulators in urban traffic environments keeping a good trade-off between accuracy and computational complexity respect to the microscopic model.

The traffic model defined in this thesis has the potential to simulate different traffic profiles but the results of this research are limited to one type of car. The CTM-UT is focused on signalized and unsignalized intersections, specific facilities like for example roundabouts are not taken into account.

## 4.2 Traffic flow modeling for an arterial

In the original model by Daganzo, the elements representing the street in the network are called cells. Thanks to the use of several types of connectors (ordinary, diverge and merge), it is possible to represent the advancement of traffic flow between two adjacent cells. While, the model in [Li (2011)] employs the connectors to divide the signalized roads section into four zones: merging, propagation, diverging, and departure zones. It allows to simulate the advancement of traffic flows at a signalized intersection. In addition, the author proposed a new enhanced diverging formulation that employs the subcell concept to represent each type of movement. The objective is that of capturing in a realistic way the queue and blockage effect among neighboring movements. As shown in the following figure, the diverging zone is presented with a diverging signalized cell (cell $i+1$), which can be further divided, on the basis of the channelization at a signalized approach, into the following three subzones: Zone 1 for left-turn traffic; Zone 2 for through traffic and Zone 3 with space shared by left-turn and through traffic. The total capacity of cell $i+1$ and link $a$ ($F^a_{i+1}$) can be divided, considering the zone 1, 2 and 3, as in the following example

$$F^{aL}_{i+1} = F^{aL}_{i+1,1} + F^{aL}_{i+1,3} \tag{4.1}$$

$$F^{aT}_{i+1} = F^{aT}_{i+1,2} + F^{aT}_{i+1,3} \tag{4.2}$$

$$F^{a}_{i+1} = F^{aL}_{i+1} + F^{aT}_{i+1} \tag{4.3}$$

In particular, the flow capacity of each subcell can be evaluated by its lane number and the lane-saturation flow rate. In the formula, the proportion of vehicles traveling from link to link is assumed as known. Another assumption is that the vehicles in the upstream cell of the diverging cell are well-mixed, namely the vehicles directed from cell $i$ to cell $i+1$ is given by the number vehicles of each

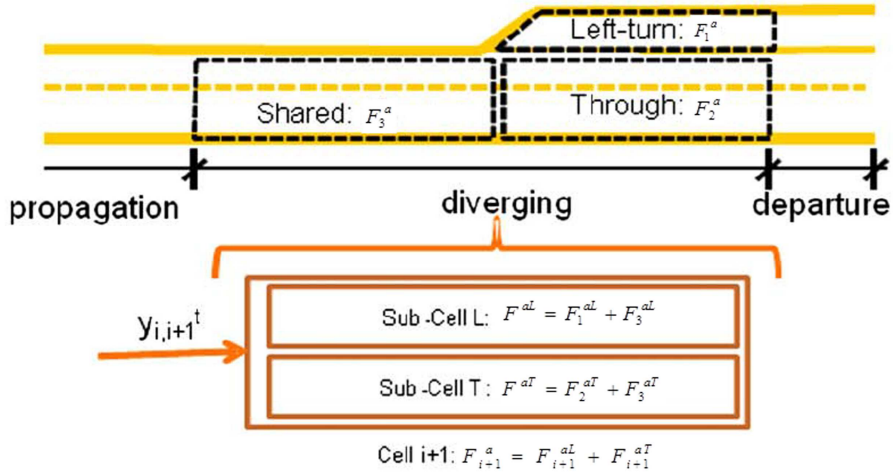


Figure 4.1: The subcell representation of diverging signalized cell (see [Li (2011)]).

movement specified by the turning ratio $\phi$. As previously described $y$ represents the flow in discrete time. The number of vehicles entering in the different cells (upstream and diverging cell) is given by the following formulation:

$$y_{i+1}^a = min \begin{cases} min\{n_i^a, Y_i^a\}, \\ \frac{w_{i+1}(\alpha^{aL} F_{i+1}^{aL} - n_{i+1}^{aL})}{v_{i+1}} \cdot \frac{1}{\phi_{i+1}^{aL}}, \\ \frac{w_{i+1}(\alpha^{aT} F_{i+1}^{aT} - n_{i+1}^{aT})}{v_{i+1}} \cdot \frac{1}{\phi_{i+1}^{aT}} \end{cases} \tag{4.4}$$

$$y_{i+1}^{aL} = y_{i+1}^a \cdot \phi_{i+1}^{aL} \tag{4.5}$$

$$y_{i+1}^{aT} = y_{i+1}^a \cdot \phi_{i+1}^{aT} \tag{4.6}$$

The proposed extension of CTM has been tested on a real environment, composed of segments of four congested intersections. As in other studies, to the new model a GA-based solution method is applied. It's employed to optimize signal timings, and it has demonstrated that it is possible to obtain a nearly optimal

signal-timing plan. The experiments compared with signal-timing plans from TRANSYT-7F, indicate that the presented model can better predict the realism both of the total delay and the resulting throughput.
In conclusion, the results of the study indicates that the presented model, with its new set of formulas for the subcell, can realistically model lane-blockage among neighboring lane groups due to queue spillback under oversaturated conditions.

### 4.2.1 A new model to capture complex flow interactions among lane groups for signalized intersections

The CMT-UT model, has the potential to accommodate the typical dynamic of flows and road conditions in urban contexts. Despite the results obtained in literature, most dynamic queue models do not integrate the multiple signal phases. In second place, the spillback phenomena has not been explicitly modeled during congested conditions. For this reason, the paper [Adacher et al., (2014)] focuses on the representation of traffic movements and signal phases. Specifically, it models capacity reduction due to flow conflicts, queue spillback effects and overflow for lane.
In the study by [Adacher et al., (2014)], the process of traffic flow propagation along the arterial link and the network road is described by three sets of formulas: propagation into network, propagation into link and flow conservation. As shown in the following figure, let $N$ the total number of cells of link and $I$ the number of cells belong to merging zone, the arterial is divided in two zones: an upstream merging zone ($1 \leq i \leq N - I + 1$) where the turning movements are mixed and a downstream queue storage zone ($N - I + 1 < i \leq N$) where vehicles are split into specific dedicated lanes, one for each different turning movements. If the vehicles choose a lane to access in the channelized zone, they cannot change their lane. The queue from channelized zone, on the bases of its length, could spill back until to merging zone and, therefore, blocks the mixed traffic. In the CTM-

UT the traffic flow is more disaggregated in relation both of its position in the network and, especially, of the kind of traffic dynamic that requires accuracy to mimic microscopic traffic components. The representation of flow is aggregated in the merging zone ($y_i^a$), because the model considers the total flow that crosses the cell, while the representation of flow is disaggregated for lanes $b$ ($y_i^{ab}$) in channelized zone.

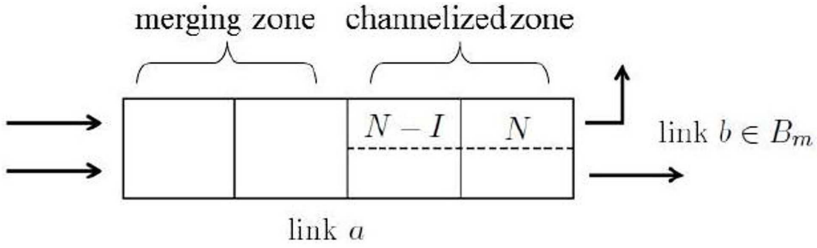


Figure 4.2: The traffic zone of link (see [Adacher et al., (2014)]).

If $i = N - I + 1$, max *flow of downstream channelized zone* is defined as

$$\widetilde{y}^{ab} = min \begin{cases} \phi^{ab}\ n^a_{N-I}\ , \\ \alpha^{ab}\ Y^a_{N-I+1}\ , \\ \frac{w\ (\alpha^{ab}\ F^a_{N-I+1} - n^{ab}_{N-I+1})}{v} \end{cases} \tag{4.7}$$

Due to the conflict between turning vehicles and ahead vehicles, the total flow incoming in the channelized zone can be calculated by

$$y^a_{N-I+1} = \min_{b \in B_m} \left\{ \frac{\widetilde{y}^{ab}}{\alpha^{ab}} \right\} \tag{4.8}$$

The inflow is calculated on the bases of previous equation, resulting in

$$y^{ab}_{N-I+1} = \phi_{ab}\ y^a_{N-I+1} \tag{4.9}$$

### 4.2.2 Cases study and Experiments

#### CTM-UT vs Long Model

To access the channelized zone, the vehicles directed to different turns may ob-

struct each other. For this reason, in oversaturated conditions, their behavior could block different movements. The following equation shows, for an hypothetical two lane link for which it is possible to go through (T) or turn on left (L) at intersection, how to represent the behavior of the incoming flow in the lane dedicated to the left-turn in case it is obstructed by through flow. In such a case, in the model proposed in [Long et al. (2011)], the queue of a spilling back turning movement, exceeding the length of its lane (of the channelized zone), strongly affects the neighboring lane, even if in free flow condition: the inflow value of the neighboring lane is largely reduced. The CTM-UT proposes a realistic model of turning movements considering the vehicular conflicts in channelized zone, its formulation is based on the inflow of the blocking movement: specifically, this conflict is assumed to be proportional to the difference of the values of blocking inflow when passing from the merging zone to the channelized one.

$$y_3^{aL} = min \begin{cases} \widetilde{y}_3^{aL} \cdot \left[1 - \left(\frac{y_2^{aT} - y_3^{aT}}{y_2^{aT}}\right) \cdot \left(1 - \phi^{aL}\right)\left(1 - \alpha^{aL}\right)\right], \\ \phi^{aL}\, n_2^a \quad , \quad \alpha^{aL}\, Y_3^a \end{cases} \tag{4.10}$$

It considers the maximum flow and substitutes (4.37) and (4.38), obviously, the constrains on capacity and supply must be satisfied.

Comparison between the CTM-UT and the Long model ([Long et al. (2011)]) has been conducted on a link with four cells and two lanes, where the through queue spills back and, therefore, reduces the left-turn traffic. The values of main variables have been set as follows:

- $F_3^a = 20$ , $y_2^{aT} = 2.44$ , $n_2^a = 6.64$ , $n_3^{aT} = 5.58$ , $n_3^{aL} = 1.87$ $[vp\Delta t]$;
- $v = 33.56$ , $w = 11.29$ $[mph]$;
- $\phi^{aL} = \phi^{aT} = 0.5$ , $\alpha^{aL} = \alpha^{aT} = 0.5$;

$\phi^{aL}$ and $n_2^a$ assume ranging values in the Fig.4.3.

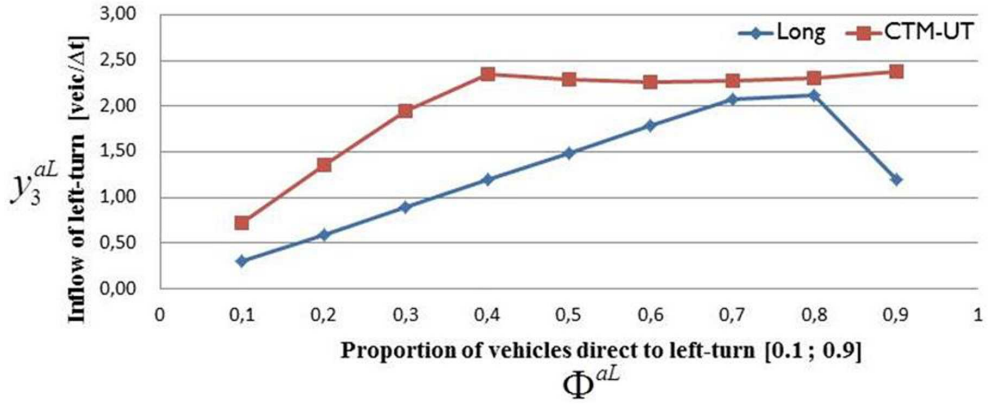


Figure 4.3: CTM-UT vs Long: left turn inflow entering the channelized zone for different proportions of left turn demand

The tests results show that the Long model underestimates the left turn inflow penalizing it with compared to the capacity of the turning lane.
The Fig.4.3 shows that when proportion of demand ranges between 0.8 and 0.9, the Long formulation decreases the inflow value. In the interval up to $\phi^{aL} = 0.4$, the value of $y_3^{aL}$ given by CMT-UT stabilizes around its maximum value irrespective of any additional increase of $\phi^{aL}$ . Also the results of Fig.4.4 confirms previous assertions.

**CTM-UT vs Microscopic Simulator (VISSIM)**

To validate the proposed model two different traffic scenarios, representing various levels of downstream congestion within a signal controlled intersection, have been simulated. A comparison between CTM-UT and VISSIM, one of the most important microscopic traffic flow simulation software, is done.
The following experiments are focused on the analyze the accuracy of travel time prediction obtained by CTM-UT. Namely, we have tested if the simulation of our macroscopic model is comparable with the microscopic one.
In this case study, CTM-UT and VISSIM are configured to simulate one approach in a hypothetical three-way signal controlled intersection. The approach is $0,1863$

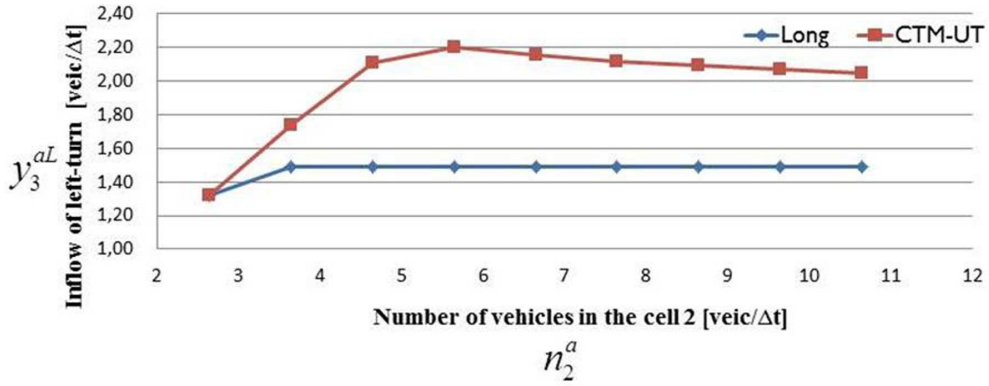


Figure 4.4: CTM-UT vs Long: left turn inflow entering the channelized zone for different number of vehicles (supply traffic)

miles (300 meter) in length and has two lanes. A signal is placed to control the movements: left-turn and through movements. Different movements through this intersection are tested, and two signal phase combinations are defined (4.1).

| Scenario | T Signal Phase | L Signal Phase |
|---|---|---|
| 1 | Green: 30 Red: 30 [*sec*] | Permanent Green |
| 2 | Green: 30 Red: 30 [*sec*] | Green: 5 Red: 25 [*sec*] |

Table 4.1: Signal phases for a signal controlled intersection

The simulation longs 18 minutes. Five travel demand levels have been simulated, 1000, 2000, 2500, 3000, 3600 vehicles/hour respectively. The cell capacity and demand are split over the two lanes fifty-fifty. The flow capacities for links is 3600 and for lanes 1800 vehicles/hour respectively.
A typical application of traffic simulation models estimates total system travel time. It can be expressed as follows:

$$TT(k) = \sum_{links \in A} \sum_{i=1}^{N} \frac{\Delta x_i}{V_i^a(k)} \tag{4.11}$$

The mean travel time is calculated:

$$MTT = \frac{\sum_{k=1}^{tot\ step} TT(k)}{tot\ step} \tag{4.12}$$

where *tot step* is the final value of index $k$ at the end of simulation, so the model capacity to predict the average travel time through a signal controlled intersection has been tested.

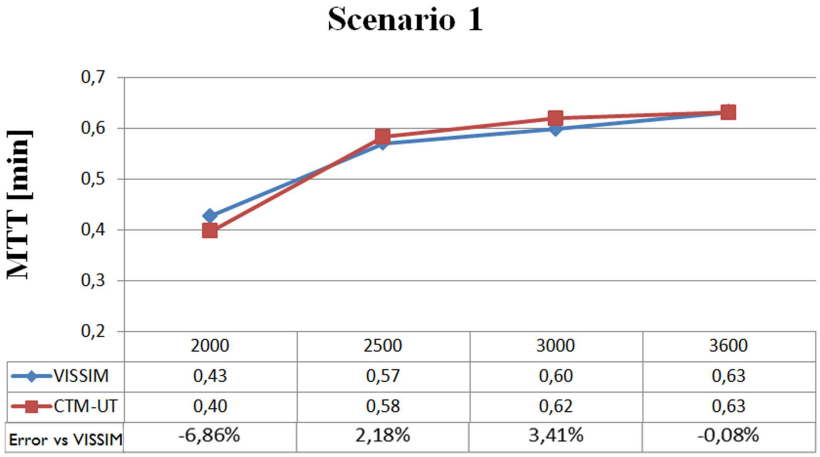


| | 2000 | 2500 | 3000 | 3600 |
|---|---|---|---|---|
| VISSIM | 0,43 | 0,57 | 0,60 | 0,63 |
| CTM-UT | 0,40 | 0,58 | 0,62 | 0,63 |
| Error vs VISSIM | -6,86% | 2,18% | 3,41% | -0,08% |

Figure 4.5: Scenario 1 - Mean Travel Time Prediction and CTM-UT error vs Vissim.

In the first scenario, the simulation shows that CTM-UT underestimated mean travel time when the flow demand is low compared to arterial capacity (see Fig.4.5 and 4.6). While, when the travel demand and the relative congestion level increased the results between software approaching.

In the second scenario, the arterial upstream of signal is under congestion conditions. In particular, the signal phase decreases the capacity of outflow for left-turn of the 75% respective to previous scenario. The results of Scenario 2 indicate that CTM-UT is more consistent in predicting travel time when left-turn is congested causing a movement blockages and queue in the intersection. Under medium and high traffic flows CTM-UT overestimates mean travel time around 4%.

As demonstrated through the results the proposed model have a good capacity to

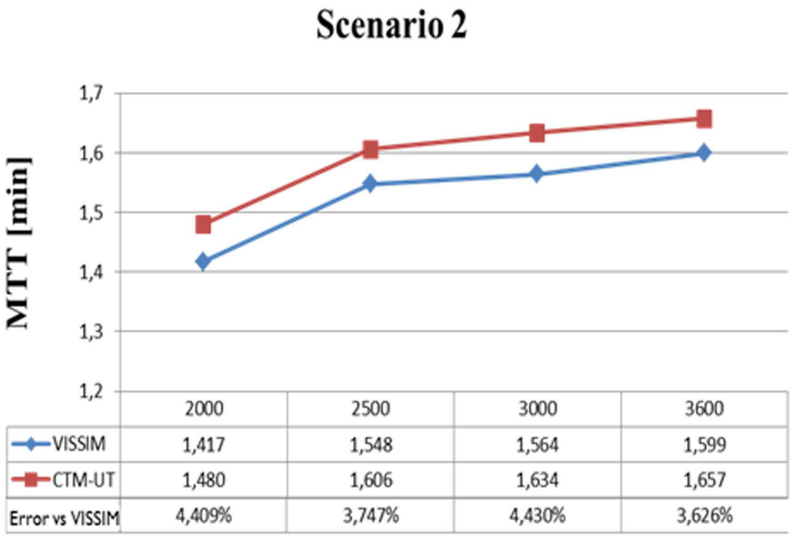


| | 2000 | 2500 | 3000 | 3600 |
|---|---|---|---|---|
| VISSIM | 1,417 | 1,548 | 1,564 | 1,599 |
| CTM-UT | 1,480 | 1,606 | 1,634 | 1,657 |
| Error vs VISSIM | 4,409% | 3,747% | 4,430% | 3,626% |

Figure 4.6: Scenario 2 - Mean Travel Time Prediction and CTM-UT error vs Vissim.

simulate oversaturated traffic conditions. On the base of test cases, the CTM-UT produces acceptable travel time prediction for medium and high congestion conditions and reproduces VISSIM simulation results with consistency. The relative errors of all simulation results are about 2%. The proposed model well simulates the lane blocking effects and shared lanes.

### 4.2.3 Conclusions

On the basis of a compared analysis of CTM-UT and VISSIM, it has been demonstrated that the proposed new model has a remarkable capacity to simulate oversaturated traffic conditions.

The traditional traffic model is extended to take into account some real aspects of traffic conditions, such as the proportion of turning and lane width, both used for different turning movement.

This paragraph describes the queue and blockage effect among neighboring movements in the approach lane of arterial upstream in the intersection. The CTM-UT

is suitable to represent this kind of approach defining the correct number of lane, and relative capacity, at the last cell of channelized zone. In particular, the CTM-UT is suitable for the representation of the flow conflicts to access in the approach lane. Such conflict modeling is based on the measure of queue spillback effects for lane.

## 4.3 Traffic flow modeling at intersection

The urban traffic is strongly conditioned by signalized intersections. For this reason, the intersection modeling is fundamental for a correct and complete representation of traffic on the road network. This representation is very difficult for the macroscopic modeling because an intersection is affected by other types of problems, also related to individual vehicles, compared to the arterial representation.

The intersection modeling is hard problem, the paper [Lebacque and Khoshyaran (2002)] has proposed three different modeling approaches: extended versus pointwise intersection models, and flow maximization. In his work, Lebacque explains that in order to extend the LWR model, so that it is suitable for networks and dynamic assignment problems, it is fundamental to consider the following aspects of traffic modeling: defining proper boundary conditions for links, modeling intersections with particular attention to their relationship with link boundary conditions, taking into account the partial densities and flows for the link and intersection models. To achieve these objectives, Lebacque proposed the following formulation. The equilibrium supply ($\Sigma_e$) and demand ($\Delta_e$) functions are defined as:

$$\Sigma_e(\rho, x) = \begin{cases} f_{max}(x^+) & if \quad 0 \leq \rho \leq \rho^c(x^+) \\ f_e(x^-) & if \quad \rho^c(x^-) \leq \rho \leq \bar{\rho}(x^+) \end{cases} \tag{4.13}$$

and

$$\Delta_e(\rho, x) = \begin{cases} f_e(x^+) & if \quad 0 \leq \rho \leq \rho^c(x^-) \\ f_{max}(x^-) & if \quad \rho^c(x^-) \leq \rho \leq \bar{\rho}(x^+) \end{cases} \tag{4.14}$$

where $f_{max}$ is the total aggregate flow for zone in free condition and $f_e$ is the total aggregate flow for zone when the density exceeds the critical density $\rho^c$ (the symbols + and - representing right- and left-hand limits).

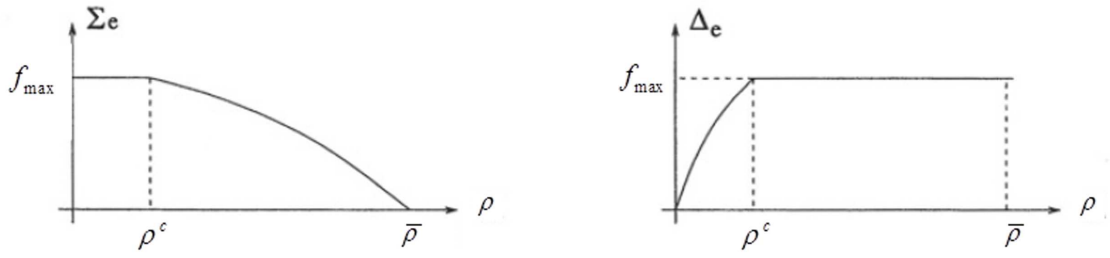


Figure 4.7: Equilibrium supply and demand functions (see [Lebacque and Khoshyaran (2002)]).

The greatest possible inflow and outflow at point $x$ is represented respectively by the local supply and demand as:

$$\begin{cases} \Sigma(x,t) = \Sigma_e(\rho(x^+,t),x) \\ \Delta(x,t) = \Delta_e(\rho(x^-,t),x) \end{cases} \tag{4.15}$$

It can be used to calculate the flow satisfying the natural condition:

$$f(x,t) = min\ \{\Sigma(x,t), \Delta(x,t)\} \tag{4.16}$$

Supply and demand are fundamental to describe discontinuities. The previous equation is suitable for the circumstance that it is valid at all discontinuity points, whether related to density (shockwaves), or to the equilibrium flow-density function $f_e$ (boundary conditions, incidents, intersections). This characteristic is the

most important, because a good intersection model should be suitable to estimate adequate supply and demand values to the upstream links and to links downstream of the intersection, respectively. An alternative to the SSMT solution, to representation of various movements that may occupy the same space at intersection, is the definition of the exchange zones. They are similar to the cells, but an exchange zone allows to define various movements in relation to multiple entry and exit points. To represent interaction among movements in the intersection model by [Lebacque and Khoshyaran (2002)], the following dynamic variables were introduced:

- $n_{in,out}(t)$ the number of vehicles having entered the zone through entry point $in$, exiting it through exit point $out$ ;
- $ni_{in}(t)$ the number of vehicles having entered the zone through entry point $in$ ;
- $no_{out}(t)$ the number of vehicles about to exit the zone through exit point $out$
- $n(t)$ the total number of vehicles of the zone.

The global zone supply and demand equilibrium functions describe the mixing of movement flows in the zone. These functions are similar to link equilibrium functions, but their argument is the total number of vehicles of the zone instead of density of the cell ( $\Sigma_e(n, z)$ and $\Delta_e(n, z)$ for a zone $z$). Therefore, the global zone supply and demand are calculated according to the following equation:

$$\begin{aligned} \Sigma(x,t) &= \Sigma_e(n(t), z) \\ \Delta(x,t) &= \Delta_e(n(t), z) \end{aligned} \tag{4.17}$$

As represented in the figure 4.8, the inflows to the exchange zone are obtained by comparing the zone partial supplies $\Sigma_{in}(t)$ and demands $\Delta_{out}(t)$ to the

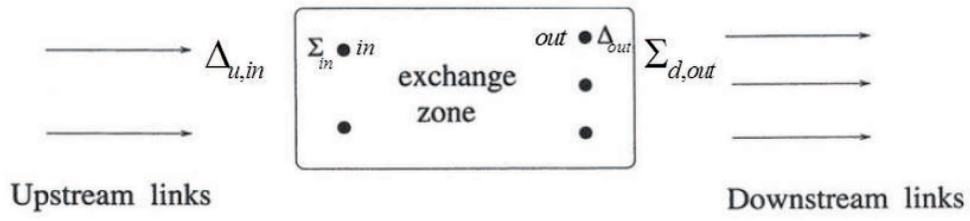


Figure 4.8: Exchange zone [Lebacque and Khoshyaran (2002)].

upstream link demands $\Delta_{u,in}$ and downstream supplies $\Sigma_{d,out}$ in the usual way. In the figure 4.8, the points in the exchange zone represent the entry (on the left) and the exit point (on the right). The major difficulty caused by the model is that of estimating correctly the behavioral component, which is represented by the zone partial supplies and demands from the available zone variables. The partial demand can be calculated, for example, by the following FIFO-like model:

$$\Delta_{out}(t) = \frac{no_{out}(t)}{n(t)} \cdot \Delta(t) \tag{4.18}$$

While, the partial supplies play an important role because the driver's behavior depends on them. There are various models to define the partial supplies. Lebacque has proposed three examples, based on the so-called supply-split coefficients $\beta_{in}$, equal for example to the relative number of lanes available in the zone for traffic entering through entry point $in$. Linear model:

$$\Sigma_{in}(t) = \beta_{in}\Sigma(t) \tag{4.19}$$

Homogeneous zone model:

$$\Sigma_{in}(t) = \beta_{in}\Sigma_e\left(\frac{ni_{in}(t)}{\beta_{in}}\ ,\ z\right) \tag{4.20}$$

Partial supply proportional to residual storage capacity:

$$\Sigma_{in}(t) = \frac{\beta_{in}n_{max}(z) - ni_{in}(t)}{n_{max}(z) - n(t)} \cdot \Sigma(t) \tag{4.21}$$

For very simple intersections, like for example merges and diverges, a simple zone is sufficient, while for complex intersections several zones may be necessary. The partial supply and demand models above-reported are based on global zone supply and demand, which capture the global behavior of the zone. Finally, Lebacque concludes that it does not exist a unique solution for intersection modeling, because it heavily depends on the drivers' behavior. This can vary widely, depending on type and complexity of the intersection, which determines the interaction among upstream demand and downstream supply. Despite the several proposals in literature for the split-supply and split-demand intersection models, the study of an analytical solutions is yet to be pursued. The simulation model based on the hydromechanical theory, allows to give an excellent representation of the freeway flows with the kinematic wave. But, such features are not suitable for urban traffic scenarios, which present dynamic flows in complex interactions. For this reason, the objective of the paper [Flötteröd and Rohde (2011)] is to define a simulation model that models the urban traffic with the kinematic wave model on the type of intersections existing in urban environment. They have proposed a new method to the macroscopic first order modeling and simulation of traffic flow in complex urban intersections. This approach is based on the generic class of node model presented in [Tampere et al., (2011)]. The purpose of the authors is to formulate an incremental node model for general road intersections and to adequately represent the flow conflicts. The classical equation for flow conservation is fundamental for the traffic flow theory, it puts in relation traffic demand and supply.

By defining the position with $x_i$, the local flow $f(x_i, t)$ is then defined as the minimum of local flow demand $\Delta(\rho(x_{i-1}, t), x_{i-1})$ and local flow supply as

$\Sigma(\rho(x_{i+1}, t), x_{i+1})$ :

$$f(x_i, t) = min \begin{cases} \Delta(\rho(x_{i-1}, t)\ ,\ x_{i-1})\ \ , \\ \Sigma(\rho(x_{i+1}, t)\ ,\ x_{i+1}) \end{cases} \tag{4.22}$$

This function, illustrated in the following figure, takes into account the case of traffic flow bounded by the flow capacity and by flow demand in the position $x$ and time $t$.

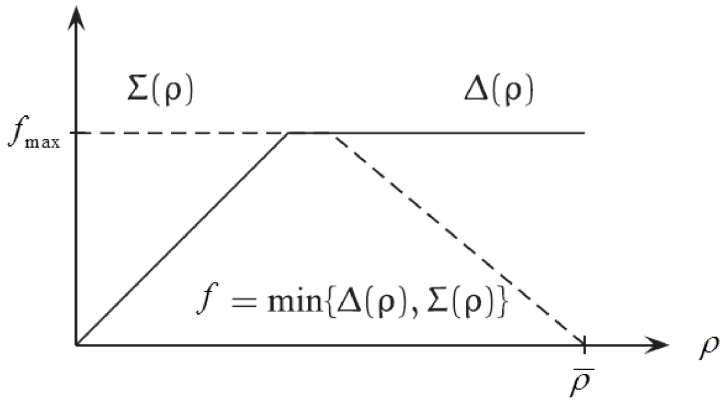


Figure 4.9: The demand function $\Delta(\rho)$ (solid) consists of an increasing part with its slope equal to the free flow speed and is limited by the flow capacity $F$. The supply function $\sum(\rho)$ (dashed) is also limited by the flow capacity. The slope of its declining part equals the backward wave speed and intersects the abscissa at the greatest possible density [Flötteröd and Rohde (2011)].

The macroscopic node model is applied to maximize the constrained flow. Such kind of model, enjoying the benefits of the solutions provided by kinematic wave models, can select physically relevant solutions making the phenomenological modeling easier through the constraints. Flötteröd has developed a generic node model that, in comparison with model of Tampere, has a simpler objective function and more detailed constraints. It is possible to define that a node model

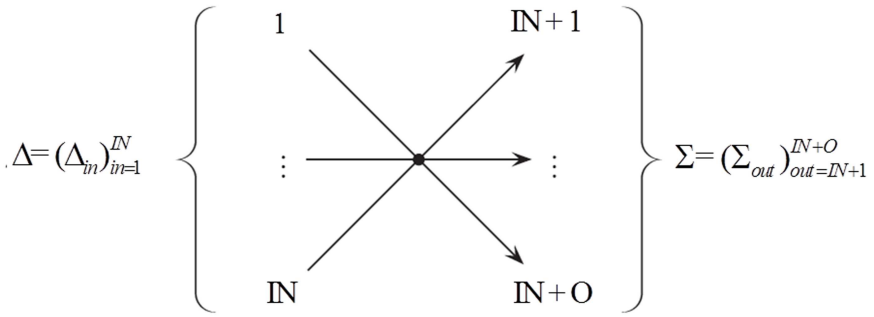


Figure 4.10: General intersection with $IN$going and $O$utgoing links [Flötteröd and Rohde (2011)].

belongs to such class of model if it solves the following:

$$\begin{aligned} \max_{\mathbf{f}^{in}} \quad & \textstyle\sum_{in=1}^{IN} f^{in} \\ \text{s.t.} \quad & \mathbf{f} \geq 0 \\ & \mathbf{f}^{out} = \mathbf{B} f^{out} \\ & \mathbf{f}^{in} \leq \boldsymbol{\Delta} \\ & \mathbf{f}^{out} \leq \textstyle\sum \\ & \mathbf{f} \text{ satisfies the invariance principle} \\ & \mathbf{f} \text{ satisfies a supply constraint interaction rule} \\ \text{optional :} \quad & \mathbf{f} \text{ satisfies node supply constraints} \end{aligned} \tag{4.23}$$

where the vector $\mathbf{f}^{in} = (f^{in})$ collects the $IN$ node inflows from upstream, the vector $\mathbf{f}^{out} = (f^{out})$ collects the $O$ node outflows towards downstream and $\mathbf{B} = (B^{in,out})$ are vectors of upstream demands and downstream supplies. As far as it concerns the node, its space dimension and traffic dynamics are not taken into consideration. In particular the invariance principle intrinsically represents both the link flow constrained from downstream and the link flow constrained from upstream. As far as it concerns the first link, the increase of the queue size on a congested upstream link has no effect on the node flows. While, the second one, has shown that making more space available on an not congested downstream link does not change the node flows. If an instance of the Incremental

Node Model (INM) is defined as a function the general node model (GNM) (4.23) can be formulated as an incremental node model. Through the piecewise constant transfers, it is possible represent the incremental transfers with a finite sum instead that with a integration of the differential equation. Such simplification allows to gain a great computational advantage in the searching of inflows and respecting the constraints GNM constraints. In [Flötteröd and Rohde (2011)] an incremental node model is presented. It maintains the intuitive aspect and the computational advantage of the incremental transfer principle. The incremental transfer principle by Daganzo was generalized in order to have varying flow transfer rates during the transmission and, at same time, it is consistent with the generic node model [Cayford et al., (2011)].

**Capacity determination based on gap acceptance**

The technique named as gap acceptance requires that in the unsignalized intersection controlled by signal stop (minor road) and yield (major road) a traveling vehicle in the minor road, that wants to enter the intersection, should wait for a safe opportunity (gap acceptance) between two vehicles of a principal road to occur. The procedure to define the vehicle movement at unsignalized intersection, presents in Highway Capacity Manual ([HCM (2010)]), requires the identification of conflicting flow rate for a movement that is, the total flow rate that conflicts with movement. Then the calculation of the capacity determination based on gap acceptance for a movement is based on the values of conflicting flow rate, critical gap times $t_c$, follow-up times $t_f$ and potential capacity. The critical gap time is defined as "*the minimum time interval in the major-street traffic stream that allows intersection entry for one minor-street vehicle*". The follow-up time is defined as "*the time between the departure of one vehicle from the minor street and the departure of the next vehicle using the same major-street gap*". In the gap acceptance procedure is present the compute of values of $t_c$ and $t_f$ . These can be calibrated against measured data or chosen by HCM and following tuned

depending of the traffic simulation or measured data.

The paper [Troutbeck and Kako (1999)] presents a gap acceptance model based on limited priority for the major stream. It models the traffic on unsignalized intersections under congested conditions. The case of study in [Troutbeck and Kako (1999)] shows that for congested traffic condition, is not appropriate to define a distribution of the available downstream supply (over the incoming links) based only on priority rules.

[Flötteröd and Rohde (2011)] also present an algorithm to maximize the local flow considering the incremental node model with constraints. For the initial run the demand constraints are not considered and the flow is done. If a capacity of minor flow $\Delta$ is reduced the new values of flow is eventually reduced according to the demand constraint function $\hat{\Delta}(f)$. The new value is defined with $\hat{\Delta} = min\left\{\Delta, \hat{\Delta}(f)\right\}$. The algorithm terminates when all constraints are satisfied for all inflow and outflow at the node. This model has the potential to employ different kinds of demand constraints function.

$$\hat{\Delta}(f_p) = \frac{1}{t_f} e^{\left(-f_p\left(t_c \frac{t_f}{2}\right)\right)} \tag{4.24}$$

where $f_p$ is the traffic flow of opposing direction, $t_c$ is critical gap times and $t_f$ is the follow-up times.

In conclusion, the incremental node model is extended with concrete node supply constraints to capture complex flow interactions inside the node through an additional fixed-point condition. In this way, has been obtained a good combination of the computational efficiency of the incremental node model and considerably increased modeling capabilities. The experiments, compared with AIMSUN, indicate that the macroscopic model well captures the microscopic traffic phenomena. However, the results show some differences for a particular outflow, because macroscopic models do not capture platoon dispersion. Therefore, it isn't a representation error but rather an inherent feature of all first order models. The author concludes that the macroscopic node model is perfectly able to capture

the flows in a complex urban intersection.

[Brilon and Wu (2001)] present an approach to the determination of capacities at unsignalized intersections based on the additive conflict flow (ACF) method (originate from conflict theory). The method can be used to define node supply constraints, for conflict point of crossing flows or merging flows.
Another kind of capacity determination, object of comparison in the next paragraph (see 4.14), is that used in paper of [Wu (1999)], where the maximal traffic flow of the minor stream is determinate as:

$$\hat{\Delta}(f_p) = \frac{f_p}{e^{\left(f_p \cdot \left(t_c - t_f\right)\right)} \cdot e^{\left(\left(t_f \cdot f_p\right) - 1\right)}} \tag{4.25}$$

### 4.3.1 A new node model based with capacity determination

In order to define a general node approach that takes into account different aspects about conflicts at intersections, has been extended the previous work based on CTM-UT framework by [Adacher et al., (2014)]. Such node model is suitable to represent traffic flows that crosses signalized and unsignalized intersections. Moreover, a new model is suitable to compute the minor streams that are limited by major stream on unsignalized intersections is presented. This model, presented in [Adacher and Tiriolo (2015a)], reduces the problems and the complexities of the capacity determination (based on gap acceptance) and it could be used for dynamic traffic assignment.
In particular, the new node model can represent: the connection of the demand upstream intersections to the supplies downstream intersection; the demand percentages of turns for every single lane; complex signalized and unsignalized inter-

section; merging flows or conflict among crossing flows. The Fig. 4.11 shows an overview of the CTM-UT's formulation. In this example are represented two arterial links upstream intersection ($a$), two arterial links downstream intersection ($c$) and all links have four cells ($i$) and two lanes ($b$).

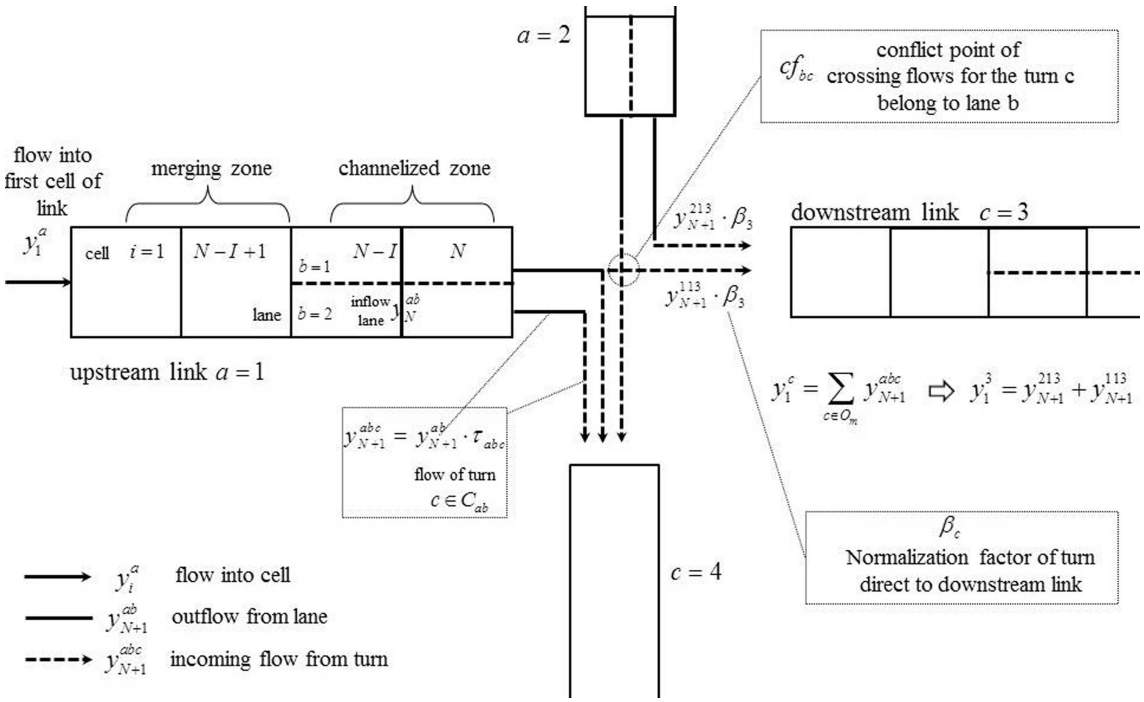


Figure 4.11: Variables of CTM-UT, example of representation of a node model

### Propagation into intersection

The following formulation defines the inflow and outflow for every intersection $m$. The model considers the total movements active in period $k$ and the turns associated with the red phases at the signalized intersection are excludes. The node model allows to maximize the incoming flows $y_{N+1}^{abc}$ at intersection, considering turning fractions $\tau_{abc}$, subject to supply constraints of the outgoing links. The model represents the flow from incoming links at intersection proportional

to the vehicle demand of the movements ($\tau_{abc}$), and the incoming links can be distributed by fractions ($\beta_c$) proportional to the capacities of the outgoing links. The normalization factor of merging flows for the downstream link $c$ is initiated by $\beta_c = 1$. $y^a_{N+1}$ represents the total outflow by link and $y^{abc}_{N+1}$ is the flow of the incoming link at intersection, which is divided over the outgoing links according to proportion of vehicle demand turning $\tau_{abc}$. For each turns from the lane $b$ belong to cell $N+1$ of link $a$, is possible calculate the incoming flow at intersection (demand) direct to downstream link $c$ in relation to its supply by:

$$y^{abc}_{N+1}(k) = \beta_c \cdot \ min \begin{cases} \tau_{abc}\ n^{ab}_N(k) & , \alpha^{ab}\ Y^a_N(k) \\ Y^a_1(k) & , \frac{w^c_1(F^c_1(k) - n^c_1(k))}{v^c_1} \end{cases} , \tag{4.26}$$

The sum of flows by incoming link at intersection $y^{abc}_{N+1}$ direct to the outgoing link $c$ must respect the supply constraints of the first cell of downstream link $c$. This supply constraint is represented by :

$$\sum_{c \in C_a} y^{abc}_{N+1}(k) > min \left\{ Y^c_1(k)\ , \frac{w^c_1(F^c_1(k) - n^c_1(k))}{v^c_1} \right\} \tag{4.27}$$

If the supply constraint is not respected, the normalization factor $\beta_c$ is computed as the capacity of first cell of outgoing link divided the total flow demand direct to the outgoing link.

$$\beta_c = \frac{min \left\{ Y^c_1(k)\ , \frac{w^c_1(F^c_1(k) - n^c_1(k))}{v^c_1} \right\}}{\sum_{c \in C_a} y^{abc}_{N+1}(k)} \tag{4.28}$$

If the demand by incoming links exceeds the supply of the outgoing link $c$ (when $\beta_c < 1$), a queue will be formed on at least one of the incoming links $a$. If the supply constraint is respected, is possible compute the total outflow by lane $b$ of link $a$ as the sum of $y^{abc}_{N+1}$ by incoming links belong to the same lane $c \in C_a$ as

$$y^{ab}_{N+1}(k) = \sum_{c \in C_a} y^{abc}_{N+1}(k) \tag{4.29}$$

, the total outflow by link $a$ as the sum of the lanes $b$ of link $a$

$$y_{N+1}^{a}(k) = \sum_{b \in B_a} y_{N+1}^{ab}(k) \tag{4.30}$$

The total inflow $c \in O_m$ in the first cell of the movement directs to downstream link $c$ as:

$$y_{1}^{c}(k) = \sum_{c \in O_m} y_{N+1}^{abc}(k) \tag{4.31}$$

All the upstream and downstream flows of the links at intersection can be calculated. The model is suitable to employ other constraints for the supply or demand.

**Propagation into network from and direct to fictitious node**

If outflow from $a$ leaves the road network by fictitious node (with infinity capacity), the equation (4.26) to calculate the outflow for turn is rewrite as:

$$y_{N+1}^{abf}(k) = min\left\{\tau_{abf}\ n_{N}^{ab}(k)\ , \alpha^{ab}\ Y_{N}^{a}(k)\ , \infty\ , \infty\right\} \tag{4.32}$$

where, in this case, the movement from link $a$ is direct to a fictitious node $f$ and $\tau_{abf}$ is the turning fractions of movements outflow the network.

The incoming flow in a upstream link connected with a fiction node coincides with the flow demand for the network. The inflow into the network from a fiction node direct to $a$ is compute as:

$$y_{1}^{a}(k) = min\left\{n^{f,a}(k)\ , Y_{1}^{a}(k)\ , \frac{w_{1}^{c}(F_{1}^{c}(k) - n_{1}^{c}(k))}{v_{1}^{c}}\right\} \tag{4.33}$$

where $n^{f,a}(k)$ is the flow demand from fictitious node $f$ at period $k$.

**Propagation into link**

*Upstream arrives*, for $i = 1$ the inflow into the first cell of link is calculated by

(4.26) . While the $y_1^{ab}(k)$ is calculated from (4.29).

Inflow of the cells belongs to the *merging zone* of link $a$ can be described with the following equation

$$y_i^a(k) = min \begin{cases} n_{i-1}^a(k) \ , Y_i^a(k) \ , \\ \frac{w_i^a \ (F_i^a(k) - n_i^a(k))}{v_i^a} \end{cases} \qquad 1 < i \leq N - I \tag{4.34}$$

and for estimate flow into cell $i$ of link $a$ and direct to lane $b$ we have:

$$y_i^{ab}(k) = \Phi_{ab} \ y_i^a(k) \ , \ \ 1 < i \leq N - I \tag{4.35}$$

When $i = N - I + 1$ , max *flow of downstream channelized zone* can be calculated by

$$\widetilde{y}^{ab}(k) = min \begin{cases} \Phi^{ab} \ n_{N-I}^a(k) \ , \alpha^{ab} \ Y_{N-I+1}^a(k) \ , \\ \frac{w_{N-I+1}^a \ (\alpha^{ab} \ F_{N-I+1}^a(k) - n_{N-I+1}^{ab}(k))}{v_{N-I+1}^a} \end{cases} \tag{4.36}$$

It permits to maximize the demand of upstream lane $n_{N-I}^{ab}$ considering the maximum capacity of lane ($\alpha^{ab} \ Y_{N-I+1}^a$) and the necessary restriction to ensure that the inflow $y^{ab}$ does't exceed the available capacity. $\frac{w_{N-I+1}^a \ (\alpha^{ab} \ F_{N-I+1}^a(k) - n_{N-I+1}^{ab}(k))}{v_{N-I+1}^a}$ represents the total space available in the downstream cell $i$.

Because of conflict between turning vehicles and ahead vehicles, the total inflow of channelized zone can be formulated as follows

$$y_{N-I+1}^a(k) = \min_{b \in B_m} \left\{ \frac{\widetilde{y}^{ab}(k)}{\alpha^{ab}} \right\} \tag{4.37}$$

Inflow of each direction can be calculated as

$$y_{N-I+1}^{ab}(k) = \Phi_{ab} \ y_{N-I+1}^a(k) \tag{4.38}$$

To access the channelized zone, the vehicles directed to different turns may obstruct each other. For this reason, in oversaturated conditions, their behavior could block different movements. The following simple case considers only the interactions between left-turn (L) and through (T) movements incoming in cell

3. In order to give a realistic representation of the vehicular conflict occurring between neighboring turning movements when entering the channelized zone, the $CTM-UT$ has a formulation based on the inflow of the blocking movement: specifically, this conflict is assumed to be proportional to the difference of the values of blocking inflow when passing from the merging zone to the channelized one.

$$y_3^{aL}(k) = \\ = min \begin{cases} \widetilde{y}_3^{aL}(k) \cdot \left[1 - \left(\frac{y_2^{aT}(k) - y_3^{aT}(k)}{y_2^{aT}(k)}\right) \cdot \left(1 - \Phi^{aL}\right)\left(1 - \alpha^{aL}\right)\right], \\ \Phi^{aL}\, n_2^a(k)\, , \alpha^{aL}\, Y_3^a(k) \end{cases} \tag{4.39}$$

It considers the maximum flow given by (4.36) and substitutes (4.37) and (4.38) in model formulation. Moreover, capacity and supply constraints must be respected.

*Channelized zone*, for $N - I + 1 < i \leq N$ the inflow of each cell can be represented as follows

$$y_i^{ab}(k) = min \begin{cases} n_{i-1}^{ab}(k) \;\; , \alpha^{ab}\, Y_i^a(k) \;\; , \\ \frac{w_i^a\, (\alpha^{ab}\, F_i^a(k) - n_i^{ab}(k))}{v_i^a} \end{cases} \qquad N - I + 1 < i \leq N \tag{4.40}$$

After applying the (4.30) for each $b \in B_a$ we can calculate the total inflow of cell $i$ as

$$y_i^a(k) = \sum_{b \in B_a} y_{N+1}^{ab}(k) \;\; , \;\; N - I + 1 < i \leq N \tag{4.41}$$

**Flow conservation**

The flow conservation equation used for $CTM-UT$ is expressed as the difference between the inflows and the outflows of the earlier time interval. The following formulation allows to update the number of vehicles contained in each lane

$$n_i^a(k+1) = n_i^a(k) + y_i^a(k) - y_{i+1}^a(k) \;\; , \;\; 1 \leq i \leq N \tag{4.42}$$

The number of vehicles presents in each cell $i$ in period $k+1$ ($n_i^a(k+1)$) is equal to the sum of the number of vehicles present, in period $k$, in the cell $i$ and vehicles moving from upstream cell $(i-1)$ to cell $i$, less the number of vehicles moving from the cell $i$ to the downstream cell $(i+1)$.

$$n_i^{ab}(k+1) = n_i^{ab}(k) + y_i^{ab}(k) - y_{i+1}^{ab}(k) \quad , \quad 1 \leq i \leq N \tag{4.43}$$

**Demand constraint for conflicting flow interactions**

Compared to the procedure to define the vehicle movement at unsignalized intersection, presents in Highway Capacity Manual ([HCM (2010)]) and based on gap acceptance for a movement compared to the conflicting flow rate for such movement, the capacity determination proposed in the CTM-UT permits to avoid the problems of definition and calibration of the values of critical gap times and follow-up times. In order to realistically capture the potential capacity of minor flow $\hat{\Delta}_{abc}$ when is obstructed, the we propose a formulation based on the demand of the minor flow $\Delta_{abc}$, considering the principal flows $f_h$.

$$\hat{\Delta}_{abc}\left(f_h, \ldots, f_{cf}\right) =$$

$$= \frac{\Delta_{abc}}{2}\left[\left(\frac{\left(\sum_{h=1}^{cf} Y_h - \sum_{h=1}^{cf} f_h\right)}{\sum_{h=1}^{cf} Y_h}\right) \exp\left(-\sum_{h=1}^{cf} f_h \left(tf^{cf}\ 1,5^{cf}\right)\right)\right] \tag{4.44}$$

The formulation considers that half of minor flow (it is diminished by the signal stop or low-priority of its kind of turn) that wants to cross the intersection is inversely proportional to the crossing major flows $f_h$ respected to their capacities $Y_h$. The exponential element depends by the principal flows $f_h$, number conflict flows $cf$ and number of total flows $tf$ for the movement direct to $c$ (including the minor flow). Higher are the values of principal flows, conflict flows and total flows, higher the minor flow is obstructed when try to cross the intersection.

The following example shows the application of (4.26) to calculate the outflow for turn $L$ considering one principal flow ( $y_{N+1}^{abT}$ through flow T), one minor flow ($y_{N+1}^{abL}$ left-turn L), one conflict point of crossing flows $cf$ and and total flow

conflicts $tf = 2$ .

$$y_{N+1}^{abL}(y_{N+1}^{abT}) = \frac{y_{N+1}^{abL}}{2}\left[\left(\frac{\left(Y_{N+1}^{T} - y_{N+1}^{abT}\right)}{Y_{N+1}^{T}}\right)\exp\left(-y_{N+1}^{abT}\left(2^{1}\ 1, 5^{1}\right)\right)\right] \tag{4.45}$$

This equation can be applied on the node model before to consider the formulation to calculate the total flow in the downstream link (4.31). An important aspect of the urban contest of traffic is that we can have a complex signalized intersection with conflict flows in the same signal phase. If this happen is necessary apply the determination of capacity for minor flow. The CTM-UT represents this traffic dynamic including the possibility to estimate the demand of the minor flow both for signalized and unsignalized intersection when the conflict occurs.

### 4.3.2 Cases study and Experiments

A comparison between CTM-UT and incremental node model with constraints (INMC) is done, implementing the model in Matlab. The new node model is suitable to compute the crossing flows at the intersection applying the supply and demand constraints. The model is applied to compute the capacity of minor streams that are limited by major stream (demand constraint), and the time to travel the intersection is not taken into account. The accuracy of representation of inflow at intersection in relation at the demand constraint has been analyzed. The results show the difference of values obtained with methods employed from the node models by Flötteröd and CTM-UT to compute the capacity of the minor flow. In the experiments, the capacity determination used by Wu is applied in the algorithm by Flötteröd to estimate the solution of INMC.
The comparison is done on some case studies presented in [Flötteröd and Rohde (2011)].

The network consists of a major street in north/south direction, which is intersected by a minor one way street that runs from east to west. There are three links for the inflows (upstream flows) at intersection and three links for the outflows (downstream flows) at intersection. In particular, the results highlight the values of $q_E^{IN}$ and $q_S^{IN}$ (in CTM-UT represented by $y_{N+1}^{abc}$ for each link $a$) , minor inflows from south and east direct to the link in west direction.

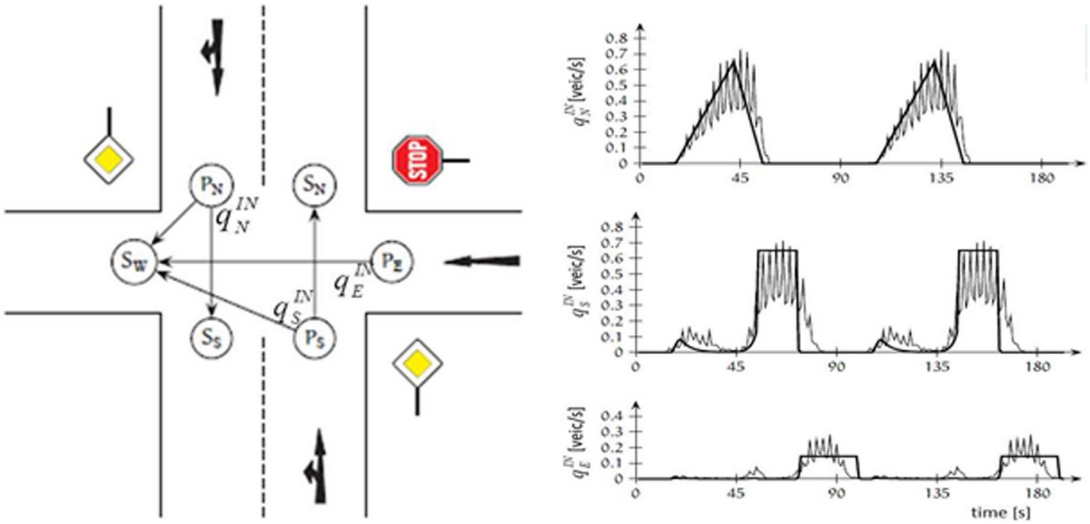


(a) (b)

Figure 4.12: Intersection for the experiments (a) and comparison of microscopic model (thin noisy curve) and Flötteröd (fat smooth curve) (b).

The supply for the major streets (yeld-controlled) consists in:

- one lane with two movements (50% of traffic demand for every movement by lane);
- length of road equal to 0.15 $[km]$; $Y = 2340$ $[vph]$;
- $\bar{\rho} = 200$ $[mph]$ $v = 50$ , $w = 16.29$ $[mph]$;

The supply for the minor street (stop-controlled) consists in:

- one lane and one movement (100% of demand by minor street only crosses the intersection);
- length of road equal to 0.10 $[km]$; $Y = 518$ $[vph]$;
- $\bar{\rho} = 200$ $[mph]$ $v = 32$ , $w = 16.29$ $[mph]$;

The right-of-way laws at the westbound merge $S_W$ are defined, for every movements direct to west link, with the priority values $p_N = 10$, $p_S = 1$ and $p_E = 0.1$. The flows that going into the network are generated by adding traffic light controlled links upstream of each ingoing link of the original network. The cycle time is 90 s , in the first scenario the green phases for the major and minor street are equal to 24 s and 9 s respectively.The analysis is focused only on the demand by first cycle of the traffic light, for the following scenarios the value of different inflow by CTM-UT are the same for every cycle. The total simulation time is 120 s and sampling period (time step) is $\Delta t = 1$ s.
To determinate the capacity has been estimated the value of

- mean error $[vp\Delta t]$: the average of the error is the difference between the same minor flow obtained by two different models for each interval times of the simulation period;
- specific error $[vp\Delta t]$: is the mean error computed only when the conflict among major and minor flows occurs;
- decreasing error: is based on the percentage gap (PG). The difference between the flow obtained by the literature model and our model divided by the flow obtained by our model. Considering only the instants in which the conflict occurs until the minor flow reaches its minimum value;
- increasing error: is based on the percentage gap (PG). Considering only the instants in which the conflict occurs until the minor flow reaches its maximum value;

- mean delay : is based on the percentage gap (PG). It is the mean of queuing delay of the last cell (N) of the link upstream intersection. It considers when the density of the cell exceeds the critical density and the velocity of the travel flow has lower value respected to the free flow speed.

**Results for the synthetic experiment**

The node model INMC ([Flötteröd and Rohde (2011)]) and CTM-UT have obtained the same values for $q_N^{IN}$ . This is the major flow that is not obstructed when crosses the intersection. In the Fig.4.13 and 4.14, $q_N^{IN}$ highlight as it limits the minor flows at intersection.

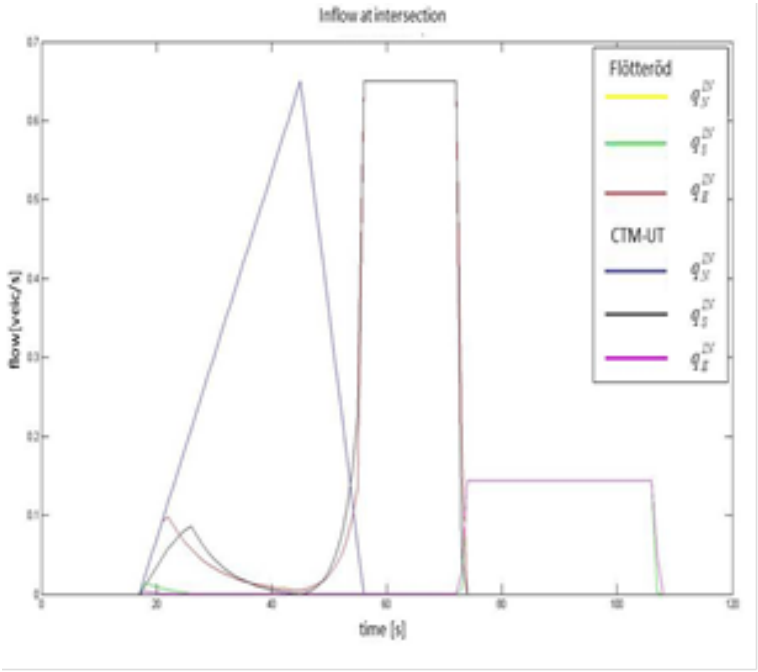


Figure 4.13: Scenario 1 (CTM-UT vs Flötteröd) - Comparison of accuracy.

The results indicate that the curve $q_S^{IN}$ obtained with CTM-UT are more close, compared to the values of Flötteröd, relatively to the values obtained by the microscopic model (see Fig.4.12b), both when $q_S^{IN}$ increases and decreases.

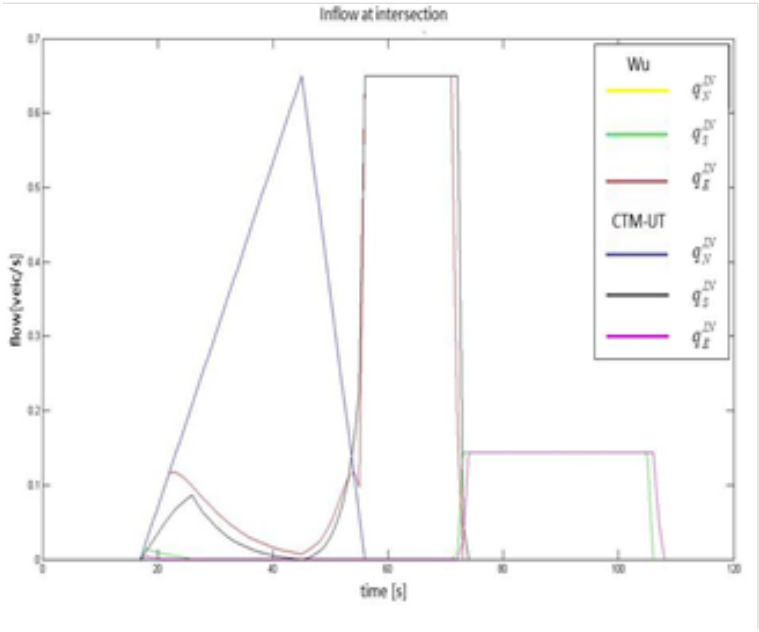


Figure 4.14: Scenario 1 (CTM-UT vs Wu) - Comparison of accuracy.

| inflow at intersection | Flötteröd vs CTM-UT | | | | | Wu vs CTM-UT | | | | |
|---|---|---|---|---|---|---|---|---|---|---|
| | mean error $[vp\Delta t]$ | specific error $[vp\Delta t]$ | decreasing capacity | increasing capacity | delay | mean error $[vp\Delta t]$ | specific error $[vp\Delta t]$ | decreasing capacity | increasing capacity | delay |
| $q_N^{IN}$ | 0 | 0 | 0% | 0% | 0% | 0 | 0 | 0% | 0% | 0% |
| $q_S^{IN}$ | 0,006 | 0.0153 ([18,56]s) | 7,8% | −19,9% | 4,7% | 0,0115 | 0.0225 ([18,56]s) | 39,1% | −4,5% | 11,5% |
| $q_E^{IN}$ | 0,0011 | 0.0015 ([18,74]s) | 86,0% | −2,8% | 4,4% | 0,0032 | 0.0035 ([18,74]s) | 86,6% | −2,9% | 4,4% |

Figure 4.15: Scenario 1 - Comparison of accuracy.

The comparison with Wu indicates a major difference with CTM-UT compared to the Flötteröd, but the curve $q_S^{IN}$ obtained with Wu is less consistent compared to the values obtained by the microscopic model. The flow $q_E^{IN}$ must give way first to $q_N^{IN}$ and then to $q_S^{IN}$ , for this reason it is obstructed until the flows $q_N^{IN}$ and $q_S^{IN}$ crosses the intersection (until 74 s ). The decreasing capacity for $q_E^{IN}$ is 86%( Flötteröd vs CTM-UT) and is 86.6% (Wu vs CTM-UT) and there is a constant error for a time period ($[18, 74]$s) longer compared to the duration of conflict between $q_N^{IN}$ and $q_S^{IN}$. On the other hand, the specific error of $q_E^{IN}$ is ten times less than $q_S^{IN}$ . For the flows $q_S^{IN}$, at 55s is obtained with INMC a not smooth representation of flow. The proposed model have a good capacity to simulate the travel delay of the last cell of the link.

**Results for the synthetic experiment with initial max inflow by minor flow**

For this experiment the inflow demand is the same of scenario 1 except for the link from south.$\Delta_S^{IN}$is equal to the value of max capacity of inflow until 25 s of the simulation time, than is equal to zero. This scenario represents as the crossing flow $q_S^{IN}$, equal to value of max capacity, is obstructed when the principal flow $q_S^{IN}$ incoming in the intersection. Due to the conflict with $q_N^{IN}$, not all demand by south can cross the intersection, but $q_S^{IN}$ must wait the decreasing of major flow. During the decreasing phase the CTM-UT overestimated compared to the values obtained by Flötteröd and Wu, but they produce a less smooth representation. Also, this experiment demonstrates that the formulation of Wu gives an inconsistent representation when the flows conflict occurs and when it ends. This problem depends by the individuation of conflicts in INMC.

**Results for the signalized intersection with conflict flows**

In the this experiment the intersection is the same of Fig.4.12a but it considers a different type of intersection control. In this case the flow is controlled by traffic

signals, we test the obstruction of the flows when they belong to the same signal phase. The traffic light cycle time consists in 70 s and two phases, the first (second) have 22 s red phase (green phase) , 40 s green phase (red phase), 8 s intergreen time between the first and second phase. This times allow to satisfy all the inflow demands at intersection, so there is not delay at the last cell of the incoming links. During the green phase, the minor flows cross the intersection only if they are not obstructed by a major, otherwise, these inflows use the phase of intergreen to free the intersection. $q_N^{IN}$ crosses the intersection until 63 s ( decreases until at zero when the green phase ends); $q_S^{IN}$ crosses the intersection in the last 3 s of the green phase (60-63 s) and for 4 s of intergreen for the CTM-UT (5 s for Flötteröd and Wu ); $q_E^{IN}$ crosses intersection in the last 3 s of intergreen phase (67-70 s) for the CTM-UT (4 s for Flötteröd and Wu ). The difference on the time of crossing flow $q_E^{IN}$, for the intergreen phase, among the models, depends on the quantity of flow $q_S^{IN}$that previously has crossed the intersection. For specific error and flow values we obtain higher values then the previous scenarios because the interval of time is very restricted. These considerations also apply to the values of decreasing capacity and increasing capacity.

The comparison between the different models to represent the capacity of minor flow demonstrates the following considerations. For the minor stream of type left-turn from major street ($q_S^{IN}$in the experiments), when the principal flow increases, for the CTM-UT the capacity of minor flow decreases more slowly and when the principal flow decreases, the capacity of minor flow increases slightly more quickly. For the minor stream of type through traffic on minor ($q_E^{IN}$ in the experiments), for scenarios 1 and 2, the CTM-UT underestimates the value of obstructed flow. This is consistent with the results of Flötteröd and Wu, the values of specific and mean error are very low for scenario 1 while, for scenario 3, percent different of decreasing capacity and increasing capacity are at most3.3%.

### 4.3.3 Conclusions

On the bases of the previously results, the capacity determination of minor streams of the CTM-UT produces a accurately and smooth representation of the flow when a conflict occurs at intersection. Also, it gives a good accuracy respected to the other macroscopic and microscopic model.
Has been proved that the CTM-UT, using a general node model, is suitable to represent traffic flows that cross signalized and unsignalized intersections. The CTM-UT allows to model complex intersections for urban contest, where many conflicts among through flows are presented. In particular, the model can represent different turn movements of the inflow at intersection and belonging at the same lane. The model takes into account also the estimation of the merge flows at the intersection.
Lastly, through a new way to compute the minor streams that are limited by major stream on unsignalized intersections, the CTM-UT reduces the problems and the complexities of the capacity determination (based on gap acceptance) and it could be used for dynamic traffic assignment.

## 4.4 A new methodology to calibrate the congestion wave

As explained in the Chapter 2, the microscopic traffic simulation software are used to simulate the real urban traffic for small and medium networks because they have need of great deal of information to management and simulation of traffic. To model the traffic demand with the microscopic simulators is need set the behavioral models for the driver-vehicle profiles.
For example *SUMO* (Simulation of Urban MObility) is a microscopic traffic simulation package, it is not only a traffic simulation, but rather a suite of applications which help to prepare and to perform the simulation of traffic. *SUMO*

allows modeling of intermodal traffic systems including road vehicles, public transport and pedestrians. The simulation uses the microscopic, space-continuous and time-discrete car-following model developed by [Krauss et al., (1997)] and a lane-changing model developed within the work on the simulation. Traffic assignment is normally performed using the iterative approach formulated by [Gawron (1999)], but further methods, such as a one-shot assignment method, exists (see [Krajzewicz et. al, (2012)]).
It is obvious that the microscopic simulation requires greater efforts in calibration than the macroscopic one, but even the macroscopic models include their difficulty in tuning and setting the physical and simulation parameters.
Define a solution to calibrate a key element of the traffic demand such as congestion wave for the macroscopic fundamental diagram.

Despite simulation models offer the possibility to select entry parameters based on the available transport literature, it is necessary to calibrate these models according to a specific type of transport network. Such calibration procedure involves the regulation of the parameters until there is a correct relation between the data collected by direct observation and those reproduced by the model. This calibration process requires a great effort in terms of time and resources.

A way to solve the calibration problems by optimization method, where a combination of values that best satisfies an objective function is searched. Studies on calibration are focused on minimizing the error between the observed data and the simulation.
The research proposed different approaches on calibration (stochastic, static, etc.). [Ma and Abdulhai (2002)] and Lee et al. [Lee et. al, (2001)] proposed a optimization tool that uses genetic algorithms to automate the calibration of traffic microsimulation models. [Muñoz et al., (2006)] proposed a piecewise-linearized

version of CTM, the $SMM$. The authors presented a semi-automated method, based on a least-squares data fitting, for calibrating the CTM and $SMM$ parameters such as free-flow speeds, congestion-wave speeds, and jam densities for specified subsections of a freeway. [Lee and Ozbay (2008)] proposed a calibration methodology using enhanced simultaneous perturbation stochastic approximation methodology.

Define a solution to calibrate a key element of the traffic demand such as congestion wave for the macroscopic fundamental diagram. In order to solve such problems, [Adacher and Tiriolo (2015b)] proposed a generalization of the CTM-UT and a new calibration model of congestion wave for CTM. The aim of the method by [Adacher and Tiriolo (2015b)] is to improve the calibration process of congestion wave speed in terms of accuracy and efficiency. In the following is described the new calibration model.

The application of triangular fundamental diagram determines the relation of congestion wave speed $w$, free flow speed $v$, jam density $\rho_J$, critical density $\rho_c$ and max capacity ( $Y_i/\Delta_t$). The total capacity of cell (storage capacity) $F_i$ is calculated on the number of vehicle and it is obtained by the product of max capacity, free flow speed and sampling period ( $\bar{\rho} \cdot v \cdot \Delta_t$ ). The storage capacity represents the max number of vehicle that can be present in the cell. The storage capacity for the lane takes into account the proportion of stop line width devoted to vehicles traveling to lane $b$ ( $\alpha^{ab} F_i^a$ ). The original model of Daganzo ([Daganzo (1994)],[Laval and Daganzo (2006)]) considers the supply constrain of the cell $\frac{w_i^a \ (F_i^a(k) - n_i^a(k))}{v_i^a}$ to ensure that the inflow $y_i^a$ does't exceeds the available capacity, it represents the total space available in the downstream cell $i$. If the inflow in the cell $y_{i+1}^a$ (equal to outflow from cell $i$ ) is restricted by supply constraint, it could influence the travel velocity of the cell $i+1$ and of the upstream

cell $i$. If we have $y_i^a$ and $y_{i+1}^a$ are restricted the density of cell $i+1$ increases. While, if density of the cell $i$ exceeds the critical density $\rho_c$, the actual speed $V_i$ decreased. For this reasons the supply constrain of the cell play an important role in the prediction of traffic.

Originally, the CTM has been designed to provide a simple representation of traffic on a highway. To apply the CTM in the urban contest is necessary to set the variables of the fundamental diagram appropriately. In this paragraph, a new model to calibrate the supply constraints of each link is presented. This model allows the variation of the congestion wave speed maintaining the same values of max capacity, free flow speed, critical and jamming density of the triangular fundamental diagram defined. With the following formulation it is possible to replace the supply constraints of the cell $i$ for the inflow $y_i^a$, when the density of cell $i$ is over the critical density.

$$y_i^a(k) = min\left\{ n_{i-1}^a(k)\ , Y_1^a(k)\ , \frac{w_i^a\ (F_i^a(k) - n_i^a(k))}{v_i^a \exp -(n_i^a(k)/w_i^a)^{-cw_i^a}} \right\} \tag{4.46}$$

The decreasing velocity of the inflow $y_i^a$ is conditioned by the exponential $\exp -(n_i^a(k)/w_i^a)^{-cw_i^a}$. The decreasing velocity of the inflow becomes quicker with increasing of the vehicle number presented in the cell $i$ ( $n_i^a(k)$ ). $cw_i^a$ represents the coefficient of congestion speed wave (if it is equal to zero we obtain the original formulation of Daganzo). For negative value of $cw_i^a$, the fundamental diagram tends to assume a trapezoidal shape. The estimation of the congestion speed wave coefficient $cw_i^a$ is obtained by an optimization method. Via optimization we obtain the minimization of the error between the congestion wave by CTM and real data (or microscopic model). We can calibrate accurately the traffic values that represent the congestion wave for each link.

As shown in the figure 4.16 and algorithm 1, we can apply the calibration model to find the minimum value of mean speed error obtained by these macroscopic and microscopic models. In this way, it is possible to find the values of $cw_i^a$ for each link $a$ of the network. Each values of $cw_i^a$ represents a different variation of

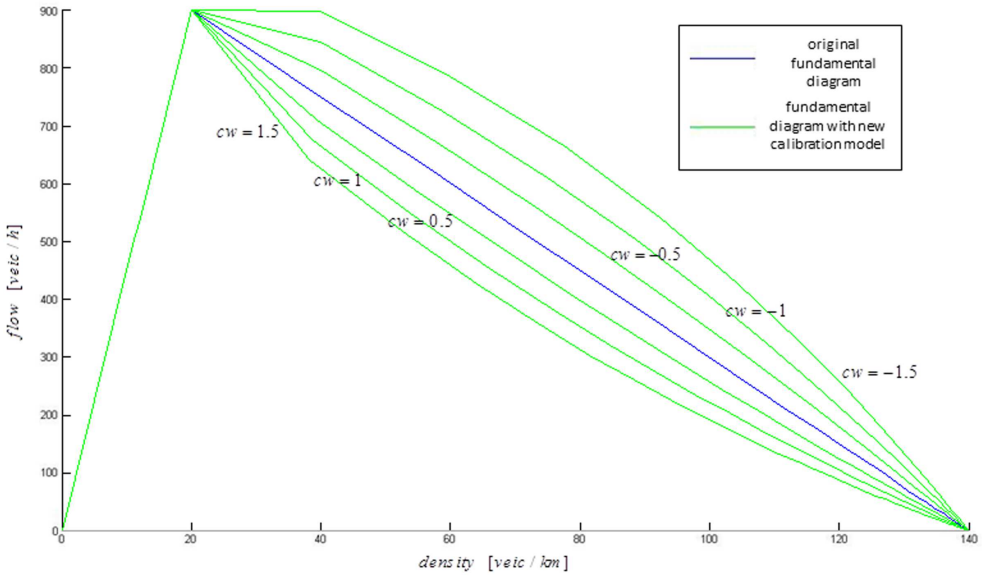


Figure 4.16: Representation of a fundamental diagram. The new calibration model changes in relation to different values of congestion wave speed

congestion wave speed.

### 4.4.1 Case studies and Experiments

#### Model Validation

The CTM-UT with the calibration of the congestion wave via simulation is compared with *SUMO*. Different scenarios are considered to obtain good values of link travel speed. The calibration of the CTM-UT is based on the minimization of mean error, calculated on macroscopic and microscopic models. The experiments are focus on the study of the accuracy of traffic prediction obtained by CTM-UT including also the calibration method.

The case study is a hypothetical four-way signal controlled intersection. It is composed by two links with one lane. One link is dedicated to the inflow into

**Algorithm 1** Calibration with optimization method

1: Definition of supply and demand of traffic
2: Calibration of Triangular Fundamental Diagram
3: Run of CTM-UT and real data (or microscopic model):
- estimation of $MTT_{realdata}$
- estimation of $MTT_{CTM-UT}$ (see (4.12))

4: Initialization
- $cw_i^a = 0$
- $TSE = \frac{MTT_{realdata} - MTT_{CTM-UT}}{MTT_{realdata}}$

5: **while** $-0.99\% \leq TSE \leq 0.99\%$ **do**
6: run of CTM-UT and estimation of $MTT_{CTM-UT}$
7: $\mathrm{cw}_i^a = \begin{cases} cw_i^a = cw_i^a + 0.01 & if \quad TSE \leq -0.99\% \\ cw_i^a = cw_i^a - 0.01 & if \quad TSE \geq 0.99\% \end{cases}$ **end while**

the network (100 meter in length) and another link upstream of intersection (75 meter in length). A signal is placed to control the incoming flow in intersection. The total simulation time is $120s$, sampling period (time step) is $\Delta t = 2s$ and for earlier state the network is empty. The cycle time considers only the red phase because we want to analyze the jam formation.

The values of $Y = 900[v/h]$, $\rho_J = 140[v/km]$, $\rho_c = 20[v/km]$ are obtained by the analysis of $SUMO$ data simulation, considering the input value of demand traffic $v = 50[km/h]$, car length= $5[m]$, the minimum space between two vehicles= $2[m]$, acceleration $ac = 0,7[m/s^2]$, deceleration $dc = 3[m/s^2]$. Applying the triangular fundamental diagram, the congestion wave speed is equal to $w = \frac{Y_i/\Delta_t}{\rho_J - \rho_c} = 7,5[km/h]$. The comparison is done on the bases of upstream link.

8: 
- travel speed error (TSE): it is based on the percentage gap (PG). The difference between the mean travel speed (calculated on the total step) obtained by $SUMO$ and CMT-UT

- density error (DE): is based on the percentage gap (PG). The difference between the mean density of link (calculated on the total step) obtained by

*SUMO* and CMT-UT

Fixed the values of triangular fundamental diagram, for the macroscopic model the congestion wave speed is calculated. Others scenarios are defined varying only the acceleration ($ac$) and deceleration ($dc$) values, fixing the same congestion wave speed. The mean travel speed and mean density are obtained by $SUMO$ varying $ac$ and $dc$ instead the values obtained by CM-UT are fixed if we don't use the calibration model.

The congestion wave speed changes if we utilized CMT-UT with calibration model ($CTM - UTwithCM$) on the bases of $ac$ and $dc$ values. It is important to notice that the congestion wave speed adapts its values when we use the $CTM - UTwithCM$ and it is not need to simulate the scenario by $SUMO$. The comparison is done between $SUMO$ vs CMT-UT and vs $CTM - UTwithCM$.

Case study 1 : $dc = 3[m/s^2]$ and $cw = 0,8$

| | **ac** | **dc** | **cw** | | **TSE** | **DE** |
|---|---|---|---|---|---|---|
| SUMO | $0,7$ | 3 | | | | |
| CTM-UT | | | | | $-4,06\%$ | $10,37\%$ |
| CTM-UT CM | | | $0,8$ | | $0,36\%$ | $5,69\%$ |

Case study 2 : $dc = 5[m/s^2]$ and $cw = -0,4$

| | **ac** | **dc** | **cw** | | **TSE** | **DE** |
|---|---|---|---|---|---|---|
| SUMO | $0,7$ | 5 | | | | |
| CTM-UT | | | | | $-3,47\%$ | $9,06\%$ |
| CTM-UT CM | | | $-0,4$ | | $0,12\%$ | $-0,34\%$ |

Case study 3 : $dc = 7[m/s^2]$ and $cw = -0,5$

| | **ac** | **dc** | **cw** | | **TSE** | **DE** |
|---|---|---|---|---|---|---|
| SUMO | $0,7$ | 7 | | | | |
| CTM-UT | | | | | $-3,47\%$ | $9,07\%$ |
| CTM-UT CM | | | $-0,5$ | | $-0,46\%$ | $-0,78\%$ |

In the case 1 the traffic condition goes in traffic jam state later compared to the case 2 and 3. In general, the macroscopic model represents the traffic more similarly to microscopic model with high volumes of traffic. For this reason in the case 1 the DE is $5,69\%$.

An optimization method is proposed to obtain a good calibration of the model. This method is based on the minimization of TSE when its value is not minor of $0,99\%$. In the initialization phase the $TSE$ is calculated by $SUMO$ and CMT-UT considering $cw = 0$. If the $TSE$ is negative, the $cw$ is increased by $0,01$ and viceversa. A new simulation is done with the new $cw$ value and the $TSE$ is calculated by $SUMO$ and CMT-UT. This process goes on until the $TSE$ is minor of $0,99\%$.

## 4.5 Conclusions

The results validate the capacity and the accuracy of the CTM-UT compared to a microscopic model.

The CMT-UT is a good model and simulator for the congestion phase. The behavior of the CMT-UT with calibration is very similar to the microscopic model. The CMT-UT, consistently compared to the microscopic model, gives a good traffic prediction in terms of mean speed and density. The relative errors of CMT-UT respects to $SUMO$ are about 4% for TSE and 10% for DE. The results demonstrate that the application of the calibration method improves the behavior obtaining 0% of TSE in comparison with $SUMO$.

# Chapter 5

# Stochastic optimization based on surrogate method for traffic problem

## 5.1 Introduction

In this chapter a new SM version gets introduced. A "surrogate problem" approach has been employed, which had been previously developed because of discrete stochastic optimization problems. It is eligible to deal with traffic signal synchronization problem in order to minimize total delay (DTSS).
The optimization model presented in this chapter, and in the general framework presented in this thesis, has been designed to obtain robust solutions. A solution to an optimization model is defined as robust if it remains "close" to optimal for all scenarios of the input data.
The proposed SM version is intended to combine the advantages of a stochastic approximation type of algorithm with the ability to obtain sensitivity estimates with compared to discrete decision variables.
Moreover, the results show that the new extensions of the SM improve its ef-

ficiency and efficacy making it suitable for urban contest, online approach and large-scale network.

## 5.2 Traffic Signal Synchronization Problem

The performance of a traffic network get worse when too many vehicles attempt to use a common transportation infrastructure with limited capacity.
The urban traffic coordination control is a very important research area in intelligent transportation systems. The performance of a traffic network can be influenced through several types of actions or decision variables. Some of these pertain to how traffic flow is controlled through the network components, such as junction utilization through signal control (supply management).
Since road congestion usually takes place at or close to junction areas, an improvement in signal settings contributes to improve travel times, driver comfort, fuel consumption efficiency, pollution and safety. In a traffic network, the signal control strategy affects the travel time on the roads and influences the drivers' route choice behavior.
Usual traffic signal optimization methods seek either to maximize the green bandwidth or to minimize a general objective function that typically includes delays, number of stops, fuel consumptions and some external costs like pollutant emissions. A major objective of Traffic Signal Synchronization at intersection is to clear maximum traffic throughput in a given time with least number of accidents, at maximum safe speed and with minimum delay.
The traffic synchronization problem can consider only the green signal times as decision variables (see (5.1)).

$$\min_{r \in A_d} J_d(r)$$

$$A_d = \{r := [r_1, \cdots r_N]^{'}, a_{min} \leq r_a \leq a_{max};, r_a \in \mathbb{Z}^+\} \tag{5.1}$$

$r$ represents a $N$-dimensional decision vector with $r_a \in \mathbb{Z}_+$ denoting the green time ratio for intersection link $i$, the capacity constraint is $A_d$ and $J_d(r) = E[L_d(r,q)]$ is the objective function, where $L_d(r,q)$ is the total delay on the network when the state (green split vector) is $r$ over a specific sample path (link flow) denoted by $q$, and $E[]$ denotes the expected value.
The following signal optimization model minimizes the value of the objective function that in this case is the total traffic delay.

## 5.3 Surrogate Method (SM)

In the research project presented in this thesis, a generalized "surrogate problem" methodology based on an on-line control scheme is applied.
The original SM by [Gokbayrak and Cassandras (2002)] can be generalized to optimize the signal setting problem. The SM is based on an on-line and stochastic control scheme. This approach has been proposed by [Adacher and Cassandras (2014)] and applied for the first time in traffic problem [Adacher and Cipriani (2010)], based on the idea of transforming a *discrete* optimization problem into a "surrogate" *continuous* optimization problem which is not only easier to solve, but also much faster using standard gradient-based approaches.

Stochastic optimization assumes that the uncertainty has a probabilistic description. This paragraph describes the SM based on gradient approach. The gradient estimation iteratively takes appropriate steps along descent directions for the problem. This analogy continues to hold through the iterations; the local search is designed to terminate at a local minimum, a point where no improving direction exists.

The traffic problem formulated in (5.1) can be solved with the following algorithm, the SM.

First, initialize $\rho_0 = r_0$ and perturb $\rho_0$ to have all components non-integer. Then, for any iteration $k = 0, 1, \ldots$

1. Determine $\mathcal{N}(\rho_k)$, the set of all *feasible neighboring discrete states of* $\rho_k$ $\mathcal{N}(\rho_k) = \{r | r = \inf \rho_k + \overline{\overline{r}} \text{ for all } \overline{\overline{r}} \in \{0,1\}^N\} \cap A_d$.
2. Determine $\mathcal{S}(\rho_k)$, a selection set to define a set whose a convex hull includes $\rho_k$ (using [Gokbayrak and Cassandras (2002)]).
3. Select a *transformation function* $f_k \in \mathcal{F}_{\rho_k}$ such that $r_k = f_k(\rho_k) = \arg\min_{r \in \mathcal{S}(\rho_k)} \|r - \rho_k\|$.
4. Evaluate the gradient estimation $\nabla L_c(\rho_k) = [\nabla_1 L_c(\rho_k), ...., \nabla_N L_c(\rho_k)]^T$, using the following relationship $\nabla_j L_c = L_d(r^j) - L_d(r^k)$, where k satisfies $r^j - r^k = e_j$.
5. Update state: $\rho_{k+1} = \pi_{k+1}[\rho_k - \eta_k \nabla L_c(\rho_k)]$.
6. If some stopping condition is not satisfied, repeat steps for $k+1$. Else set $\rho^*$.

Finally, we obtain $r^*$ as one of the neighboring feasible states in the set $\mathcal{S}(\rho^*)$. It is important to notice that to evaluate the gradient estimation in step 4, we need to calculate $n+1$ times the value of the objective function, so this estimation is dependent of the decision vector dimension.

The basic idea of this approach is to solve the continuous optimization problem above with standard stochastic approximation methods and establish the fact that when (and if) a solution $\rho^*$ is obtained it can be into some point $r = f(\rho^*) \in A_d$ which is in fact the solution of step 4. Note, however, that the sequence $\{\rho_k\}$, $k = 1, 2, \ldots$ generated by an iterative scheme for solving step 5, consists of real-valued allocations which are infeasible, since the actual system involves only

discrete resources. Thus, a key feature of this approach is that at every step $k$ of the iteration scheme involved in solving step 5, the discrete state is updated through $r_k = f_k(\rho_k)$ as $\rho_k$ is updated. This has two advantages: first, the cost of the original system is continuously adjusted (in contrast to an adjustment that would only be possible at the end of the surrogate minimization process); and second, it allows us to make use of information typically employed to obtain cost sensitivities from the *actual* operating system at every step of the process.

## 5.4 Stochastic Optimization for Macroscopic Urban Traffic Model with Microscopic Elements

In the last years, the development of ITS has increased the need to define the simulation methods to accurately estimate the travel time prediction but at the same time they must be efficient to be applicability for the optimization of real-time traffic. For example, optimization tools that use multiple traffic simulations have been defined (e.g., TRANSYT-7F and SYNCHRO) and also optimization tools based on hybrid traffic flow models (e.g. [Burghout (2004)], [Zhang et al., (2014)], [Bourrel and Lesort (2014)]) are introduced. These last combine macroscopic (or mesoscopic) model with microscopic model. The choice of the correct optimization method in relation to the characteristics of the traffic network is complicated, studies have not defined exhaustively the reasons behind the inconsistencies between optimization and simulation tool results.

In order to define an effective optimization system suitable to efficiently optimize the urban traffic signal synchronization this paragraph presents a version of SM to optimize the signal synchronization problem considering every turns in accord with the CMT-UT framework(see [Adacher and Tiriolo (2016c)]). Moreover,

some extensions to improve the efficiency and efficacy of the surrogate method are proposed. A node algorithm for urban traffic to define the inflow and outflow of every intersection $m$ respecting all boundaries constraints is presented. In particular, the algorithm calculates the flows disaggregated by turn $y^{abc}$, lane $y^{ab}$, intersection outflow $y_1^c$, intersection inflow $y_{N+1}^{abc}$ with the relative constraints of total demand $\Delta$ and total supply $\Sigma$. The demand and supply constraints could define the normalization factors $\beta_{ab}$ ((5.2)) and $\beta_c$ ((5.3) ) to limit the flows. When the demand of flow turn ($\Delta_{abc}$) exceeds the maximum capacity of the lane $Y_{ab}$ or demand of intersection otuflow ($\Delta_c$) exceeds maximum capacity of intersection outflow ($\Sigma_c$), are calculated the normalization factor for lane or for intersection outflow, respectively.

Following is described the simplified node algorithm, developed in Matlab, divided in three parts: calculation of normalization factor for lane (Alg. 2); calculation of intersection outflow with a normalization factor for lane and for downstream link (Alg. 3); calculation of intersection inflow (Alg. 4). The term *aux* refers to auxiliary variables to the algorithm and $\Delta_{abc}$ represents the number of vehicles of the movement $abc$ from lane $b$ that requires to cross intersection.

**Algorithm 2** Calculation of normalization factor for lane

```
1: for all upstreamLink(a) do
2:     for all lane(ab) do
3:         if #turn(abc) ∈ lane(ab) > 1 then
4:             for all turn(abc) ∈ downstreamLink(c) do
5:                 auxy^abc = min{Δ_abc, Y^ab}
6:                 auxy^ab = auxy^ab + auxy^abc
7:             end for
8:             if auxy^ab > Σ_ab then
9:                 compute β_ab
10:            end if
11:        end if
12:    end for
13: end for
```

**Algorithm 3** calculation of outflow with a normalization factor for lane and for downstream link

**for all** upstreamLink($a$) **do**
  Outflow=false
  $\beta_c = 1$
  **while** Outflow=false **do**
    $y^c = 0$
    **for all** turn($abc$) $\in$ downstreamLink($c$) **do**
      $y^{abc} = \beta_{ab} * min\{\Delta_{abc}, Y^c\}$
      $y^{abc} = \beta_c * y^{abc}$
      $y^c = y^c + y^{abc}$
    **end for**
    **if** $y^c \leq min\{\Delta_c, \Sigma_c\}$ **then**
      Outflow=true
    **else**
      **compute** $\beta_c$
    **end if**
  **end while**
**end for**

**Algorithm 4** calculation of intersection inflow

**for all** upstreamLink($a$) **do**
  **for all** turn($abc$) $\in$ lane($ab$) **do**
    $y^{ab} = y^{ab} + y^{abc}$
  **end for**
  **for all** lane($ab$) $\in$ upstreamLink($a$) **do**
    $y^a = y^a + y^{ab}$
  **end for**
**end for**

Where, the normalization factor $\beta_{ab}$ is calculated as

$$\beta_{ab} = \Delta_{abc} \sum_{c \in ab} y_{N+1}^{abc}(k) \tag{5.2}$$

The normalization factor $\beta_c$ is computed as the capacity of first cell of outgoing link divided the total flow demand direct to the outgoing link.

$$\beta_c = \frac{min\left\{Y_1^c(k)\ , \frac{w_1^c(F_1^c(k) - n_1^c(k))}{v_1^c}\right\}}{\sum_{c \in C_a} y_{N+1}^{abc}(k)} \tag{5.3}$$

This general algorithms can be useful to support the transportation researchers to develop node macroscopic models with microscopic advantages in order to solve open issues on optimization of urban traffic.

**Extensions for SM: Database of solutions**

To evaluate the gradient estimation the SM needs to calculate $n + 1$ times the value of the objective function (see step 4), and this estimation is required many time for one solution. For this reason to increase the efficiency of SM we have memorized every solution with relative objective function (OF). If the SM requires the OF for one solution, the software avoids the run of simulation model if the OF has already been calculated.

The dimension for the Database of Solution ($sizeDB$) depends both on the number of calculation of the objective function at every run of the SM ($n + 1$) and the number of total runs of SM ($stepSM$) less the saving of calculation of the objective function ($solDB$).

$$sizeDB = ((n + 1) * (stepSM)) - solDB \tag{5.4}$$

The use of database resources relative to the evaluation of the value of the objective function, increases with increasing of the number of the following events: very small size of gradient step and/or high stop condition(much beyond the final solution). In the example shown in 5.1, when the database of solution it is applied

with the classic gradient step estimation (SM-DS) there is an efficiency improvement of 64%, in term of computational time we have a saving of 288 min on a computer with Intel Xeon CPU E5 3,40GHz 2 processor; RAM 32GB; Windows 10 Pro 64bit.

**Extensions for SM: Dynamic gradient step estimation**

It is possible that different solutions give the same value for OF, consequently the corresponding component of the gradient, given by the difference of these solutions, is equal to 0. When the component is blocked and doesn't change toward a better solution, we have defined a formulation to randomly increase the component of gradient equal to 0 considering the SM iterations for which the component of gradient remains equal to 0. To counts these iterations we used the counter $z$.

$$\eta = 0.5/k \tag{5.5}$$

Moreover, compared to classic step size definition where $k$ represents the number of SM iteration, we used the value $u$ that counts the number of SM iteration and it becomes zero when a better solution is founded.

The calculation of the dynamic step size is described in the following algorithm 5.

**Extensions for SM: Green splits constraints**

In the optimization signal setting problem, the decision variables have to respect the constraints of green time limitation and cycle. Given an intersection with fixed-time cycle and more of two alternative phases, when the optimization method explores the possible solutions, the sum of green splits have to be equal to time cycle. To respect this constraint we proposed the following formulation

$$\sum_{p \in \Pi_m(p)} r_m(p) = C_m \ , \ \forall m \in M \tag{5.6}$$

**Algorithm 5** Dynamic gradient step estimation

**if** $OF(\rho^k) \leq \min OF(\rho^{k-1})$ **then**
    $u = 1$
**else**
    $u = u + 1$
**end if**
**for** $i = 1 : n$ **do**
    **if** $\nabla_i L$ ¡ $\epsilon$ and $\nabla_i L > \epsilon$ **then**
        $z = z + 1$
        $\nabla_i L = rand \in [-z, z]$
        $\eta_i = 0.5$
    **else**
        $\eta_i = 0.5/u$
    **end if**
**end for**

where, $M$ is the set of intersection, $\Pi_m(p)$ the set of phase $p$ indices of intersection $m$, $r(p)$ the green split of phase $p$ belong to intersection $m$. Defining with $\psi_m$ the decision vector of the green times $r(p)$ of the phases for intersection link $m$ the set of neighboring feasible states, in accord to the cycle time, is defined as

$$P(\psi_m) = \left\{ \psi_m + \bar{r}, \forall \bar{r} \in 0, 1^{\Pi_m(p)} \mid \sum_{p \in \Pi_m(p)} r_m(p) = C_m \right\} \tag{5.7}$$

For each phases of one intersection only one green time is defined as decision variable. If the green time changes, the neighboring feasible states changes in accord to the cycle time. For example, for one intersection with cycle time of 100 sec and three alternative phases, given the green times $[50, 25, 25]$ sec the decision vector considers only the first element. If this element is changed of $+1$ sec, the set of neighboring feasible states corresponds to ([51,24,25], [51,25,24]). The complete decision vector is evaluated with either solutions and the green times are fixed for intersection that returns the best OF value.

### 5.4.1 Cases study and Experiments

The following results show the effects in terms of traffic predictions and efficiency of the CMT-UT compared to the macroscopic model. The analysis is based on the following microscopic elements are used:

- queues dissipation in the channelized lanes at upstream intersection;
- conflict flows that could occur when the vehicles try to enter in channelized lanes;
- representation of different turn movements belonging at the same lane.

**Effects of microscopic elements on traffic prediction**

We have defined an hypothetical test network with 9 four-way signal controlled intersection and 12 centroids for the flow of input/output of network. All links (300 meters in length) have max capacity ($Y$) equal to 900 [veic/hour] and two lanes. The capacity and demand of the links are split over the two lanes fifty-fifty, excepted for the principal paths where the demands are represented in the Fig.5.1.

The traffic light cycle of each intersection consists in two alternative phases and one right-turn not controlled as represented in the Fig.5.2.

A comparison between the original CTM and CTM-UT in terms of network delay prediction is presented. The analysis is focused on the evaluating of the total delay based on different microscopic elements.

The delay represents the number of vehicles obstructed in the road section. For each cell the delay is defined as the difference between the number of vehicles that could travel in the downstream cell less the vehicles that travel in the downstream cell. The total delay ($TD$) includes both the upstream and the downstream node

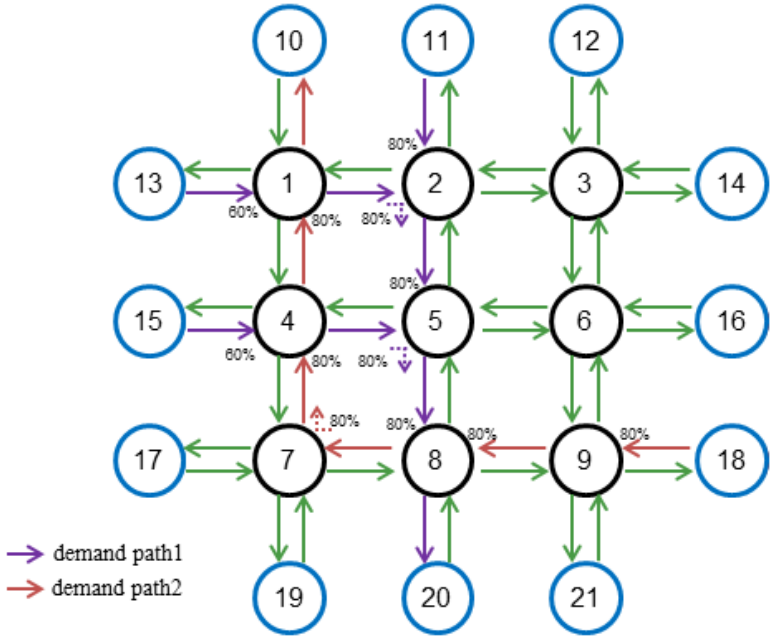


Figure 5.1: Representation of network test with centroid (blue), signalized intersections (black), links (green), demands and paths.

delay.

$$D(h) = \sum_{a=1}^{\#link} \sum_{i=1}^{N+1} n_{i-1}^{a}(h) - y_{i}^{a}(h) \tag{5.8}$$

$$TD = \sum_{h=1}^{H} D(h) \tag{5.9}$$

The CTM-UT represents all links with a channelized zone of 120 meters, instead the macroscopic model does not represent channelized zone and vehicular conflict along the link. In the representation with the original CTM, the delay caused by spillback phenomena affects on the total flow, but in real cases we can have delay effects only for one lane and for one direction. In case of urban channelized zone, the CTM-UT allows to obtain a correct representation of the urban dynamics with a loss of efficiency around 4% compared to classical CTM. Such loss of efficiency is due to the additional representation of the propagation

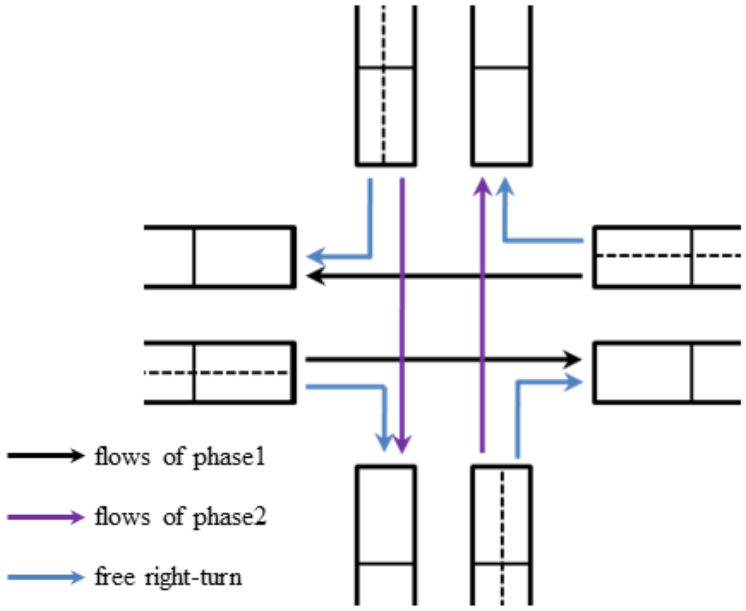


Figure 5.2: Representation of phases of signalized intersection in the network test.

into the channelized zone of the link.

The CTM-UT can represent behaviors of urban drivers, its peculiarity improves the efficacy of travel prediction for complex urban intersections. It is possible considered an additional movement belonging to the right-turn so that the demand lane is split in right-turn (95% turn demand) and through (5% turn demand) movements. This through demand is applied to all lanes for right-turn of network and it belong to the phase 1 for east-west/west-east directions and to phase 2 for south-north/north-south. These percent represent drivers that must move forward but for error take the channelized lane for right-turn.
Such analysis highlighted that to obtain efficacy solutions for urban traffic optimization, it is necessary to model flows that crosses the channelized lanes, flow upstream intersection and the complex flow intersection with detail level quite close to the microscopic models.

**Surrogate Model with new extensions**

In this section are presented the results of the new SM extensions applied to the test network in Fig. 5.1 with the inflow demands of 800 [veic/h] from the nodes 11,13,15,18 during a simulation time of $6,66$ min.

Four versions of the optimization method based on CTM-UT are defined: classic SM with step size presented in (5.5); SM with Database of Solutions (SM-DS); SM with Dynamic Gradient step estimation (SM-DG) and SM both with DS and DG (SM-DSDG). Each version of SM are compared in terms of efficacy (value of $TD$) and efficiency (number of times that the OF must be calculated $NOF$). The initial state is defined with the total cycle time over the two phases fifty-fifty, 50 sec for each decision variables. The optimization model is stopped after 29 iterations ($k$).

Table 5.1: Comparison of SM versions based on CTM-UT

| | **TD** | $\Delta_{TD}$ | **NOF** | $\Delta_{NOF}$ |
|---|---|---|---|---|
| SM | 7906 | | 291 | |
| SM-DS | 7743 | $-2\%$ | 106 | $-64\%$ |
| SM-DG | 7124 | $-10\%$ | 291 | |
| SM-DSDG | 6999 | $-11\%$ | 208 | $-4\%$ |

Both the results in table 5.1 that the many results presented in the next section highlight the improvement of robustness of the SM-DSDG. With different runs of the optimization method is obtained the same solution both with the same starting conditions that with different starting conditions. The method has robust performances and well works on scenarios with different traffic demands and network size. Moreover an analysis on the object function has demonstrated

that the solution obtained is really the optimal solution.

## 5.5 Conclusions

To obtain effective optimization solutions for urban network it is important that the simulation model represents with accuracy the flows upstream intersection. The experiments presented above, put in evidence that CTM-UT can be well-applied for the real-time signal setting problem.

The results obtained with the proposed SM extensions demonstrated that the new dynamic gradient step estimation improves the efficacy about 10% compared to the classic step estimation; and when the Database of Solutions extension is applied the improvement is 4%. The new dynamic gradient step estimation permits to avoid the local optimum and it increases the number of times that the objective function is calculated.

The new SM based on CTM-UT characteristics has the potential to settle some unresolved critical issues on the real-time applicability of the ITS for urban traffic networks on large-scale.

# Chapter 6

# Network traffic clustering: decomposition and cooperation

## 6.1 Introduction

In this chapter a new distributed procedure to obtain a decomposition to reduce the complexity of the Traffic Signal Synchronization problem is proposed. Spatial problem decomposition refers to the process of partitioning the network through which the problem is optimized into small subnetworks considering some intersections of the entire network. A good policy in this respect should divide the considered area in relation to the geographical area. Alternatively, this research project offers a decomposition based on the importance of nodes. In a new decomposition approach, the classification of nodes is integrated with a clustering algorithm based on topological characteristics of the network. Moreover, a cooperation approach is adopted and decisions are made based on neighboring intersection areas.

## 6.2 Distributed urban traffic signal optimization based on macroscopic model

A major objective of Traffic Signal Synchronization at intersection is to clear maximum traffic throughput in a given length and time with least number of accidents, at maximum safe speed and with minimum delay (see [Goliya and Kumar (2012)], [Adacher (2012)], [Adacher L. et al.,2015]). It has been widely accepted that improving traffic flow has been one of the strategies to reduce vehicle emissions and fuel consumption. In urban areas, frequent stop-and-go driving and excessive speed variations contribute to higher fuel consumption and emissions (see [Adacher and Cipriani (2010)], [Khaki and Haghighat (2014)], [Xiaojian H. et al.,2015], [Stevanovic A. et al.,2009]).

In order to improve the algorithm, several authors combined in a different way the two synchronization approaches, that are the minimum delay and the maximal bandwidth. [Cohen S.L.,1983] used the maximal bandwidth as initial solution of the former problem; [Cohen and Liu (1986)] constrained the solution of the former problem to fulfill maximum bandwidth; [Hadi and Wallace (1993)] used the bandwidth as objective function; [Malakapalli and Messer (1983)] added a simple delay model to the maximal bandwidth algorithm; [Gartner and Hou (1994)] introduced a flow-dependent bandwidth function; [Papola and Fusco (2000)], [Adacher and Cipriani (2010)] have expressed the delay at nodes as a function of the maximal bandwidth solution.

It is important to notice, that the minimum delay is related to physical variables that are to be minimized; anyway, it is a non-convex problem and existing solution methods do not guarantee to achieve the optimal solution. The maximal bandwidth method maximizes an opportunity of progression for drivers and does not reduce delays necessarily; nevertheless, it is a quasi-concave problem and efficient solving algorithms exist to find the optimal solution.

The centralized solution of the traffic signal problem may provide better performance if it can be derived, but it has several shortcomings as a solution strategy. Firstly, solving this problem is usually intractable and hence not suitable for online decision making because the problem is complex (NP-hard) and of large-scale (especially when the problem involves a large time horizon and several intersections). Secondly, centralized solutions require global information about the status of the network. Thirdly, solving the problem centrally is not highly dependable, the failure of the central unit will result in complete failure of the system. On the other hand, distributed strategies can better avoid failures and the distributed approaches finds good application in different fields ([Adacher L. et al.,2014b], [Adacher L. et al.,2014a]).

## 6.3 Clustering algorithm

In general, clustering algorithms can be grouped into two groups: hierarchical or partitional. Both methods are applied in transport.
An hierarchical algorithms function either by, starting with each individual data point, progressively merging similar pairs of points to form a cluster hierarchy or, starting with all the data points in one cluster, by dividing clusters into smaller clusters successively. The optimal number of clusters is determined afterwards, using a dendrogram, which visualizes the variation within the clusters for different steps of the clustering procedure.
Instead, partitional clustering leads to only one partition, depending on the number of clusters that is chosen in advance. The K-means is the most popular partitional algorithm due to its simplicity when compared to other alternatives, but suffers from the issue to specify a value for the cluster count. Therefore is advisable to run the algorithm several times with different numbers of clusters to choice the best number of output clusters. k-means is also limited by the original

data of different size. For example, the use of Euclidean distance means that certain data relationships (for example spirals or/and lines) may not be clustered in the best manner.

As mentioned in Chapter 2, traffic supply can be represented as a network graph, where an intersection corresponds to a node, a road segment to a link. In aspect of key node assessment or subdivision of network, several approaches can be referred, e.g., the betweenness method, node deletion method, node contraction method, network nodes nearness and neighborhood key degrees assessment. In aspect of network subarea division, it is found be similar with the network community discovery. The Newman algorithm is a fast hierarchical method used to detect communities built around the idea of using centrality indices to find community boundaries. The advantage to use the Newman algorithm, based on topological characteristics of the network, is that it is considerably fast $O(N^2)$. Moreover the algorithm no need a prior knowledge of the community sizes nor of the number of communities.
In order to reduce the complexity of the Traffic Signal Synchronization problem, in this thesis the advantages of the k-means (simplicity and good to work on a large number of variables) and of the Newman(calculation of community and velocity) are considered to define new strategy for network clustering.

### 6.3.1 K-means clustering algorithm

K-means is one of the simplest unsupervised learning algorithms that solve the well known clustering problem. The procedure follows a simple and easy way to classify a given data set through a certain number of clusters (assume k clusters) fixed a priori. The main idea is to define k centers, one for each cluster. These centers should be placed in a cunning way because of different location causes different result. So, the better choice is to place them as much as possible far away from each other. The next step is to take each point belonging to a given

**Principal steps of K-means algorithm**

Given $K$ the number of clusters:

1 Initialize the center of the clusters

2 Attribute the closest cluster to each data point

3 Set the position of each cluster to the mean of all data points belonging to that cluster

4 Repeat Steps 2 and 3 until the centroids no longer move.

Figure 6.1: Steps of $KM$

data set and associate it to the nearest center. When no point is pending, the first step is completed and an early group age is done. At this point we need to re-calculate k new centroids as barycenter of the clusters resulting from the previous step. After we have these k new centroids, a new binding has to be done between the same data set points and the nearest new center. A loop has been generated. As a result of this loop we may notice that the k centers change their location step by step until no more changes are done or in other words centers do not move any more. This produces a separation of the objects into groups from which the metric to be minimized can be calculated. The steps for K-means algorithm are summarized in Fig6.1

Although it can be proved that the procedure will always terminate, the K-means algorithm does not necessarily find the most optimal configuration, corresponding to the global objective function minimum. The algorithm is also significantly sensitive to the initial randomly selected cluster centers. The K-means algorithm can be run multiple times to reduce this effect. For more details see ([Kanungo T. et al.,2002]).

### 6.3.2 Newman clustering algorithm

The basic requirements for a general community finding algorithm are that it should find natural divisions among the vertices without requiring the investigator to specify how many communities there should be, or placing restrictions on their sizes, and without showing the pathologies evident in the hierarchical clustering method, the Girvan-Newman algorithm detects communities by progressively removing edges from the original network. The connected components of the remaining network are the communities. Instead of trying to construct a measure that tells us which edges are the most central to communities, the Girvan-Newman algorithm focuses on edges that are most likely "between" communities. The Girvan-Newman algorithm extends the betweenness concept to the case of edges, defining the "edge betweenness" of an edge as the number of shortest paths between pairs of nodes that run along it. If there is more than one shortest path between a pair of nodes, each path is assigned equal weight such that the total weight of all of the paths is equal to unity. If a network contains communities or groups that are only loosely connected by a few inter-group edges, then all shortest paths between different communities must go along one of these few edges. Thus, the edges connecting communities will have high edge betweenness (at least one of them). By removing these edges, the groups are separated from one another and so the underlying community structure of the network is revealed. For more details see ([Girvan and Newman (2002)]). The algorithm's steps for community detection are summarized in Fig.6.2.

## 6.4 Nodes classification

The nodes of the network are classified considering three different parameters:

- *Degree*: Degree is the simplest of the node centrality measures by using the local structure around nodes only. In a binary network, the degree is the

**Principal steps of Newman algorithm**

1 The betweenness of all existing edges in the network is calculated first.

2 The edge with the highest betweenness is removed.

3 The betweenness of all edges affected by the removal is recalculated.

4 Steps 2 and 3 are repeated until no edges remain.

Figure 6.2: Steps of Newman

number of ties a node has.

- *Betweenness*: Betweenness centrality is an indicator of a node's centrality in a network. It is equal to the number of shortest paths from all vertices to all others that pass through that node.

- *Flow*: flow is the amount of flow directed into node. A flow must satisfy the restriction that the amount of flow into a node equals the amount of flow out of it, unless it is a source, which has only outgoing flow, or sink, which has only ingoing flow.

The node classification gives a score for each node based on its degree or its betweennees or its flow or weighted arithmetic mean of these three parameters.

On the bases of these scores is possible to understand the importance of each node compared to the network. We also utilize this nodes classification to give a score for each subnetwork. The score of the subnetwork is given by the sum of score of each node in the subnetwork. Given the partition, for each node and for each subnetwork the score is calculated. It is important for deciding on which subnetwork apply the surrogate method. A scheme of our approach to give a score for each subnetwork is given in Fig.6.3.

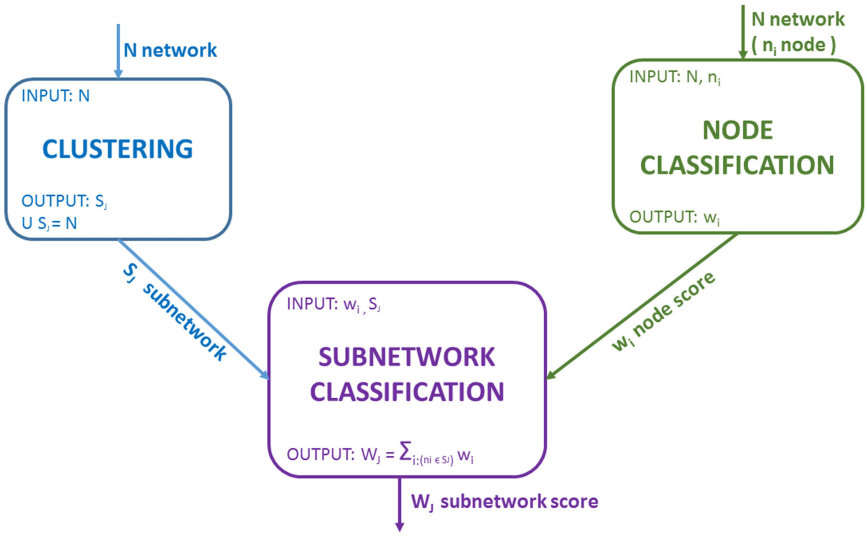


Figure 6.3: Procedure to give the subnetwork score

In Fig.6.4 is reported on left the clustering obtained by K-means partition and on right in red the main subnetwork (i.e. the subnetwork with the biggest score) and the most important nodes for each subnetwork.

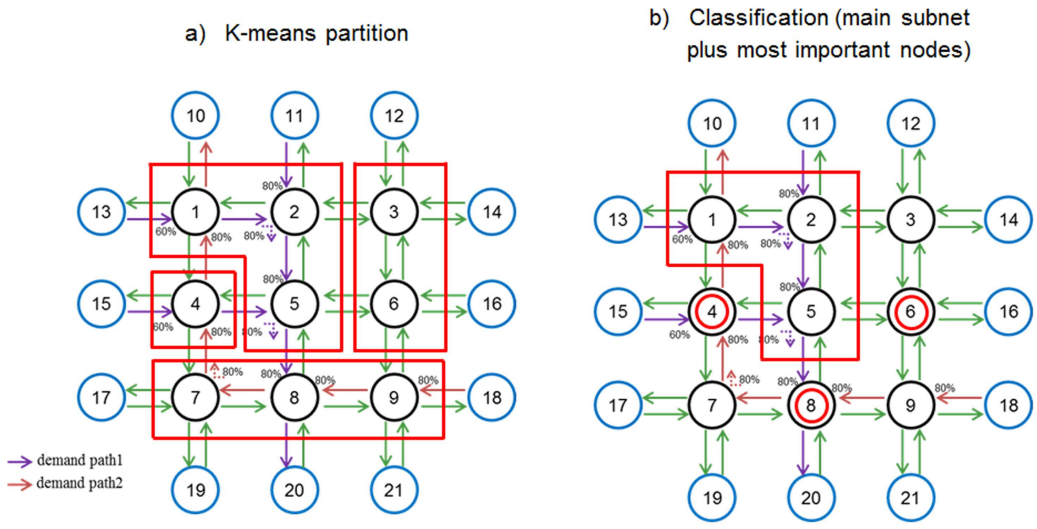


Figure 6.4: Subnetworks individuated with K-means partition and selection of important nodes.

**Principal steps of Hybrid algorithm**

0 Definition of $K$ clusters given by Newman

1 Calculate the score of each node by Classification Method.

2 Selection of the main nodes ($mn$) with the highest score. The size of the $mn$ is define with the equation

$$\frac{tot\ nodes}{K + (K - 1)}$$

If the $mn$ don't has at least one node from each cluster, the most important node from the not included clusters is added to $mn$.

3 The new clustering is given by the $K$ clusters defined with Newman plus the main subnet fixed in step 2

Figure 6.5: Steps of Hybrid algorithm

It is important to notice that the two clustering algorithms don't take in to account the classification method. For this reason we have also considered an hybrid algorithm see Fig. 6.5. This hybrid algorithm adds a set of $K + 1$ nodes, ($k$ is the number of clusters) selecting from the nodes with highest score, and at least one node for each cluster identified in the clustering process.
Although these experiments are still in progress, the new decomposition approaches give comforting results also for large scale network.

Another new algorithm based on K-means is proposed in Fig6.6 . Also in this clustering, the idea behind the algorithm, is to integrate the classification of nodes with topological characteristics of the network. In the *K-Means connected* algorithm, first original K-Means is applied and then, if it is necessary, the clusters are changed to define only cluster with nodes connected to each other. To apply the *K-Means connected* algorithm in best way, the initialization of number of clusters could be obtained by Newman algorithm or with the run of algorithm several times with different numbers of output clusters.

**Principal steps of *K-Means connected* algorithm**

0 Selection of the $K$ value

1 Definition of $K$ clusters given by K-Means based on the normalized values of degree, btw, inflow

2 Connection of the clusters in step 1:
WHILE all clusters are not connected DO
FOR all clusters

- IF cluster is connected → OK
- ELSE → moves node into the connected cluster

Figure 6.6: Steps of *K-Means connected*

## 6.5 Cooperation strategies

In addition to define new clustering algorithms, we have proposed different levels of cooperation. The choice of the cooperation strategy may depend from the traffic control system, it could be decentralized or centralized.

- **COOP** means that the $SM$ is applied on the subnetwork with the biggest score plus the most important nodes, one for each subnetworks fixed by the clustering approach (we call this new subnetwork coopnet).
- **COOP1** means that the $SM$ is before applied on coopnet, and then in parrallel way on the other subnetworks, considering fixed all the nodes also presented in coopnet.
- **COOP2** means that the $SM$ is before applied on coopnet, and the in series way on the other subnetworks. The $SM$ is applied to other subnetworks in

descending order of importance, but considering the most important node of each subnetworks fixed at the value of the precedent optimization.

- **COOP3** means that the $SM$ is applied as in COOP2 but the objective function considering in the $SM$ is calculated on subnetwork considered plus all nodes already optimized.

### 6.5.1 Cases study and Experiments

This paragraph summarized the results presented in [Adacher and Tiriolo (2016a)], [Adacher and Tiriolo (2016b)], [Adacher and Tiriolo (2016c)].
To obtain efficacy solutions for urban traffic we applied the optimization approach to different subnetworks.
We have compared the results of optimization approach applied on total network (centralized approach) with the results obtained considering different network partitions and different levels of cooperation. We want to analyze if the optimization must be applied on the total network or it is possible to obtain good results applying the surrogate method only on subnetworks. Each method is compared in terms of efficacy (value of $\Delta_{TD}$) and efficiency (value of $\Delta_{CT}$) its solution is calculated with the percentage difference compared to the optimization of the total net (Tot Net).
The initial state is defined with the total cycle time over the two phases fifty-fifty, 50 sec for each decision variables. The optimization model is stopped after 50 iterations ($k$) or if the solution is not improved after 20 iterations.

In the following 6.1 is considered the Newman partition and in Tab.6.2 is considered the K-means partition. We have also reported the results for the Hybrid decomposition (see Tab.6.3) and for the K-means with cluster connected (see Tab .6.4). Except for the Newman, the others partitions are based on the scores of inflow, degree and betweenness.

A comparison between the centralized approach (Tot Net) and the decentralized with different levels of cooperation is done. It is possible notice that if we increase the cooperation the solution improve but the approach needs more time.

**Test network with medium level of congestion**

For the preliminary experiments on clustering algorithms, we have used the same network with 9 four-way signal controlled intersection shown in the Fig. 5.1. Where the inflow demands is 500 [veic/h] from the nodes 11,13,15,18 during a simulation time of 400 sec.

For example, in Tab. 6.3 we considered the clustering given by the Newman algorithm: **[1,2,3,5,6]**,[**4**,7],[**8**,9] (in bold the main subnetork and the main nodes). In $COOP$ the $SM$ is applied on main subnetwork plus main nodes ([**1,2,3,4,5,6,8**]). In $COOP1$ it is applied before on coopnet ([1,2,3,4,5,6,8]) and the in parallel way on [**4**,7] considering the value of green time ratio for intersection 4 fixed, on [**8**,9] considering 8 fixed. In $COOP2$ the approach is the same but the $SM$ is applied in series. In $COOP3$ we need more information. The $SM$ is applied on coopnet ([**1,2,3,4,5,6,8**]), then on [**4**,7] considering the value of green time ratio for intersection 4 fixed, but the delay is calculated on the subnetowrk [**1,2,3,4,5,6,8**,7], and so on.

These results put in evidence that is possible find a good trade off between efficacy and efficiency. We get a worsening of objective function from 0.01% to 5.9%, against an improved calculation from 29% to 93%. It is evidence that the cooperation gives optimal solution very near to the centralized approach but with a significant reduction of calculate time.

**Test network with high level of congestion**

This case is the same of the previous one but has inflow demands higher. Inflow de-

Table 6.1: Decentralized vs centralized with Newman decomposition

| | subnetworks | **TD** | $\Delta_{TD}$ | $\Delta_{CT}$ |
|---|---|---|---|---|
| Newman | **[1,2,3,5,6]**,[**4**,7],[**8**,9] | | | |
| Tot Net | [**1,2,3,4,5,6,7,8,9**] | 5997 | | |
| main net | [**1,2,3,5,6**] | 6330 | 5.6% | −84% |
| COOP | [**1,2,3,4,5,6,8**] | 6318 | 6.5% | −34% |
| COOP1 | [1,2,3,4,5,6,8],[**4**,7],[**8**,9] | 6137 | 2.3% | −31% |
| COOP2 | [1,2,3,4,5,6,8],[**4**,7],[**8**,9] | 6135 | 2.3% | −31% |
| COOP3 | [1,2,3,4,5,6,8],[**4**,7],[**8**,9] | 5999 | 1.0% | −29% |

Table 6.2: Decentralized vs centralized with 4-Means decomposition

| | subnetworks | **TD** | $\Delta_{TD}$ | $\Delta_{CT}$ |
|---|---|---|---|---|
| 4-Means | **[1,2,5]**,[**6**,3],[**8**,7,9],[**4**] | | | |
| Tot Net | [**1,2,3,4,5,6,7,8,9**] | 5997 | | |
| main net | **[1,2,5]** | 6233 | 3.9% | −93% |
| COOP | **[1,2,4,5,6,8]** | 6081 | 1.4% | −50% |
| COOP1 | [1,2,4,5,6,8],[**6**,3],[**8**,7,9] | 6051 | 0.9% | −48% |
| COOP2 | [1,2,4,5,6,8],[**6**,3],[**8**,7,9] | 6051 | 0.9% | −48% |
| COOP3 | [1,2,4,5,6,8],[**6**,3],[**8**,7,9] | 5999 | 0.03% | −42% |

Table 6.3: Decentralized vs centralized with Hybrid decomposition

| | subnetworks | **TD** | $\Delta_{TD}$ | $\Delta_{CT}$ |
|---|---|---|---|---|
| Hybrid | [**1,2**,3,**5**,6],[**4**,7],[**8**,9] | | | |
| Tot Net | [**1,2,3,4,5,6,7,8,9**] | 5997 | | |
| COOP | [**1,2,4,5,8**] | 6352 | 5.9% | −43% |
| COOP1 | [1,2,4,5,8], [**1,2**,3,**5**,6],[**4**,7],[**8**,9] | 6324 | 3.9% | −29% |
| COOP2 | [1,2,4,5,8], [**1,2**,3,**5**,6],[**4**,7],[**8**,9] | 6302 | 5.1% | −37% |
| COOP3 | [1,2,4,5,8], [**1,2**,3,**5**,6],[**4**,7],[**8**,9] | 6031 | 0.6% | −78% |

mands is equal to 800 [veic/h] from the nodes 11,13,15,18 during a simulation time of 400 sec.

The following results present the same decompositions of the network test with different values of $TD$. Whereas the inflow demands are higher, and the transport supply is the

Table 6.4: Decentralized vs centralized with 3-Means connected decomposition

| | subnetworks | **TD** | $\Delta_{TD}$ | $\Delta_{CT}$ |
|---|---|---|---|---|
| 3-Means conn | **[1,2,4,5]**,[**8**,7,9],[**6**,3] | | | |
| Tot Net | [**1,2,3,4,5,6,7,8,9**] | 5997 | | |
| main net | **[1,2,4,5]** | 6352 | 5.9% | −43% |
| COOP | [**1,2,4,5,6,8**] | 6081 | 1.4% | −50% |
| COOP1 | [1,2,4,5,6,8],[**8**,7,9],[**6**,3] | 6051 | 0.9% | −48% |
| COOP2 | [1,2,4,5,6,8],[**8**,7,9],[**6**,3] | 6051 | 0.9% | −48% |
| COOP3 | [1,2,4,5,6,8],[**8**,7,9],[**6**,3] | 5997 | 0.01% | −36% |

same, the value of total delay is higher compared to the previous case.

Table 6.5: Decentralized vs centralized with Newman decomposition

| | subnetworks | **TD** | $\Delta_{TD}$ | $\Delta_{CT}$ |
|---|---|---|---|---|
| Newman | **[1,2,3,5,6]**,[**4**,7],[**8**,9] | | | |
| Tot Net | [**1,2,3,4,5,6,7,8,9**] | 6999 | | |
| main net | [**1,2,3,5,6**] | 7319 | 4.6% | −84% |
| COOP | [**1,2,3,4,5,6,8**] | 6318 | 7.5% | −56% |
| COOP1 | [1,2,3,4,5,6,8],[**4**,7],[**8**,9] | 7362 | 5.2% | −54% |
| COOP2 | [1,2,3,4,5,6,8],[**4**,7],[**8**,9] | 7354 | 5.1% | −53% |
| COOP3 | [1,2,3,4,5,6,8],[**4**,7],[**8**,9] | 7189 | 2.7% | −51% |

Table 6.6: Decentralized vs centralized with 4-Means decomposition

| | subnetworks | **TD** | $\Delta_{TD}$ | $\Delta_{CT}$ |
|---|---|---|---|---|
| 4-Means | **[1,2,5]**,[**6**,3],[**8**,7,9],[**4**] | | | |
| Tot Net | [**1,2,3,4,5,6,7,8,9**] | 6999 | | |
| main net | **[1,2,5]** | 7667 | 9.5% | −93% |
| COOP | **[1,2,4,5,6,8]** | 7481 | 6.9% | −70% |
| COOP1 | [1,2,4,5,6,8],[**6**,3],[**8**,7,9] | 7440 | 6.3% | −64% |
| COOP2 | [1,2,4,5,6,8],[**6**,3],[**8**,7,9] | 7443 | 6.3% | −44% |
| COOP3 | [1,2,4,5,6,8],[**6**,3],[**8**,7,9] | 7439 | 6.3% | −41% |

Table 6.7: Decentralized vs centralized with Hybrid decomposition

| | subnetworks | **TD** | $\Delta_{TD}$ | $\Delta_{CT}$ |
|---|---|---|---|---|
| Hybrid | [**1,2**,3,**5**,6],[**4**,7],[**8**,9] | | | |
| Tot Net | [**1,2,3,4,5,6,7,8,9**] | 6999 | | |
| COOP | [**1,2,4,5,8**] | 7461 | 6.6% | −83% |
| COOP1 | [1,2,4,5,8], [**1,2**,3,**5**,6],[**4**,7],[**8**,9] | 7422 | 6.0% | −65% |
| COOP2 | [1,2,4,5,8], [**1,2**,3,**5**,6],[**4**,7],[**8**,9] | 7422 | 6.0% | −62% |
| COOP3 | [1,2,4,5,8], [**1,2**,3,**5**,6],[**4**,7],[**8**,9] | 7154 | 2.2% | −59% |

Table 6.8: Decentralized vs centralized with 3-Means connected decomposition

| | subnetworks | **TD** | $\Delta_{TD}$ | $\Delta_{CT}$ |
|---|---|---|---|---|
| 3-Means conn | [**1,2,4,5**],[**8**,7,9],[**6**,3] | | | |
| Tot Net | [**1,2,3,4,5,6,7,8,9**] | 6999 | | |
| main net | [**1,2,4,5**] | 7488 | 7.0% | −92% |
| COOP | [**1,2,4,5,6,8**] | 7481 | 6.9% | −70% |
| COOP1 | [1,2,4,5,6,8],[**8**,7,9],[**6**,3] | 7525 | 7.5% | −45% |
| COOP2 | [1,2,4,5,6,8],[**8**,7,9],[**6**,3] | 7525 | 7.5% | −45% |
| COOP3 | [1,2,4,5,6,8],[**8**,7,9],[**6**,3] | 7163 | 2.3% | −61% |

Found the optimal solution with an high level of congestion is more difficult and require computational time higher compared to the previous case. For this reason, the decomposition approaches get a small worsening of efficacy but major efficiency. In the last case, we get a worsening of objective function from 2.2% to 9.5%, against an improved calculation from 41% to 93%.

In some cases, the results of COOP1 and COOP2 are really close because, with a small network, the difference between the two cooperations is only for the optimization of the last node. In these cases, the perturbation of the last node (the least important) fails to improve the solution and the optimization algorithm stops in a short time, after the calculation of the OF for a few times (4 or 5).

In general the most efficacy is obtained with the COOP3. The results put in evidence that with the new proposed algorithms (Hybrid and *K-means connected*) is possible find a good trade off between efficacy and efficiency. For medium and high level of

congestion, the most efficacy solution is obtained by Hybrid or *K-means connected* algorithms.

From these previous experiments is not possible to well understand the influence of flow and topological characteristics on the solution optimality. It seems that a small cooperation of the most important nodes gives a good solution compared to the optimal. In the following experiments, we test if these encouraging results are still true for large networks.

**Large network with medium level of congestion**

To deepen the analysis of the clustering algorithms, has been defined a large scale network with 194 links, 42 signalized intersections and 26 centroids. The large network mimics the supply and demand of the test network with the principal paths represented in the test network (see the paths of Fig.5.1 ).

The inflow demands is 800 [veic/h] from the input centroids of principal paths during a simulation time of 600 sec.

This analysis is still in progress, we have started to calculate the results applying the COOP3 strategy because it has obtained the most efficacy solution for the small network.

When K-means algorithm is applied the values of $K$ is equal to the number of clusters given by Newman plus one. While, for the large network, the Tab. 6.10 reports the results calculated with the $K$ value equal to the the number of clusters given by Newman. The comparison between the Tab. 6.10 and 6.11 demonstrates that applying the K-means algorithm with $K$ equal to the number of clusters given by Newman plus one we can obtain better results in terms of efficacy and efficiency.

Table 6.9: Large Net: dec. vs cen. with Newman decomp.

| | subnetworks | **TD** | $\Delta_{TD}$ | $\Delta_{CT}$ |
|---|---|---|---|---|
| Newman | [**1 2 3 4 5 6 7 8 9 14 16 18**] [32 33 34 38 39 40 41 45 46 47 48] [**19** 20 21 31 35 36 37 42 43 44][22 23 24 25 26 27 **28** 29 30] | | | |
| Tot Net | [**1 2 3 4 5 6 7 8 9 14 16 18 19 20 21 22 23 24 25 26 27 28 29 30 31 32 33 34 35 36 37 38 39 40 41 42 43 44 45 46 47 48**] | 15146 | | |
| COOP | [**1 2 3 4 5 6 7 8 9 14 16 18 19 28**] | 17639 | 16% | −47% |
| COOP3 | [1 2 3 4 5 6 7 8 9 14 16 18 19 28] [32 33 34 38 39 40 41 45 46 47 48] [**19** 20 21 31 35 36 37 42 43 44] [22 23 24 25 26 27 **28** 29 30] | 15515 | 2.4% | −36% |

Table 6.10: Large Net: dec. vs cen. with 4-Means decomp.

| | subnetworks | **TD** | $\Delta_{TD}$ | $\Delta_{CT}$ |
|---|---|---|---|---|
| 4-means | **[3 5 6 8 9 16 18 20 21 25 26 28 29 31 32 33 36 37 38 39]** [4 7 **19** 34 35 41 48] [1 **2** 22 23 24 27 43 44 45 46 47] [14 **16** 30 40 42] | | | |
| Tot Net | **[1 2 3 4 5 6 7 8 9 14 16 18 19 20 21 22 23 24 25 26 27 28 29 30 31 32 33 34 35 36 37 38 39 40 41 42 43 44 45 46 47 48]** | 15146 | | |
| COOP | **[2 3 5 6 8 9 16 18 19 20 21 25 26 28 29 31 32 33 36 37 38 39]** | 18168 | 20% | −71% |
| COOP3 | [2 3 5 6 8 9 16 18 19 20 21 25 26 28 29 31 32 33 36 37 38 39] [4 7 **19** 34 35 41 48] [1 **2** 22 23 24 27 43 44 45 46 47] [14 **16** 30 40 42] | 15204 | 0.4% | −41% |

Table 6.11: Large Net: dec. vs cen. with 5-Means decompo.

| | subnetworks | **TD** | $\Delta_{TD}$ | $\Delta_{CT}$ |
|---|---|---|---|---|
| 5-means | **[4 7 19 34 35 41 48]** [ 5 8 14 16 **20** 30 33 36 40][6 9 **18** 21 28 31 32 ][ 2 3 22 25 26 29 37 **38** 39 ][ 1 23 24 27 **42** 43 44 45 46 47] | | | |
| Tot Net | **[1 2 3 4 5 6 7 8 9 14 16 18 19 20 21 22 23 24 25 26 27 28 29 30 31 32 33 34 35 36 37 38 39 40 41 42 43 44 45 46 47 48]** | 15146 | | |
| COOP | **[4 7 19 34 35 41 48 42 20 18 38]** | 16233 | 7.2% | −89% |
| COOP3 | [4 7 19 34 35 41 48 42 20 18 38] [ 5 8 14 16 **20** 30 33 36 40][6 9 **18** 21 28 31 32 ] [ 2 3 22 25 26 29 37 **38** 39 ][ 1 23 24 27 **42** 43 44 45 46 47] | 15192 | 0.3% | −69% |

Also the results for the large scale network confirms the previous assertions. The results show that the Hybrid algorithm obtains best results compared to Newman and K-means algorithms. In particular, whit the Hybrid algorithm we get a worsening of objective function from 0.09% to 0.2%, against an improved calculation from 53% to 89%.

Table 6.12: Large Net: dec. vs cen. with Hybrid decomp.

| | subnetworks | **TD** | $\Delta_{TD}$ | $\Delta_{CT}$ |
|---|---|---|---|---|
| Hybrid | [1 2 3 **4** 5 **6 7** 8 **9 14 16 18**] [32 33 **34** 38 39 40 **41** 45 46 47 **48**] [**19 20** 21 **31 35** 36 37 42 43 44] [22 23 24 25 26 27 **28** 29 30] | | | |
| Tot Net | **[1 2 3 4 5 6 7 8 9 14 16 18 19 20 21 22 23 24 25 26 27 28 29 30 31 32 33 34 35 36 37 38 39 40 41 42 43 44 45 46 47 48]** | 15146 | | |
| COOP | **[4 6 7 9 14 16 18 19 20 28 31 34 35 41 48]** | 15177 | 0.2% | −79% |
| COOP3 | [4 6 7 9 14 16 18 19 20 28 31 34 35 41 48] [1 2 3 **4** 5 **6 7** 8 **9 14 16 18**] [32 33 **34** 38 39 40 **41** 45 46 47 **48**] [**19 20** 21 **31 35** 36 37 42 43 44] [22 23 24 25 26 27 **28** 29 30] | 15159 | 0.09% | −53% |

Table 6.13: Large Net: dec. vs cen. with 4-Means connected decomp.

| | subnetworks | **TD** | $\Delta_{TD}$ | $\Delta_{CT}$ |
|---|---|---|---|---|
| 4-Means conn | [ 3 6 8 9 18 21 25 26 28 29 31 32 33 37 38 39][ 1 2 22 23 24 27 42 43 44 45 46 47 5 30 **40** ][ 4 7 19 34 35 **41** 48][14 **16** 20 36] | | | |
| Tot Net | **[1 2 3 4 5 6 7 8 9 14 16 18 19 20 21 22 23 24 25 26 27 28 29 30 31 32 33 34 35 36 37 38 39 40 41 42 43 44 45 46 47 48]** | 15146 | | |
| COOP | **[3 6 8 9 16 18 21 25 26 28 29 31 32 33 37 38 39 40 41]** | 17890 | 18.1% | −75% |
| COOP3 | [ 3 6 8 9 18 21 25 26 28 29 31 32 33 37 38 39][ 1 2 22 23 24 27 42 43 44 45 46 47 5 30 **40** ][ 4 7 19 34 35 **41** 48][14 **16** 20 36] | 15181 | 0.2% | −14% |

### 6.5.2 Conclusions

Urban signal timing is a non-convex problem and finding an optimal solution for not very small networks may take a long time. For this reason it is very heavy apply the

optimization of traffic lights for large networks and in real-time. In order to solve that problem, in this thesis is proposed a robust optimization algorithm for signal setting problem based on the CTM-UT.

The experiments demonstrate that the CTM-UT is suitable to obtain good accuracy (between the 2% and 4%) compared to microscopic simulation tools (i.e., VISSIM and SUMO). At the same time, the CTM-UT framework is suitable to take into account the urban complexity keeping the benefits of macroscopic model (i.e., low computational time and not too many information to manage).

To improve the calibration process of macroscopic models, which require a great effort in terms of time and resources, a new method to calibrate the congestion wave speed via optimization is proposed.

In order to minimize total traffic delay with signal synchronization, the SM has been improved. The new version of the optimization model is suitable to obtain solution with more efficiency (at least the 4%) and efficacy (at least the 10%) compared to the classic SM.

Lastly, new decompositions of network nodes are proposed where the nodes classification is integrated with a clustering algorithm based on topological characteristics of the network. Given the subnetworks, the SM is applied to solve the traffic signal synchronization problem. Compared to considering the total network, the optimization integrated with the new "hybrid" decomposition approaches can reduce the computational time with a small loss of accuracy. For example, on a small network, an improved efficiency of 78% and a efficacy loss of 0.6% have been obtained. While, on a large network, an improved efficiency of 53% and a efficacy loss of 0.09% have been obtained.

Such results demonstrate that the network decomposition proposed in this thesis allow to make Synchronizing Traffic Signals suitable for real-time decision and for large-scale networks.

The knowledge of the variations of travel time is fundamental in the evaluation of Dynamic Traffic Assignment (DTA) strategies and in the travelersâ choices. Since that the CTM-UT is suitable to predict the travel time for traffic demands detailed at urban level (link, lane, turning movement), an interesting future research will be focused

to the application of the DTA combined to the new proposed optimization algorithm. The integration of the assignment model into the defined control strategy might lead to increase the computational time but this problem can be reduced with the presented decomposition approaches.

# Bibliography

[EU Explained: Transport (2016)] 'Transport Connecting Europe's citizens and businesses. The European Union Explained ', *European Commission*, 2016

[Urban mobility (2014)] Ariane D., 'Urban mobility: Shifting towards sustainable transport systems ', *European Parliamentary Research Service Blog* , 2014

[Urban Mobility Scorecard (2015)] Schrank D., Eisele B., Lomax T., and Bak Jim 'Urban Mobility Scorecard ', *Texas Transportation Institute, The Texas AM University System.*, 2015

[Papageorgiou et al., (2003)] Papageorgiou, M., Diakaki, C., Dinopoulou, V., Kotsialos, A., Wang, Y.: 'Review of Road Traffic Control Strategies ', *Proceedings of the IEEE, Vol. 91, issue 12*, 2003, pp.2043–2067

[Alecsandru and Ishak (2007)] Alecsandru C. and Ishak S. Modeling Randomness In Driving Behavior Within A Cell Transmission Based Framework , *National Research Council* , 2007

[Kang (2000)] Kang Y.-S.: Delay, stop and queue estimation for uniform and random traffic arrivals at fixed-time signalized intersections , *PhD thesis , Virginia Polytechnic Institute and State University* , 2000

[Hu et al., (2010)] Hu X., Wang W. and H. Sheng: Urban Traffic Flow Prediction with Variable Cell Transmission Model , *J Transpn Sys Eng IT, 10(4)* , 2010

[Daganzo (1994)] Daganzo C.: 'The cell transmission model: a dynamic representation of highway traffic consistent with the hydrodynamic theory. ', *Transportation Research, Part B, 28(4)*, 1994, pp.269–287

[Daganzo (1995)] Daganzo C.: 'The cell transmission model, Part II: Network traffic. ', *Transportation Research, Part B, 29(2)*, 1995, pp. 79–93

[Lighthill and Whitham (1955)] Lighthill, M., Whitham, G.: 'On kinematic waves I: Flow movement in long rivers. II: A theory of traffic flow on long crowded roads ', *Proc. Royal Society of London, Part A, 229(1178)*, 1955, pp.281–345

[Richards (1956)] Richards, P.: 'Shock waves on the highway ', *Operations Research, 4(1)*, pp.42–51, 1956

[HCM (2010)] 'Highway Capacity Manual , *3rd Ed., National Research Council, Transportation Research Board, Washington, D.C* , 2010

[Dotoli and Fanti (2006)] Dotoli M. and Fanti M. P.: An urban traffic network model via coloured timed Petri nets , *Control Engineering Practice Volume 14, Issue 10* , 2006

[van den Berg et al., (2003)] Van den Berg A., Hegyi B., De Schutter, Hellendoorn J.: A macroscopic traffic flow model for integrated control of freeway and urban traffic networks. , *In: 42nd IEEE International Conference on Decision and Control, Hawaii, 2774 - 2779* , 2003

[Kashani and Saridis (1983)] Kashani, H.R., Saridis, G.N.: 'Intelligent control for urban traffic systems ', *Journal Automatica (Journal of IFAC) archive Volume 19 Issue 2*, pp. 191–197, 1983

[Chevallier and Leclercq (2007)] Chevallier E., Leclercq L.: 'A macroscopic theory for unsignalized intersections ', *Transportation Research Part B, Vol. 41* , 2007

[Abu-Lebdeh et al., (2007)] Abu-Lebdeh, G., Chen, H., Benekohal, R.F.: 'Modeling traffic output for design of dynamic multi-cycle control in congested conditions', *Journal of Intelligent Transportation Systems 11 (1)*, pp. 25–40 , 2007,

[Tonguz et al., (2009)] Tonguz, O.K., Viriyasitavat, W., Fan Bai: 'Modeling urban traffic: A cellular automata approach ', *IEEE Communications Magazine*, 2009

[Flötteröd and Nagel (2005)] Flötteröd, G., Nagel K.: 'Some Practical Extensions to the Cell Transmission Model. ', *Proceedings of the 8th International IEEE Conference on Intelligent Transportation Systems*, 2005

[Kurzhanskiy (2007)] Kurzhanskiy, A.A.: 'Modeling and Software Tools for Freeway Operational Planning ', *Electrical Engineering and Computer Sciences University of California at Berkeley*, 2007

[Godunov (1959)] Godunov, S.K.: 'A Difference Scheme for Numerical Solution of Discontinuous Solution of Hydrodynamic Equations ', *Math. Sbornik*, 1959

[Daganzo et al., (1997)] Daganzo, C., Lin, W.-H., del Castillo, J.: 'A simple physical principle for the simulation of freeways with special lanes and priority vehicles ', *Transportation Research Part B 31 (2)*, 1997, pp.103–125

[Daganzo (1997)] Daganzo, C.F.: 'A Continuum Theory of Traffic Dynamics for Freeways with Special Lanes ', *Transportation Research, Vol. 31B, No. 2*, 1997

[Lin and Ahanotu (1995)] Lin, W.-H., Ahanotu, D.: 'Validating the basic cell transmission model on a singlefreeway link ', *University of California: Berkeley*, 1995

[Smilowitz and Daganzo (1999)] Smilowitz, K.R., Daganzo, C.F.: 'Predictability of time dependent traffic backups and other reproducible traits in experimental highway data ', *California PATH Program, Institute of Transportation Studies, Berkeley*, 1999

[Lin and Daganzo (1994)] Lin, W.-H., Daganzo, C.F.: 'Technical descrip tion of NETCELL: general framework and data structure ', *University of California: Berkeley*, 1994

[Cayford (1997)] Cayford, R., Lin, W.-H., Daganzo, C.F.: 'The NETCELL simulation package: technical description ', *University of California: Berkeley*, 1997

[Jin and Zhang (2004)] Jin, W.L., Zhang, H.M.,: 'Multicommodity kinematic wave simulation model of network traffic flow', *Transportation Research Record 1883, 5967.*, 2004

[Ni and Leonard (2005)] Ni, D., Leonard, J.D.,: 'A simplified kinematic wave model at a merge bottleneck', *Applied Mathematical Modelling 29 (11), 10541072*, 2005

[Daganzo (1999)] Daganzo, C.F.: 'The lagged cell-transmission model ', *14th ISTTT Symposium, Jerusalem, Israel*, 1999

[Szeto (2008)] Szeto, W.Y.: 'Enhanced Lagged Cell-Transmission Model for Dynamic Traffic Assignment ', *Transportation Research Record: Journal of the Transportation Research Board, No. 2085, Washington, D. C.*, 2008, pp.76–85

[Muñoz et al., (2006)] Muñoz, L., Sun, X., Horowitz, R., Alvarez, L.: 'Piecewise-Linearized Cell Transmission Model and Parameter Calibration Methodology ', *Transportation Research Board of the National Academies, Washington, D.C.*, 2006 pp.183–191

[Gomes and Horowitz (2006)] Gomes, G., Horowitz, R.: 'Optimal freeway ramp metering using the asymmetric cell transmission model', 2006

[Laval and Daganzo (2006)] Laval, J. A., Daganzo, C.F.: 'Lane-changing in traffic streams. ', *Transportation Research Part B, Vol. 40*, 2006, pp.251–264

[Ziliaskopoulos and Lee (1997)] Ziliaskopoulos, A.K., Lee, S.: 'A Cell Transmission Based Assignment Simulation Model for Integrated Freeway/Surface Street Systems ', *In Paper presented at the 76th TRB Annual Meeting*, 1997

[Ishak et al., (2006)] Ishak, S., Alecsandru, C., Seedah, D.: 'Improvement and Evaluation of the Cell-Transmission Model for Operational Analysis of Traffic Networks: A Freeway Case Study ', *Transportation Research Record: Journal of the Transportation Research Board, No. 1965, Washington, D.C.*, 2006, pp.171–182

[Hoogendoorn (1996)] Hoogendoorn, S.P.: 'Multiclass continuum modeling of multilane traffic flow ', *Transport and Planning. Delft, Delft University of Technology. PhD*, 1996

[Helbing (1996)] Helbing, D.: 'Modeling multilane traffic flow with queuing effects ', *Physica A 242*, 1997, pp. 175–194

[Ngoduy (2006)] Ngoduy, D.: 'Macroscopic discontinuity modeling for multiclass multilane traffic flow operations ', *Transport and Planning. Delft, Delft University of Technology. PhD.*, 2006

[Rouphail (1989)] Rouphail, N., Akcelik, R.: 'Progression adjustment factors at signalized intersections ', *Transportation Research Record 1225*, 1989, pp.8–17

[Liu (2008)] Liu, Y., Yu, J., Chang, G.L., Rahwanji, S.: 'A Lane-group Based Macroscopic Model for Signalized Intersections Account for Shared Lanes and Blockages ', *Intelligent Transportation Systems, 11th International IEEE Conference*, 2008

[Liu et al., (2011)] Liu, Y., Yu, J., Chang, G.L.: 'An arterial signal optimization model for intersections experiencing queue spillback and lane blockage ', *Transportation Research Part C: Emerging Technologies. Vol. 19*, 2011

[Lo (1999)] Lo, H.K.: 'A Novel Traffic Signal Control Formulation ', *Transportation Research Part A. Vol. 33*, 1999

[Lo (2001)] Lo, H.K.: 'A Cell-Based Traffic Control Formulation: Strategies and Benefits of Dynamic Timing Plans ', *Transportation Science, Vol. 35, No. 2*, 2001

[Lo (2004)] Lo, H.K., Chow, A.H.F. : 'Control Strategies for Oversaturated Traffic ', *Journal of Transportation Engineering, Vol. 130, No. 4*, 2004

[Lebacque (1984)] Lebacque, J.: 'Semi-macroscopic simulation of urban traffic ', *In: Proceedings of the International AMSE Conference Modelling Simulation, vol. 4. Minneapolis, USA*, 1984, pp.273–292

[Elloumi et al., (1994)] Elloumi, E., Hadj Salem, H., Papageorgiou, M.: 'METACOR, a macroscopic modelling tool for urban corridors ', *TRISTAN II Int. Conf., Capri*, 1994

[Wang (2010)] Wang, P.: 'Conditional cell transmission model for two way arterial in oversaturated conditions ', *USA: University of Alabama*, 2010

[Buisson (1996)] Buisson, C., Lebacque, J.P., Lesort, J.: 'STRADA. A discretized macroscopic model of vehicular traffic flow in complex networks based on the Godunov scheme ', *In: Symposium on Modelling, Analysis and Simulation, held at CESA 1996 IMACS Multiconference, vol. 2*, 1996

[Pohlmann and Friedrich (2010)] Pohlmann, T., Friedrich, B.: 'Online control of signalized networks using the cell transmission model ', *Inntelligent Transportation Systems (ITSC), 13th International IEEE Conference on*, 2010

[Ziliaskopoulos (2000)] Ziliaskopoulos, A.K.: 'A Linear Programming Model for the Single Destination System Optimum Dynamic Traffic Assignment Problem ', *Transportation Science Volume 34 Issue 1*, 2000, pp. 37–49

[Li (2011)] Li, Z.: 'Modeling Arterial Signal Optimization with Enhanced Cell Transmission Formulations ', *Journal of Transportation Engineering, Vol. 137, No. 7, July 1* , 2011

[Adacher et al., (2014)] Tiriolo, M., Adacher, L., Cipriani, E.: 'An urban traffic flow model to capture complex flow interactions among lane groups for signalized intersections ', *Procedia - Social and Behavioral Sciences Volume 111, 5* , 2014, pp.839–848

[Adacher and Tiriolo (2015a)] Adacher L. and Tiriolo M., : 'A New Node Model based on CTM-UT with Capacity Determination , *Transportation Research Procedia - Social and Behavioral Sciences Volume 10, Pages 21-30* , 2015

[Adacher and Tiriolo (2015b)] Adacher L. and Tiriolo M., : 'A New Methodology to Calibrate the Congestion Wave for the Cell Transmission Model for Urban Traf-

fic. ', *IEEE 18th International Conference on Intelligent Transportation Systems, Las Palmas* , 2015, pp.606-611

[Long et al. (2011)] Long J., Gao Z., Zhao X., Lian A. and Orenstein P., Urban Traffic Jam Simulation Based on the Cell Transmission , *Networks and Spatial Economics, Vol. 11* , 2011

[Lebacque and Khoshyaran (2002)] Lebacque, J. P., Khoshyaran, M. M.: 'First-Order Macroscopic Traffic Flow Models for Networks in the Context of Dynamic Assignment ', *Transportation Planning: State of the Art, Edited by M. Patriksson an M. Labbe, Kluwer Academic Publishers, Dordrecht, Netherlands*, 2002

[Flötteröd and Rohde (2011)] Flötteröd, G., Rohde, J.: 'Operational macroscopic modeling of complex urban road intersections ', *Transportation Research Part B 45,* , 2011, pp.903–922

[Tampere et al., (2011)] Tampere, C., Corthout, R., Cattrysse, D., Immers, L.: 'A generic class of first order node models for dynamic macroscopic simulations of traffic flows ', *Transportation Research Part B 45 (1)*, 2011, pp.289–309

[Cayford et al., (2011)] R. Cayford, W.-H. Lin, C. F. Daganzo , 'The NETCELL simulation package: technical description ', *University of California: Berkeley* , 1997

[Troutbeck and Kako (1999)] Troutbeck, R., Kako, S.: 'Limited priority merge at unsignalized intersections ', *Transportation Research Part A 33 (34), 291304* , 1999

[Brilon and Wu (2001)] Brilon W. and Wu N.: 'Capacity at unsignalized intersections derived by conflict technique', *Transportation Research Record, 82-90* , 2001

[Troutbeck and Brilon (1999)] Troutbeck R., Brilon, W.: 'Chapter 8: unsignalized intersection theory', *In: Gartner, N., Messer, C., Rathi, A. (Eds.), Monograph on Traffic Flow Theory.Oak Ridge National Laboratory, Federal Highway Administration.*,1999

[Wu (1999)] Wu N.: 'An Approximation for the Distribution of Queue Lengths at Unsignalised Intersections ', *In Akcelik, R. (ed.), Proceeding of the second International Symposium on Highway Capacity, Sydney, 1994, Volume 2, pp. 717-736* , 1999

[Krauss et al., (1997)] Krauss S., Gawron C., Wagner P. : 'Metastable States in a Microscopic Model of Traffic Flow', *Front Cover.. Univ.- 12 pages* , 1997

[Gawron (1999)] Gawron C.: 'Simulation-Based Traffic Assignment – Computing User Equilibria in Large Street Networks ', *Ph.D. Thesis, Universitat zu Koln*, 1999

[Krajzewicz et. al, (2012)] Krajzewicz D., Erdmann J., Behrisch M. and Bieker L., 'Recent development and applications of SUMO - simulation of urban mobility.' ternational Journal On Advances in Systems and Measurements 5.3 and 4: 128-138, 2012

[Ma and Abdulhai (2002)] Ma T., Abdulhai B., 'Genetic Algorithm-Based Optimization Approach and Generic Tool for Calibrating Traffic Microscopic Simulation Parameters ', Transportation Research Record: Journal of Transportation Research Board, No.1800, pp.6-15, 2002

[Lee et. al, (2001)] Lee D. H., Yang X., Chandrasekar P.: 'Parameter Calibration for PARAMICS Using Genetic Algorithm ', Preprint CD-ROM 80th Annual Meeting , Transportation Research Board 01-2399, 2001

[Lee and Ozbay (2008)] Lee J.-B., Ozbay K.: 'Calibration of a Macroscopic Traffic Simulation Model Using Enhanced Simultaneous Perturbation Stochastic Approximation Methodology ', Preprint CD-ROM 87th TRB Annual Meeting, Transportation Research Board, Washington, D. C., 2008.

[Adacher and Cipriani (2010)] L. Adacher and E. Cipriani: 'A surrogate approach for the global optimization of signal settings and traffic assignment problem '*Intelligent Transportation Systems (ITSC) 13th International IEEE Conference on , vol., no., pp.60,65, 19-22 doi: 10.1109/ITSC.2010.5624975* , Sept 2010

[Gokbayrak and Cassandras (2002)] Gokbayrak K. and Cassandras C. G., : 'A Generalized Surrogate Problem Methodology for On-Line Stochastic Discrete Optimization', *J. of Optimization Theory and Applic., Vol. 114, 1,pp. 97-132,* 2002.

[Adacher and Cassandras (2014)] Adacher L. and Cassandras C.G.,: 'Lot size optimization in manufacturing systems: the surrogate method ', *International Journal of Production Economics, Volume 155, September 2014, Pages 418-426, ISSN 0925-5273, http://dx.doi.org/10.1016/j.ijpe.2013.07.026.* , 2014

[Burghout (2004)] Burghout W., : 'Hybrid microscopic-mesoscopic traffic simulation', PhD thesis, Division of Transportation and Logistics, Royal Institute of Technology, 2004

[Zhang et al., (2014)] L. Zhang, Y. Ma, and L. Shi 'A hybrid traffic flow model for real-time freeway traffic simulation', KSCE Journal of Civil Engineering, 18, (4), 1160-1164, 2014

[Bourrel and Lesort (2014)] E. Bourrel and J.-B. Lesort , *Mixing microscopic and macroscopic representations of traffic fow: Hybrid model based on Lighthill-Whitham-Richards theory.* Transportation Research Record: Journal of the Transportation Research Board 1852(1): 193, 2003

[Adacher and Tiriolo (2016c)] Adacher L. and Tiriolo M., 'Stochastic Optimization for Macroscopic Urban Traffic Model with Microscopic Elements' *Computer Modelling and Simulation (UKSim), 2016 UKSim-AMSS 18th International Conference on, IEEE*, 2016

[Goliya and Kumar (2012)] Goliya H. S. and Nitin K.,'Jain Synchronization of Traffic Signals :A Case Study Eastern Ring Road ', *Indore. International Journal of Advanced Technology in Civil Engineering, ISSN: 2231 721, Volume-1, Issue-2.* ,2012

[Adacher (2012)] Adacher L.:'A global optimization approach to solve the traffic signal synchronization problem', *Procedia - Social and Behavioral Sciences, Volume 54, 4 October 2012, Pages 1270-1277, ISSN 1877-0428*,2012

[Adacher L. et al.,2015] Adacher L.:'The global optimization of signal settings and traffic assignment combined problem: a comparison between algorithms', *Advances in Transportation Studies.Issue 36, p35-48.* ,2015

[Khaki and Haghighat (2014)] Khaki A. M. and Haghighat P. J.,:'The impacts of traffic signal timings optimization on reducing vehicle emissions and fuel consumption by Aimsun and Synchro software's (Case study: Tehran intersections) ', *International journal of civil and structural engineering, Volume 5, No 2.* , 2014

[Xiaojian H. et al.,2015] Xiaojian H. et al.,:'Reserach article traffic signal syncronitation in the saturated high-density grid road. ', *Network computational intelligence and neuroscience* , 2015

[Stevanovic A. et al.,2009] Stevanovic A. et al.,:'Optimizing Traffic Control to Reduce Fuel Consumption and Vehicular Emissions Integrated Approach with VISSIM, CMEM, and VISGAOST. ', *Transportation Research Record: Journal of the Transportation Research Board, No. 2128, Transportation Research Board of the National Academies, Washington, D.C., pp. 105-113. DOI: 10.3141/2128-11.*, 2009

[Cohen and Liu (1986)] Cohen S. and Liu C.,:'The Bandwidth Constrained TRANSYT Signal-Optimization Program ', *Transportation Research Record, Vol. 1057, pp.1-7.* 1986

[Cohen S.L.,1983] Cohen S.L.,:'Concurrent Use of MAXBAND and TRANSYT Signal Timing Programs for Arterial Signal Optimization', *Transportation Research Record, Vol. 906, pp. 81-84.* , 1983

[Hadi and Wallace (1993)] Hadi M. and Wallace C.,:'Algorithm to Optimize Signal Phasing ', *Transportation Research Record, Vol. 1421.*, 1993

[Malakapalli and Messer (1983)] Malakapalli M.P. and Messer C.J.,:'Enhancements to the PASSER II-90 Delay Estimation Procedures ', *Transportation Research Record, Vol. 1421, pp. 94-103* ,1983

[Gartner and Hou (1994)] Gartner N. and Hou G.,:'Performance Evaluation of Multi-Band Progression Method ', *7th IFAC/IFORS Symposium on "Transportation Systems: Theory and Application of Advanced Technology", Tianjin, China, pp. 981-986, 24-26 August.* ,1994

[Papola and Fusco (2000)] Papola N. and Fusco G.,:'A new analytical model for traffic signal synchronization', *Proc. of the 2nd ICTTS Conference, Beijing, China, 31 July-2 August*, 2000.

[Adacher L. et al.,2014a] Adacher L. et al.,'Decentralized Spatial Decomposition for Traffic Signal Synchronization' , *Transportation Research Procedia, Volume 3, Pages 992-1001, ISSN 2352-1465.*

[Adacher L. et al.,2014b] Adacher L. et al., 'Decentralized Assignment for Intelligent Electric Vehicles to Recharge Stations ' , *16th International Conference on Computer Modelling and Simulation (UKSim), pp. 357-362.*, 2014

[Girvan and Newman (2002)] Girvan M. and Newman M. E. J., 'Community structure in social and biological networks. ' *Proc. Natl. Acad. Sci. USA 99, 78217826* ,2002

[Adacher and Tiriolo (2016a)] Adacher L. and Tiriolo M., 'Distributed urban traffic signal optimization based on macroscopic model ' , *Innovative Computing Technology (INTECH) 2016 Sixth International Conference on, pp. 605-610, Dublin (Ireland)*, 2016

[Adacher and Tiriolo (2016b)] Adacher L. and Tiriolo M., 'A Distributed Approach for Traffic Signal Synchronization Problem ' , *Mathematics and Computers in Sciences and in Industry (MCSI), 2016 Third International Conference on, Chania(Greece)*, 2016

[Adacher and Tiriolo (2016c)] Adacher L. and Tiriolo M., 'Decentralized Vs Centralized Traffic Signal Optimization' , IEEE ITS Transactions, submitted

[Kanungo T. et al.,2002] Kanungo T. et al., 'An efficient k-means clustering algorithm: analysis and implementation ' , in IEEE Transactions on Pattern Analysis and Machine Intelligence, vol. 24, no. 7, pp. 881-892, Jul 2002.